Studies on crystallization of lactose in permeates and the use of modified milk protein concentrate in high-protein dairy beverages

by

Karthik Pandalaneni

B.Tech., Bharath University, India, 2009
M.Sc., University of Leeds, UK, 2010

AN ABSTRACT OF A DISSERTATION

submitted in partial fulfillment of the requirements for the degree

DOCTOR OF PHILOSOPHY

Food Science

KANSAS STATE UNIVERSITY
Manhattan, Kansas

2018

Abstract

Lactose is commercially produced from whey, whey permeate, or milk permeate as α-lactose monohydrate in crystalline form. Focused Beam Reflectance Measurement (FBRM) as a potential tool for *in situ* monitoring of lactose crystallization at concentrations relevant to the dairy industry was evaluated. Applicability of FBRM at supersaturated lactose concentrations 50%, 55%, and 60% (w/w) was reported in comparison with Brix values obtained from a Refractometer during isothermal crystallization at temperatures 20ºC and 30ºC. FBRM technique was shown to be a valuable tool for monitoring chord length distributions during lactose crystallization. In a different study, the influence of cooling rate during crystallization of lactose in concentrated permeates was studied. Three cooling rates accounting for approximately 17, 11, and 9 h were applied during lactose crystallization to evaluate the lactose crystal yield and quality of lactose crystals. There was no significant difference ($P>0.05$) found in lactose crystal yield, mean particle size obtained at the end of crystallization. This study suggested that increasing the cooling rate during lactose crystallization within the range explained in this study can save approximately 8 h of crystallization time. These studies evaluated FBRM as a potential tool to monitor lactose crystal chord lengths and counts. Also, process improvements were suggested to increase the productivity of lactose crystallization process by reducing the crystallization time.

In chapters 5 and 6, calcium-reduced milk protein concentrates (MPCs) were used as an ingredient to improve the stability of high-protein dairy beverages. Heat stability increased significantly ($P>0.05$) in 8% protein solutions made from 20% calcium-reduced MPC. A significant increase in heat stability was observed in beverages formulated with 20% calcium-reduced MPC in the absence of chelating agent. In another study, it was evident that the dairy

beverage formulation with 20% calcium-reduced MPC showed no sedimentation and age gelation indicating an improved storage stability. These studies confirmed that 20% calcium reduced MPC contributed towards improved heat stability and storage stability of the high-protein beverages.

Studies on crystallization of lactose in permeates and the use of modified milk protein concentrate in high-protein dairy beverages

by

Karthik Pandalaneni

B.Tech., Bharath University, India, 2009
M.Sc., University of Leeds, UK, 2010

A DISSERTATION

submitted in partial fulfillment of the requirements for the degree

DOCTOR OF PHILOSOPHY

Food Science

KANSAS STATE UNIVERSITY
Manhattan, Kansas

2018

Approved by:

Major Professor
Dr. Jayendra Amamcharla

Copyright

Abstract

Lactose is commercially produced from whey, whey permeate, or milk permeate as α-lactose monohydrate in crystalline form. Focused Beam Reflectance Measurement (FBRM) as a potential tool for *in situ* monitoring of lactose crystallization at concentrations relevant to the dairy industry was evaluated. Applicability of FBRM at supersaturated lactose concentrations 50%, 55%, and 60% (w/w) was reported in comparison with Brix values obtained from a Refractometer during isothermal crystallization at temperatures 20ºC and 30ºC. FBRM technique was shown to be a valuable tool for monitoring chord length distributions during lactose crystallization. In a different study, the influence of cooling rate during crystallization of lactose in concentrated permeates was studied. Three cooling rates accounting for approximately 17, 11, and 9 h were applied during lactose crystallization to evaluate the lactose crystal yield and quality of lactose crystals. There was no significant difference ($P>0.05$) found in lactose crystal yield, mean particle size obtained at the end of crystallization. This study suggested that increasing the cooling rate during lactose crystallization within the range explained in this study can save approximately 8 h of crystallization time. These studies evaluated FBRM as a potential tool to monitor lactose crystal chord lengths and counts. Also, process improvements were suggested to increase the productivity of lactose crystallization process by reducing the crystallization time.

In chapters 5 and 6, calcium-reduced milk protein concentrates (MPCs) were used as an ingredient to improve the stability of high-protein dairy beverages. Heat stability increased significantly ($P>0.05$) in 8% protein solutions made from 20% calcium-reduced MPC. A significant increase in heat stability was observed in beverages formulated with 20% calcium-reduced MPC in the absence of chelating agent. In another study, it was evident that the dairy

beverage formulation with 20% calcium-reduced MPC showed no sedimentation and age gelation indicating an improved storage stability. These studies confirmed that 20% calcium reduced MPC contributed towards improved heat stability and storage stability of the high-protein beverages.

Table of Contents

List of Figures

List of Tables

Acknowledgements

I would like to express my gratitude to my major advisor, Dr. Jayendra Amamcharla, for his support and guidance throughout my doctoral program. I am greatly thankful to my committee members, Dr. Karen Schmidt, Dr. Scott Smith, Dr. Weiqun Wang for their kind words and support during my doctoral program. Special thanks to Dr. John Tomich for serving as my outside chair.

My special thanks to my friends and fellow graduate students at the Food Science Institute for their support and motivation during this journey. I also thank the support I received from other faculty and staff who is always ready to help to make this learning process easier.

I would like to thank my parents Kondala Rao Pandalaneni and Syamala Devi Pandalaneni who supported and encouraged me and always had me in their prayers. My special thanks to my wife, Haripriya Naidu for the love, support and encouragement towards completing my doctorate degree.

Dedication

I would like to dedicate this doctoral dissertation to all my teachers who mentored me to become what I am today.

Chapter 1 - General Introduction

Traditionally, bovine milk is consumed as liquid milk as well as products milk such as cheese, yogurt, or ice cream. In addition, bovine milk is also a valuable source for the milk derived ingredients such as milk protein concentrate and whey protein concentrate that are in global demand. Major components of milk include water, lactose, fat, proteins, and minerals along with many other minor components. Lactose constitutes 4.9-5.4% of milk and is the major component of milk solids. Because of its low sweetness and ability to participate in browning reactions such as Maillard reaction, it is valued as an ingredient in the bakery and pharmaceutical industries. On the other hand, milk proteins (caseins and whey proteins) are the most valued components of milk. Milk proteins are valued for their functional and nutritional properties in the food and beverage industries. According to Food and Health Survey, US (USDEC, 2017) shoppers are more inclined to prefer protein-rich drinks due to their health benefits. The importance of lactose and milk proteins is discussed in detail in the further chapters.

Lactose is crystallized as a stable α-lactose monohydrate from concentrated permeates. Crystallized and refined lactose powder has a wide range of applications in the food and pharmaceutical production. From a recent Global Dairy Report (USDEC, 2018) lactose exports reached 35,469 tons in December 2017 which is 14% higher compared to the exports 32 months ago. With growing demand for lactose, it is important to improve the lactose crystallization process to be more efficient. Productive and economical lactose crystallization processing can be optimized by using better monitoring techniques during crystallization to minimize the losses (McLeod et al., 2011). Using efficient monitoring techniques can help control the crystal growth and secondary nucleation during the crystallization and give an opportunity to the manufacturer

to minimize the loss caused by fine crystals (Wong et al., 2012; Pandalaneni and Amamcharla, 2016).

The protein-rich fraction of skim milk obtained after ultrafiltration is spray dried to obtain milk protein concentrate (MPC). MPCs are considered as a complete dairy protein because of their casein to whey ratio is same as milk (Marella et al., 2015). They are a preferred source to enrich the dairy beverages and energy bars. However, complications during storage should be considered when developing a beverage with increased protein content. Due to the protein-protein and protein-mineral interactions during storage of high-protein dairy beverages, defects like sedimentation and age gelation are possible (Datta and Deeth, 2001; Malmgren et al., 2017). Especially calcium associated with caseins as colloidal calcium phosphate (CCP) plays an important role in inducing the changes to caseins that influence the stability of proteins in the beverages (Dalgleish and Law, 1989). To delay the storage defects, additives like calcium chelating agents are extensively used in the dairy-based beverages (de Kort et al., 2011). But calcium chelating salts contribute towards high sodium content on the nutrition label which can affect the consumer acceptability. Hence, manufacturers are aiming for label-friendly additives in the formulations to improve storage stability. With advancements in separation technologies, improved and modified MPCs are used in the formulations of high-protein dairy beverages in this study.

The following chapters address the issues related to lactose crystallization process and also the application of modified MPCs in the formulations of high-protein dairy beverages.

Objectives

- Chapter 3- Evaluate the effectiveness of focused beam reflectance measurement (FBRM) at concentrations relevant to the industrial scale crystallization of lactose.
- Chapter 4- Characterizing the lactose crystallization and quality of lactose crystals at different cooling rates in concentrated permeates. Influence of cooling rate and naturally present impurities in the concentrates permeates on lactose crystallization and quality were evaluated.
- Chapter 5- Evaluate the application of calcium-reduced MPCs in dairy beverage formulation.
- Chapter 6- Investigate the influence of calcium-reduced MPCs and the presence of chelating agent on the storage stability of high-protein dairy beverages.

Bibliography

Dalgleish, D.G., and A.J.R. Law. 1989. pH-induced dissociation of bovine casein micelles. II. Mineral solubilization and its relation to casein release. J. Dairy Res. 56:727 – 735.

Datta, N., and H.C. Deeth. 2001. Age Gelation of UHT Milk—A Review. Food Bioprod. Process. 79:197–210.

de Kort, E., M. Minor, T. Snoeren, T. van Hooijdonk, and E. van der Linden. 2011. Effect of calcium chelators on physical changes in casein micelles in concentrated micellar casein solutions. Int. Dairy J. 21:907–913.

Malmgren, B., Y. Ardö, M. Langton, A. Altskär, M.G.E.G. Bremer, P. Dejmek, and M. Paulsson. 2017. Changes in proteins, physical stability and structure in directly heated UHT milk during storage at different temperatures. Int. Dairy J. 71:60–75.

Marella, C., P. Salunke, A.C. Biswas, A. Kommineni, and L.E. Metzger. 2015. Manufacture of modified milk protein concentrate utilizing injection of carbon dioxide. J. Dairy Sci. 98:3577–3589.

McLeod, J., A.H.J. Paterson, J.R. Jones, and J.E. Bronlund. 2011. Primary nucleation of alpha-lactose monohydrate: The effect of supersaturation and temperature. Int. Dairy J. 21:455–461.

Pandalaneni, K., and J.K. Amamcharla. 2016. Focused beam reflectance measurement as a tool for in situ monitoring of the lactose crystallization process. J. Dairy Sci. 99:5244–5253.

Wong, S.Y., R.K. Bund, R.K. Connelly, and R.W. Hartel. 2012. Designing a lactose crystallization process based on dynamic metastable limit. J. Food Eng. 111:642–654.

USDEC, 2017. U.S Dairy proteins and permeates in ready-to-drink beverages. Accessed Mar. 22, 2017. http://www.thinkusadairy.org/resources-and-insights/resources-and-insights/application-and-technical-materials/ready-to-drink-beverage-monograph

USDEC, 2018. Global Dairy- Market outlook. Apr. 7, 2018. http://www.usdec.org/member-services/periodicals/global-dairy-market-outlook

Chapter 2 - Literature Review

Lactose Crystallization

Introduction

Lactose is the principal carbohydrate and the second major component in bovine milk constituting 4.4-5.2%. Lactose is also a major fraction of permeates such as milk permeate and whey permeate which are obtained during manufacturing of milk protein concentrate and whey protein concentrate, respectively. Lactose constitutes 70-90% of dry matter in permeate powders and about 50-55% in non-fat dry milk (NFDM) (McSweeney and Fox, 2009). The global market for the dry commodities of dairy increased because of their nutritional value and ease of transportation. Lactose plays an important role in retaining the quality and shelf-life of these dried dairy ingredients. Manufacturers need to optimize the processing conditions to obtain the stable lactose form to avoid the customer complaints and loss of product quality during transportation and storage.

In addition to playing an important role in dairy ingredient stability, lactose as α-lactose monohydrate is also crystallized and recovered from the concentrated permeates. Due to its low sweetness (30% less than sucrose) and flavor, lactose has a wide range of applications in the food and pharmaceutical industries (Lifran et al., 2010). Also, since lactose is a reducing sugar that can enhance color by Maillard browning, it is used in bakery and confectionery products for improving color (McSweeney and Fox, 2009).

The storage stability of the dairy ingredients is influenced by form of lactose and hence optimizing the processing conditions to obtain a stable lactose form is required. The objective of this review is to highlight the research that focused on improving processing, functionality, and storage stability of lactose and lactose-rich dairy powders.

Structure

Lactose is a disaccharide consisting of one galactose and one glucose molecule connected by a β (1→4) glycosidic linkage as shown in Figure 2.1. Because of its steric configuration around C-1 on the glucose, lactose is present in two forms (anomers) as α-lactose and β-lactose. The interchange between α and β anomers of lactose is called mutarotation. α and β anomers of lactose can be distinguished by their specific rotation, shape of crystals, solubility, and sweetness. The specific rotation of α-lactose is $[\alpha]_D^{20} = +89.4°$, whereas for β-lactose is $[\alpha]_D^{20} = +35.0°$ (McSweeney and Fox, 2009). α-lactose crystallizes as monohydrate and predominantly exists in tomahawk shaped crystals with the ability to change depending on the crystallization conditions, whereas, β-lactose crystallizes as uneven sided diamond shaped crystals above 93.5°C. The α-lactose is less soluble than β-lactose which leads to crystallization in supersaturated lactose solutions. Also, α-lactose is less sweet when compared to β-lactose (Gänzle et al., 2008).

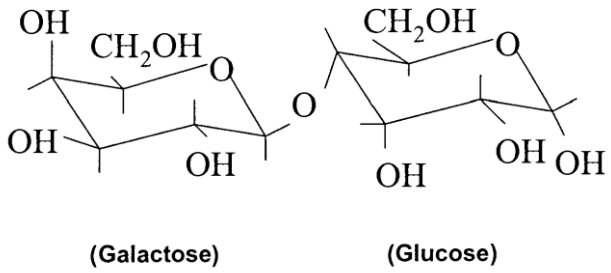

Figure 2.1. Chemical structure of α-lactose (Adapted from Nonnemacher (2004))

Mutarotation

The interchange between α and β anomers occurs in aqueous solutions through a process called mutarotation. In lactose solutions at equilibrium, the specific rotation of $[\alpha]_D^{20} = +55.3°$

exists and β:α lactose ratio is approximately 1.5:1 (Gänzle et al., 2008; Wong and Hartel, 2014). Mutarotation is dependent on the temperature, pH, and presence of other sugars and salts. When a supersaturated lactose solution is cooled gradually, α-lactose crystallizes out due to its lower solubility. To maintain the equilibrium between α and β anomers, the β-lactose mutarotates to α-lactose thus, continuing the crystallization. It is often considered that the rate of mutarotation is higher than the rate of crystallization in the unseeded or very small amount of seeded crystallization process and considered as not a limiting factor (Raghavan et al., 2001). However, mutarotation is still considered in the crystallization kinetics in few studies (Gernigon et al., 2013).

Physical State of Lactose

Depending on the molecular arrangement of lactose, the state of lactose can be classified as crystalline and amorphous. In the crystalline state, lactose molecules are arranged in an orderly fashion with space lattice, whereas in the amorphous state, lactose molecules are not organized (Mullin, 2001; Carpin et al., 2016). The transition of lactose from a crystalline state to amorphous (non-crystalline) state and vice-versa is dependent on the temperature and water content in the system. The non-crystalline amorphous state of lactose is a non-equilibrium system, which on the absorption of water transitions into stable lactose form. However, the transition from amorphous to a stable crystalline form is a time-dependent phenomenon and is often accelerated by factors like relative humidity (**RH**) and temperature (Roos, 2002). The transition of the amorphous glassy state to the rubbery state is called glass transition, and the temperature at which the amorphous glassy state transition is referred to as the glass transition temperature (T_g) (McSweeney and Fox, 2009). When a glassy state of lactose absorbs moisture at a favorable temperature, a glassy state with restricted molecular mobility converts into the

rubbery state with increased molecular mobility. Water acting as a plasticizer promotes the molecular mobility and transforms glassy state to a rubbery state. Rubbery amorphous lactose tends to form liquid bridges between powder particles (stickiness) or eventually crystallize into a stable form (caking). It was suggested that glassy amorphous state holds its stability without forming rubbery amorphous phase below the T_g (Roos, 2002). Hence, it is important that various forms of lactose should be well understood to avoid the storage defects. Influence of these forms on storage stability of dairy ingredients was discussed in detail in the later sections. Known forms of crystalline and amorphous lactose are given in Table 2.1.

Table 2.1. State and forms of lactose (Listiohadi et al., 2005a; Carpin et al., 2016)

State of lactose	Form of lactose
Amorphous	Mixture of α- lactose and β-lactose
Crystalline	α-lactose monohydrate
	α-lactose anhydrous- stable
	α-lactose anhydrous- unstable
	β -lactose

Amorphous Lactose

Amorphous lactose is formed when concentrated lactose is rapidly dried during spray drying or freeze drying without crystallization and exists as a mixture of both α and β-lactose (Carpin et al., 2016). Though solubility of amorphous lactose is high compared to stable α-lactose monohydrate, because of it is hygroscopic and state transition behavior, formation of amorphous lactose is minimized during dairy powders processing. However, continuous mass of

amorphous lactose is present in the spray dried particles of whole milk powder and skim milk powders because of the rapid water dehydration during spray drying (Walstra et al., 1999).

Alpha-Lactose Monohydrate

It is the most stable form aimed during lactose crystallization at temperature < 93.5°C. Monohydrate form of α-lactose has one water molecule attached to the lactose molecule which also accounts for 5% of its crystal mass (Mimouni et al., 2005). Because of the very few hydrophilic groups available in the crystal form, they are non-hygroscopic and have less solubility (Zadow, 1984). Most common crystal shape of α-lactose monohydrate is tomahawk shaped as shown in Figure 2.2. However, due to its polymorph characteristic, the crystal shape can vary depending on the crystallization process parameters and impurities present (Nonnemacher, 2004; Mimouni et al., 2009; Carpin et al., 2016). Stable monohydrate form of lactose is predominantly observed in dairy powders which are crystallized before spray drying (Goulart and Hartel, 2017). This pre-crystallization step promotes formation of α-lactose monohydrate form increasing stability of the dairy powders.

Figure 2.2. A typical tomahawk shape of lactose crystal.

Stable and Unstable α-Lactose Anhydrous

When the water molecule attached to α-lactose monohydrate is removed by extensive heating to higher temperatures (100°C- 190°C), anhydrous forms of α-lactose are formed (Gänzle et al., 2008). The stable form is formed by the loss of water molecule, whereas on extending the heating of anhydrous form, a highly porous lactose crystal lattice is formed in unstable form (Carpin et al., 2016). According to Listiohadi et al. (2009) both the anhydrate forms are hygroscopic, but the unstable form is more hygroscopic than the stable form. Stable and unstable anhydrate forms convert to α-lactose monohydrate upon absorbing moisture. Anhydrous α-lactose forms are more valued in pharmaceutical industries for tableting purposes in mixture with amorphous lactose (Lallukka and Heikonen, 1986).

Anhydrous β-Lactose

Anhydrous β-lactose is the only anomeric crystal form of lactose that can be recovered during crystallization above 93.5°C and exists as uneven sided diamond shaped crystals (Gänzle et al., 2008). Anhydrous β-lactose is a stable form and less hygroscopic than anhydrous forms of α-lactose. It is commercially manufactured by roller drying the thin film of supersaturated lactose at a temperature above 93.5°C (Carpin et al., 2016). Hourigan et al. (2013) reported that the obtained mixture from the roller drying method has high β-lactose percentage (70-80%) and anhydrous α-lactose. Because of its structural similarity to α-lactose, β-lactose tends to bind on $\{0\ \bar{1}\ 1\}$sides of tomahawk shaped lactose crystal during crystallization inhibiting the growth (Garnier et al., 2002).

Lactose Crystallization from Supersaturated Solutions

Recovery of lactose from the permeates gained importance after the strict environmental regulations concerning increase in biological oxygen demand (BOD) on disposal of whey (Patel and Murthy, 2012). Because of the high lactose content in whey, permeates of whey and milk

(76-85%) are considered the major sources to manufacture commercial grade lactose by crystallization (Pandalaneni and Amamcharla, 2016). Commercial lactose production involves several steps of which crystallization was an important one. As the lactose rich permeates are collected, concentrated, and gradually cooled to induce lactose crystallization. Lactose crystals are recovered after centrifugation and subsequently washed, refined, dried, and sieved for commercial bagging (Paterson, 2017) as described in Figure 2.3.

Pretreatment and Concentration

Concentration of permeates is the first step in the process of crystallization. However, to increase the lactose crystal yield and reduce the fouling and corrosion, permeates are pretreated to reduce the mineral content. Lactose rich permeate is pretreated to improve lactose recovery during subsequent crystallization (Wong and Hartel, 2014) and is generally concentrated to 65-70% total solids with 39-56% lactose concentration using vacuum evaporation. Evans and Young (1982) pretreated the whey permeate with chelating salts followed by a filteration step at 80°C prior to improve the purity of α-lactose monohydrate crystals by removing minerals.

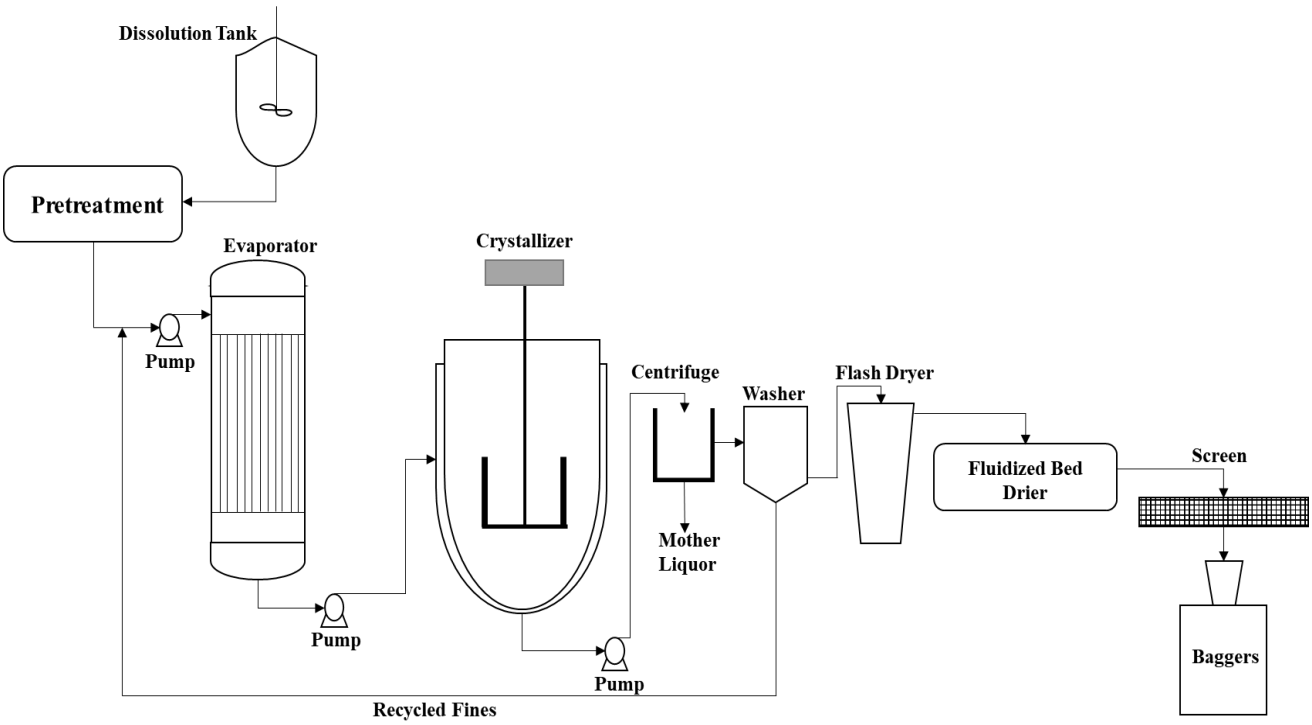

Figure 2.3. Typical process flow diagram for refined pharmaceutical grade α-lactose monohydrate

In addition to chemical addition, a combination of membrane filtration techniques like ultrafiltration and nanofiltration are also used to pretreat and partially demineralize whey to improve the lactose crystal yield (Guu and Zall, 1991; Lifran et al., 2010). Due to low pH (~ 4.5) contributed by the presence of high lactic acid and mineral concentrations, acid whey and greek yogurt whey (GYW) have limited industrial applications as a source to recover lactose. Although lactose is also the major component in acid whey and GYW, the presence of lactic acid hinders its recovery by the crystallization and subsequent drying process. Lactic acid forms strong hydrogen bonds with water and requires high energy to remove water molecules during evaporation in order to concentrate lactose (Wijayasinghe et al., 2015). To reduce the lactic acid and mineral concentration of acid whey and GYW, some researchers proposed pretreatment methods like nanofiltration to partially remove minerals (Chandrapala et al., 2015).

Nucleation

During lactose crystallization, supersaturation is the driving force which promotes nucleation by diffusing lactose from the liquid phase to solid phase. Ulrich and Strege (2002) explained that supersaturated solutions exhibit an allowable supersaturation level during crystallization called metastable zone as shown in Figure 2.4. The supersaturation concentration between solubility and super-solubility curve is called metastable zone width (MSZW). Spontaneous nucleation can only occur if the supersaturation concentration increased beyond super-solubility to reach labile zone. Above super-solubility curve, spontaneous primary nucleation is induced due to supersaturation driving force. If the nucleation is induced by the crystalline component itself (ex. addition of lactose seeds) then it is called homogeneous nucleation, whereas, if nucleation is induced by the presence of foreign particle or roughness of a surface, it is referred to as heterogeneous nucleation. If the supersaturation concentration is in the MSZW then crystal growth is dominant with some extent of secondary nucleation (Wong et al., 2011). Secondary nucleation occurs from an already formed crystal boundary layer or from broken crystals formed by agitation and collision with crystallizer walls and with each other (Pandalaneni and Amamcharla, 2016).

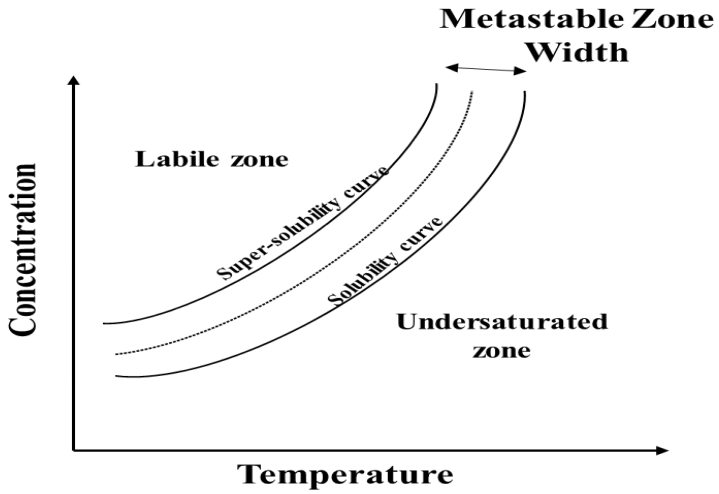

Figure 2.4. Illustration of metastable zone width (MSZW), primary and secondary nucleation of lactose in supersaturated solution

Nucleation is considered a key phase in determining the crystal size distribution and yield of lactose crystallization process (Ulrich and Strege, 2002). Concentrated permeate is transferred to a crystallizer and cooled gradually under agitation to induce nucleation by supersaturation driving force. The time required to form stable nuclei from the nuclei cluster is called induction time (Mullin, 2001). Rapid nucleation restricting the lactose crystal growth can result in small lactose crystals towards the end of crystallization that can eventually lead to product loss during centrifugation and washing steps (Wong et al., 2012).

Several researchers worked on improving the crystallization process by promoting nucleation to reduce the induction time. Reduction of induction time facilitates more time for the crystal growth and hence bigger crystals and reduced losses. Few factors that determine the nucleation of lactose are the cooling rate, agitation rate, impeller design, and the crystallizer design (Wong et al., 2012). McLeod et al. (2016) also concluded that increased agitation rate in supersaturated lactose solution increased the nucleation rate because of the increased molecular collisions and improved mass transfer. Lactose seeding is another conventional industrial

practice to improve the crystal yield by reducing the induction time during crystallization. Refined lactose crystals are added to the supersaturated lactose solution to promote the nucleation when the supersaturation concentration is in the metastable zone (Hourigan et al., 2013). Instead of adding lactose seeds, additives like soybean polysaccharide (0.1%) were added to 40% lactose solutions to promote spontaneous nucleation without decreasing the lactose purity. However, increasing the concentration of soybean polysaccharide to 0.5 and 1.0% resulted in the increased viscosity and reduced the yield (Shi and Zhong, 2014). On the other hand, the presence of impurities like whey proteins and precipitated minerals trigger heterogenous nucleation in concentrated permeates during lactose crystallization (Butler, 1998 and Mimouni et al., 2009).

Recent developments in the processing technologies introduced ultrasound to reduce the induction time during crystallization. It was explained that vibrational energy from the ultrasonic energy promotes nucleation and crystal growth by enhancing heat and mass transfer (Hartel, 2013). Zisu et al. (2014) used ultrasound to promote rapid nucleation in concentrated whey and obtained smaller lactose crystals with narrow size distribution. In another study by Xun et al. (2016), supersaturated 50% lactose solution was carbonated prior to the ultrasound treatment to promote nucleation and narrow the crystal size distribution. However, Paterson (2017) explained that the application of ultrasound in industrial scale crystallization can be difficult because of its limitation to achieve uniform field across the crystallizer. The author also suggested controlling the cooling rate and the agitation rate to obtain uniform nucleation.

Crystal Growth

After the nucleation, crystal growth occurs upon continuous diffusion of lactose onto already formed crystal lattice. Crystal growth is dependent on the supersaturation driving force

and temperature (Hourigan et al., 2013). Crystal growth can be divided into three steps, mass transport from the liquid phase to the solid phase, followed by surface integration, and transport of latent heat away from the growing crystals (Wong and Hartel, 2014). Influence of impurities on the lactose crystal growth and yield is extensively studied and addressed by many researchers and the collective summary of these studies were discussed further (Modler and Lefkovitch, 1986; Guu and Zall, 1991; Bhargava and Jelen, 1996; Garnier et al., 2002; Lifran et al., 2007; Mimouni et al., 2009; Chandrapala et al., 2016). Whey proteins are one of the common components present in the concentrated permeates and it was observed that whey proteins restrict the water molecules, creating isolated nucleation sites, and restrict the growth of lactose crystals. A similar observation was made when lactose crystal growth was investigated in presence of lactic acid in acid whey. Because of the ability of the lactic acid to bind to lactose molecules, the bulk complex of lactose molecules was formed restricting the molecular mobility and hence negatively impacting the crystal growth. As calcium and phosphates constitute the majority of mineral impurities, deposition of their salt (calcium phosphate) in the lactose crystal can hinder crystal growth. Along with calcium phosphate, other salts that proved to decrease the growth rate of lactose crystals were lactose phosphate and dipotassium phosphate. When additives with the similar molecular structure as lactose were added, they associate selectively on the lactose crystal and limiting its growth on specific face. It was observed that β-lactose anomer and lactose phosphate associated with tomahawk shaped lactose crystals during lactose crystallization inhibit the growth on specific sides. On the other hand, another major impurity in whey permeates that proved to inhibit lactose crystal growth is riboflavin. However, riboflavin adheres to the surface of lactose crystals and can be easily removed during washing steps after the crystallization.

Techniques Used to Evaluate and Characterize Lactose Crystallization Process

With advancements in technology, better ways to monitor and control lactose crystallization evolved over the years. Few monitoring techniques to characterize lactose anomers, lactose crystallization and kinetics are summarized in Table 2.*2*.

Table 2.2. Monitoring techniques to characterize lactose anomers, lactose crystallization, and its kinetics

Monitoring Technique	Summary of the method	Feasibility	Reference
Nuclear Magnetic Resonance (NMR)	Glass transition temperature (T_g) to determine the crystallinity of powders was measured. As the lactose passes through T_g, the internuclear distance increases along with amplitude of molecular vibrations during the transition from glassy to a rubbery state. These changes are measured as a function of temperature using a proton spin-lattice relaxation time analysis	▪ Rapid ▪ No sample preparation ▪ Skilled Technician	Lloyd et al., 1996
X-Ray Diffraction (XRD)	The lactose powder was poured into a brass capsule with one side covered with an adhesive X-ray transparent plastic film. Diffraction pattern was obtained at 1200W and 40kV. Quantification of α-lactose monohydrate and β-lactose was done in the lactose powder sample.	▪ Skilled technician ▪ Qualitative and Quantitative determination of lactose forms in dairy powders	Drapier-Beche et al., 1997
Differential Scanning Calorimetry (DSC)	Lactose powder was sealed in hermetic pans and heated from 20 to 240 °C at 5°C/min rate. Thermogram was obtained identifying the amorphous lactose by exothermic peak (167 °C), loss of crystalline water by endothermic peak (144 °C) and melting endothermic peaks of α (210 °C) and β (216 °C) anomers.	▪ Qualitative and quantitative analysis of dairy powders can be done ▪ Skilled Technician	Gombas et al., 2002
Laser light scattering	Crystal suspension was added into dispersant medium for the laser light scattering particle analyzer. Diffracted light from the particles was analyzed to determine the crystal size and distribution	▪ Rapid ▪ No sample preparation ▪ Expensive Equipment ▪ Cannot differentiate between lactose crystals to other particles	Mimouni et al., 2005
Refractometry	Determines the concentration of soluble solids from a small amount (1mL) of the sample. A calibration curve	▪ Rapid ▪ Easy to use	Mimouni et al., 2005;

	was used to determine the soluble lactose concentration during crystallization to determine the crystallization kinetics	▪ Used in combination with other in-situ methods ▪ Cannot provide the information about lactose crystal nucleation or growth ▪ Can only give accurate results in pure lactose system	Pandalaneni and Amamcharla, 2016
HPLC	β/α- anomer proportions were determined in the lactose powder. The lactose powder was rapidly dissolved (< 1 min) into distilled water and injected into HPLC with C18 column. B-anomer appears first followed by α-anomer	▪ Skilled Technician ▪ Not reproducible because of mutarotation sensitivity ▪ Qualitative and Quantitative determination of lactose forms in dairy powders	Listiohadi et al., 2009
Thermogravimetric Analysis (TGA)	The accurate amount of sample was weighed into crucibles and heated from 25 to 300 °C at a rate of 5 °C. Change in the mass as the function of temperature was recorded to evaluate the thermal properties in different forms of lactose.	▪ Qualitative and Quantitative determination of lactose forms in dairy powders ▪ Skilled Technician	Listiohadi et al., 2009
Focused Beam Reflectance Measurement (FBRM)	Determined the nucleation, crystal growth, and secondary nucleation in supersaturated lactose solutions. The laser beam from the FBRM probe detects the surface of the particle and backscatters to the probe. Chord length was measured from the time of backscattering reflection and velocity of the laser beam	▪ Rapid ▪ No sample preparation ▪ Sensitive ▪ Expensive Equipment ▪ Cannot differentiate between lactose crystals to other particles in the suspension ▪ Can only be used in combination with another technique to determine lactose	Huang et al., 2010; Pandalaneni and Amamcharla, 2016

		concentration to calculate crystallization kinetics	
Ultrasound	Crystallization was determined by ultrasonic waves. An ultrasonic transducer with 2.25 MHz frequency was used to generate ultrasonic waves into the gelatin gel. Ultrasonic velocity and attenuation are used to measure crystal growth and crystal load during crystallization	▪ Sensitive ▪ Good for measuring crystallization in gel environments ▪ Can only be used in opaque systems at higher crystal loads ▪ Can only be used in combination with absorbance to evaluate crystallization	Yucel and Coupland, 2011
Spectrophotometry	Absorbance and Turbidity of the supersaturated lactose solutions were measured to determine the induction period during lactose crystallization	▪ Rapid ▪ Can be insensitive if crystal load increase ▪ Can only be measured in pure lactose systems	McLeod et al., 2011; Yucel and Coupland, 2011
Microscopic Analysis	A representative sample was collected during lactose crystallization and viewed using an optical microscope to observe the change in crystal growth and distribution	▪ Qualitative analysis ▪ Cannot determine the crystallization kinetics ▪ Can be used in complementary to other particle analysis technique	Pandalaneni and Amamcharla, 2016

Solid-phase Lactose Crystallization in Dairy Powders

The state and forms of lactose present in the dairy powders play an important role in determining the functionality and stability of the lactose-rich dairy powders. Stable and non-hygroscopic α-lactose monohydrate form is desirable in dairy powders to avoid the storage defects. However, during spray drying, amorphous lactose is formed in the dairy powders leading to the stickiness and caking (Saffari and Langrish, 2014). Of the four forms of lactose, amorphous lactose is the most hygroscopic and unstable, which undergoes solid-phase crystallization to form stable monohydrate form depending on the storage conditions. It was reported that commercially available spray dried dairy powders contains approximately 10-15% of amorphous lactose (Hourigan et al., 2013). Hence, to obtain a stable monohydrate form with a controlled degree of crystallinity several studies proposed changes during processing of dairy powders.

One of the ways to improve the crystallinity in spray-dried dairy powders is by pre-crystallization. Pre-crystallization of concentrated permeates proved to obtain approximately 50-75% crystallinity, consequently improving the storage stability of spray-dried powders (Darcy and Buckton, 1998; McSweeney and Fox, 2009). However, the pre-crystallization process must be controlled to avoid bigger crystals that can damage the spray drying equipment as well as to maintain the acceptable viscosity for the ease of spray drying (Goulart and Hartel, 2017). Pre-crystallization is followed by spray drying and post-spray drying processes like fluidized bed drying and milling which also influence the degree of crystallinity in the dairy powders. This section reviews the research that focused on the effect of processing and storage conditions on the solid-phase crystallization in dairy powders.

Effect of Spray Drying Operating Conditions on Degree of Crystallization in Powders

Spray drying is one the conventional processing techniques used in the manufacturing of dairy powders (Schuck, 2002). Operating conditions during spray drying of lactose-rich dairy powders had proven to influence the degree of lactose crystallization in the formed particles. Sugars like lactose are slow to crystallize because of their higher T_g (101°C) which results in the faster formation of dehydrated particle before crystallization can occur (McSweeney and Fox, 2009; Shakiba et al., 2018). Because of this property of lactose, dehydration of water occurs faster during spray drying leaving glassy state amorphous lactose in the particle. However, to avoid the rapid dehydration from the particle during spray drying and to facilitate time to crystallize lactose, changes in operating conditions like inlet temperature and drying air humidity are evaluated. Islam and Langrish (2010) observed that spray drying 10% lactose solution at 200°C inlet gas temperature in an insulated drying chamber increased lactose crystallinity compared to 170°C inlet temperature. But higher inlet temperature resulted in lower yield (0.16%) compared to 170°C (47%) inlet temperature. Though the increase in crystallinity was observed, particles exhibited formation of β-lactose anomer in the particles, which resulted in sticking to the walls of the drying chamber. A similar observation was made by Chiou et al. (2008), where an inlet temperature was increased from 134 to 210°C during spray drying of 15% lactose solution, which resulted in an increase in the degree of crystallinity in powders. But contrasting results were obtained by Das et al. (2010) where higher inlet temperatures resulted in lower percentage of crystallinity. Their study observed 72% crystallinity at 170°C compared to 25% at an inlet temperature of 230°C. Das et al. (2010) justified that the observed contrasting results were attributed to the particle size obtained in pilot-scale spray dryer. Bigger particle size

of 15 µm was observed in pilot-scale spray dryer compared to smaller particles (5-7 µm) formed from laboratory scale spray dryer from Chiou et al. (2008) and Islam and Langrish (2010). The degree of crystallization in dairy powders is defined by the temperature difference between particle temperature (T) and the glass transition temperature (T_g) and with increase in T- T_g, the degree of crystallization increases (Haque and Roos, 2004). In the case of smaller particles, the T - T_g difference is high promoting rapid crystallization, whereas, in the case of bigger particles because of the presence of more non-aqueous composition, T_g increases along with particle temperature (T) reducing the degree of crystallinity. On reviewing these three studies, it is evident that particle size of the droplets should also be considered when addressing the degree of crystallinity during spray drying. As an alternative to increasing the inlet temperature, Shakiba et al. (2018) proposed an intermediate stage of drying during spray drying of 10% lactose solution. The author increased the humidity of the drying chamber by inserting a nozzle horizontally in the spray dryer. This study observed an increase in the degree of crystallinity as humidity was introduced during particle transition from the liquid phase to the solid phase. Humidifying the drying chamber when the particle is still in the liquid phase or after the transition to solid phase completely resulted in sticky powders. Increasing the humidity proved to increase the "wet time", thus promoting nucleation and crystal growth in the particle resulting in an increased degree of crystallinity.

Effect of Additives and Composition of Feed on Solid-phase Lactose Crystallization in Spray-Dried Powders

In addition to controlling the operating conditions of spray drying, extensive research was done on the effect of additives and composition of feed on solid-phase crystallization of lactose during spray drying. When lactose is associated with other components in the matrix, the

interactions between lactose and associated molecules determine the properties of spray dried powder. Because of the surface-active property of proteins, they migrate to the surface of the droplet during spray drying. Presence of proteins on the surface of the spray dried particle proved to delay solid-phase crystallization of amorphous lactose reducing stickiness (Wang et al., 2010; Shi and Zhong, 2015). Presence of amorphous lactose form in the spray dried powders is unavoidable which eventually leads to stickiness when stored at high RH. But Thomas et al. (2005) and Wang et al. (2010) postulated that presence of casein and β-lactoglobulin delay the onset of crystallization even when stored at higher RH. Studies witnessed a significant delay in lactose crystallization in spray-dried amorphous lactose with as low as 0.5% casein concentration. A similar observation was made in lactose and β-lactoglobulin mixtures, because of the hydrogen bonds formed during lyophilization. Along with a delay in onset of crystallization, both of these studies exhibited similar sorption properties as well. At higher RH, lactose/casein and lactose/β-lactoglobulin mixtures exhibited absorption but there was no desorption of water observed. It was explained that because of the hygroscopic property of proteins, they absorb water and increase the moisture content, however, this does not lead to crystallization of amorphous lactose. So, these two studies explain that increase in the moisture content of the lactose/protein mixtures cannot be mistaken for crystallization of amorphous lactose until further analysis is done.

Other additives which have similar surface active properties like proteins were also added to the lactose mixtures to delay the onset of crystallization and consequently stickiness in the powders. Das et al. (2010) investigated the effect of whey protein isolate (WPI) and gum arabic on solid-phase lactose crystallization. The author explained that mixture of WPI and gum arabic are efficient at delaying the onset of crystallization even at low concentrations. However, due to

the emulsion property of gum arabic, it is distributed through the particle interacting with lactose by restricting its molecular mobility to crystallize. Presence of gum arabic not only delayed the onset of crystallization on the surface but also throughout the particle. Shi and Zhong (2015) also evaluated the effect of branched polymer with a small fraction of protein called soluble soybean polysaccharide (SSPS) on solid-phase crystallization. Because of the similar surface active and hygroscopic properties of SSPS as proteins, the author observed a delay in onset crystallization in amorphous lactose powders when stored at 65% RH.

In addition to the additives discussed so far, another naturally present component associated with the lactose in acid whey is lactic acid. Due to the strong binding of lactic acid to lactose molecules, molecular mobility was restricted, resulting in hindered lactose crystallization (Wijayasinghe et al., 2015). However, in the study done by Chandrapala et al. (2016), it was observed that low concentration of lactic acid can lower the T_g drastically and initiate the lactose crystallization. When calcium was also added to lactic acid to increase the solids percentage the interfacial energy decreased and nucleation was initiated. This study explained that calcium and lactic acid work synergistically when one being at high concentration and another being at low concentration or vice versa, can increase the lactose crystallization.

Effect of Post-Spray Drying Processes on the Solid-phase Crystallization of Lactose and Storage of Dairy Powders

In addition to studies summarized on increasing the degree of crystallinity in powder particles during spray drying, Yazdanpanah and Langrish (2011) focused on post-spray drying crystallization during fluidized bed drying. Because of high heat transfer and low retention times, fluidized bed drying is considered as a robust technique to produce dry dairy powders. To increase the degree of crystallinity in skim milk powder and amorphous lactose powder, authors

further dried the powders at increased RH and temperatures. Amorphous lactose powders dried at 60°C and at RH of 40% for 60 min exhibited no absorption and desorption. This consistency of mass when stored at 75% RH at 25°C indicates that lactose was crystallized during fluidized bed drying, consequently, no absorption was observed. However, when amorphous lactose powders dried at a lower temperature (50°C) for lower times (30 min) were stored at same conditions absorption and desorption was observed during storage indicating the onset of lactose crystallization. A similar observation was seen in skim milk powder during storage as well. This study concluded that increasing RH and temperature during fluidized bed drying deceased the degree of amorphicity by 60-100% in both amorphous lactose and skim milk powders. However, particle size increased due to agglomeration during fluidized bed drying.

Another post-spray drying process that also effects the particle size and degree of crystallization in the dairy powder particles is milling. Milling is a unit operation that involves optimizing the particle size to obtain a narrow particle size distribution (Badal Tejedor et al., 2018). However, due to high shear and collision forces during milling, unintended surface amorphicity can occur (Trasi et al., 2010). Badal Tejedor et al. (2018) observed that particle size was decreased on milling for 1 h but further increase in milling time to 20 h increased particle size due to agglomeration of particles. During milling, along with topographical changes in the particles, the formation of different crystalline forms occurs depending on the milling time. Authors noted that the surface amorphicity in 1 h milled lactose powder but on increasing the milling time to 20 h, melting and recrystallization of lactose occurred, which led to the formation of new crystalline form not characterized as α or β-lactose. Authors were unclear of the nature of crystalline form and it was attributed to surface recrystallization because of increased RH in the sealed milling chamber along with the loss of crystalline water.

Changes occurred in the crystalline form and the particle size during milling proved to influence the storage of dairy powders. As evident from the discussion so far surface amorphicity on the of the particles influence the moisture absorption and desorption during storage. Presence of amorphous lactose even in the percentages as low as 5% resulted in the formation of harder cakes when stored at RH of 75%. Hardness progressed from the perimeter to the center of the lactose plugs due to the crystallization of amorphous lactose (Listiohadi et al., 2005b). Along with amorphicity, particle size is another important factor that determines the storage stability of dairy powders. Hourigan et al. (2013) explained that when lactose crystals with a median particle size smaller than 300 μm resulted in caking of powders with 5% water content. The caking was attributed to the increased possibility of liquid bridges among the smaller particles as compared to the bigger particles. However, this was observed to be not valid when the water content is below 0.5%. Enhanced caking of powders with smaller particle size was also supported by an extensive research done by Carpin et al. (2017). The author concluded that presence of fine particles (<80 μm) led to larger surface area increasing the water adsorption promoting "humidity caking". It was also observed that the presence of smaller particles increased the contact points associated with other particles promoting capillary condensation, which also led to caking.

Effect of Storage Conditions on Storage Stability of Dairy Powders

Commercial dairy powders have a shelf life of 12 months when stored in closed bags and at cool and dry conditions, however, following inadequate storing instructions can result in reduced shelf life (Robertson, 2009). One of the major problems during storage of lactose-rich dairy powders is caking, which is associated with the presence of unstable and hygroscopic amorphous lactose form. Paterson et al. (2005) explained caking as a two-step process, where

particles bridge together resulting in stickiness or lumps, which eventually lead to caking on solidification of these bridges. The onset of stickiness is initiated depending on the storage conditions like RH, water activity, forms of lactose, and temperature. In a detailed study by Listiohadi et al. (2008), the author addressed the effect of storing different forms of lactose at 33, 43, 57, and 75% RH and at 25°C. The study summarized that stable α-lactose anhydrous form was less hygroscopic compared to unstable anhydrous form of α-lactose. Stable form exhibited hygroscopicity only above 57% RH, whereas unstable form exhibited hygroscopicity at all RH studied, and increased with increase in RH. On the other hand, β-lactose showed a constant absorption until 57% RH and increased drastically with increase in RH to 75%. Whereas, spray dried lactose with approximately 5-12% amorphous lactose exhibited hygroscopicity at all the RH studied and α-lactose monohydrate on contrary absorbed moisture initially and then stayed stable. Upon moisture absorption, the transition of unstable amorphous lactose to stable monohydrate is evident from this study. The stable and unstable anhydrous forms of α-lactose transitioned to α-lactose monohydrate, likewise, β-lactose transitioned to its anomer α-lactose. Spray dried lactose powder also exhibited crystallization and caking at all RH levels studied. Increasing the water activity from 0.11 to 0.85 during storage of hygroscopic whey powder also resulted in the transition of amorphous lactose to monohydrate form (Saltmarch and Labuza, 1980). The onset of lactose crystallization on adsorption of moisture was evident at 0.40 water activity. When amorphous lactose was stored at constant water content, progressive recrystallization of amorphous lactose occurred, resulting in accelerated crystallization. Whereas, when stored at constant RH, crystallization of amorphous lactose increases with temperature and time (Roos and Karel, 1992). These studies summarized that controlling just one parameter

during storage cannot delay the caking. All the factors contributing to caking should be taken into account to increase the shelf life of the lactose-rich dairy powders.

High-protein Dairy Beverages

Introduction

Protein enriched beverages are the most sought out commodity among US customers according to a study published in 2017 by Food Information Council Foundation. Dairy ingredients rich in proteins are used in the formulation due to their rapid digestive and absorptive properties (Lagrange et al., 2015). Whey protein concentrates (WPC) or milk protein concentrates (MPC) are preferred ingredients for the manufacturing whey protein rich and milk protein rich dairy beverages (Cahalane and Ward, 2012; Agarwal et al., 2015). Storage stability of the dairy beverages along with sensory attributes like texture, flavor, and color is influenced by the composition, amount of protein, and processing conditions during manufacture (Grygorczyk, 2009). To meet the consumer demand, the dairy and food industry is striving to develop beverages with blends of new and functional ingredients. However, dairy protein-rich beverages go through a complex storage changes leading to premature failure. This review briefly summarizes the role of proteins and composition on the stability of dairy beverages.

Effect of Milk Proteins and their Interactions in Dairy Beverages

Milk is composed of 3.4% of proteins, of which caseins constitute 80% and whey proteins constitute the remaining 20%. Caseins (α_{s1}, α_{s2}, β, and κ-caseins) exist in association with each other as a porous integrated structure called micelle. Casein micelles are held together by colloidal calcium phosphate (CCP), hydrogen bonds, hydrophobic interactions, and van der Walls forces (Walstra et al., 1999). Casein micelle integrity is maintained by the presence of CCP which constitute approximately 7% of the dry weight of the micelle (Panouillé et al., 2004). According to a popular hypothesis, casein micelles are formed together by small aggregates of caseins called sub-micelles. The average hydrodynamic diameter of the casein micelle is

approximately 200 nm and β-caseins are present in the inner part of the micelle. On the other hand, α_{s1}- and α_{s2}-caseins are distributed across the micelles. κ-casein is predominantly present on the surface of the casein micelle as an outer hairy layer and helps casein micelles stable in the serum phase by electrostatic repulsions due to glycosylated hydrophilic part. Casein micelles are mostly stable at high temperatures (<100°C) because of their disorganized structures. However, they aggregate at an isoelectric point at pH 4.6 due to the reduction in electrostatic forces (Walstra et al., 1999; Dalgleish and Corredig, 2012).

On the other hand, whey proteins are globular and soluble proteins present in the serum phase. Some of the major whey proteins are β-lactoglobulin, α-lactalbumin, bovine serum albumin, and immunoglobulin, which constitute 57, 27, 6, and 10%, respectively. Whey proteins are heat sensitive and denature at temperature > 60°C by unfolding from their tertiary structure. Hydrophobic disulfide bonds are formed between unfolded whey proteins at higher temperatures and consequently leading to aggregation (Creamer et al., 2004).

During processing of dairy beverages, heat treatment results in heat-induced protein interactions between caseins and whey proteins. Heating the milk system above 90°C for 20 min, resulted in denaturation of 80% of the β-lactoglobulin and disulfide bonds with κ-casein was observed (Smits and Brouwershaven, 1980). However, the heat-induced interactions between proteins are influenced by the pH of the milk system. Vasbinder and de Kruif (2003) observed that interaction between denatured whey proteins and casein micelles was prominently observed when heated at a pH<6.6. Whereas, when heated at pH >6.6, denatured whey proteins were found to aggregate themselves in the serum phase with only a limited interaction with casein micelles. These results suggest that the pH of the dairy beverage should be taken into account during the development of dairy beverages.

Heat treatments used during the dairy beverage manufacturing are ultra-high temperature (UHT) which involves heating product to 130-150°C for 1 - 20 s, high temperature-short time (HTST) where products are heated to 105-120°C for 30 s - 2 min, and retort processing which involves heating sealed beverage containers to 110-120°C for 5-20 min (Datta and Deeth, 2001). Heat treatment step is characterized by protein denaturation followed by the structural changes due to interaction among denatured whey proteins and casein micelles. During the heat treatment, beverages develop color from Maillard browning. Although retort sterilization is considered as a severe heat treatment, extensive denaturation of whey proteins modifies the interactions between whey proteins and caseins resulting in extending shelf life during storage (Harwalkar, 1982; Walstra et al., 1999).

It was explained by Datta and Deeth (2001) that these heat-induced structural changes influence the rate at which storage defects occur in the beverages. Sedimentation and age-gelation are two main storage defects that are often encountered in the dairy beverages and are associated with protein-protein and protein-mineral interactions. Sedimentation can be identified as the formation of a clear serum layer on the top and the protein-rich sediment layer at the bottom of the container as a result of heat-induced protein aggregation (Dalgleish, 1992). The author also explained that the network between proteins is not strong enough to form a gel but prolonged storage can lead to gelation. Grygorczyk (2009) explained one of the accepted theories of gel formation in milk-based beverages. Gel formation starts with interactions between β-lactoglobulin and κ-casein through disulfide linkages which are followed by the dissociation of β-κ-complexes from the casein micelle. These free complexes form a network with each other, as well as with other proteins to form a gel.

Effect of Ingredients in the Dairy Beverages

In addition to structural changes in the proteins, the non-protein composition also influences the storage stability of the dairy beverages. Below are some of the most common non-protein components and their properties in the dairy beverages.

Mineral content

Protein functionality and the distribution of the protein in colloidal and serum phase are influenced by minerals in the system. It is an accepted theory that the CCP is an integral part of casein and distribution of calcium and phosphate between colloidal phase and serum phase influences the casein micelle stability (Augustin, 2000). Heat stability is an important functionality that should be considered during the dairy beverage manufacturing. Heat stability is defined as the ability to withstand high processing temperatures without any visible coagulation (Singh, 2004). During the heat treatment step, as the temperature is increased, CCP precipitates as calcium phosphate resulting in decreasing the pH. Precipitation of CCP leads to casein micelle destabilization resulting in aggregate formation (Singh and Fox, 1987). Mineral composition is often manipulated to improve the heat stability of the beverages. By reducing the available calcium, precipitation during heat treatment can be controlled which consequently controls the pH reduction and casein micelle aggregation. Augustin and Clarke (1990) observed both casein micelle stabilization and destabilization when phosphates were added at a constant pH. Authors described that the addition of phosphates reduced the calcium ion activity which had a stabilizing effect on casein micelle. On the other hand, the addition of phosphates also contributed to increase CCP which had a destabilizing effect on casein micelle. In the same study, when $CaCl_2$ was added to at a fixed pH, authors observed a decrease in heat stability due to increased ionic calcium content and CCP leading to destabilizing the casein micelle.

Chelating salts

Heat stability can also be improved by the addition of chelating salts in the formulation of dairy beverages to reduce the available calcium. Addition of chelating salts results in solubilization of the CCP and dissociates casein micelles into sub-micelles (Udabage et al., 2000). Reducing the available calcium by forming a chelating salt and calcium complexes reduced the mineral-protein interactions, consequently dissociating casein micelles and stabilizing them. With chelating salts having different affinities for calcium during chelation, amount of casein dissociation varies depending on the type and concentration of the chelating salt used in the dairy beverage (Kaliappan and Lucey, 2011). Chelating salts used in the formulations of the dairy beverages are sodium hexametaphosphate (SHMP), sodium uridine monophosphate, disodium hydrogen phosphate, trisodium citrate, and sodium phytate. Extensive research was done on investigating the efficient chelating salt to improve the heat stability in the milk systems. Because of the presence of six negative charges, SHMP has high adhesion to calcium and have the ability to cross-link with casein micelles as well to form complexes. Due to this ability of SHMP, available calcium was reduced on the addition of SHMP with increased dissociation of casein micelles (de Kort et al., 2011). A similar observation was made by Kaliappan and Lucey (2011) where chelating salt mixtures containing SHMP were effective in casein micelle dissociation and formation of calcium hexametaphosphate complexes. These findings explain that the concentration of calcium chelating agents should be evaluated. Addition of chelating salt in higher concentrations can lead to chelation of calcium beyond a critical limit resulting in casein micelles destabilization and thereby reduce the heat stability (Tsioulpas et al., 2010; de Kort et al., 2012).

Gums

The primary role of gums in the dairy beverages is to stabilize the proteins in the beverage and delay storage defects like sedimentation. Phillips and Williams (2009) explained that the addition of carboxymethyl cellulose (CMC) to increase the viscosity of the high-protein beverages and to maintain the emulsion stability during storage. Similarly, the application of carrageenan delayed the sedimentation and visual phase separation in UHT- products (Walstra et al., 1999).

These studies discussed illustrated that heat and storage stability of the high-protein dairy beverages are influenced predominantly by protein-protein and protein-mineral interactions. Non-protein additives like chelating salts and gums in the dairy beverages also contribute towards improving the storage stability in the high-protein dairy beverages.

References

Agarwal, S., R.L.W. Beausire, S. Patel, and H. Patel. 2015. Innovative Uses of Milk Protein Concentrates in Product Development. J. Food Sci. 80: A23–A29.

Augustin, M.A. 2000. Mineral salts and their effect on milk functionality. Aust. J. Dairy Technol. 55: 61–64. (Abstr.)

Augustin, M.-A., and P.T. Clarke. 1990. Effects of added salts on the heat stability of recombined concentrated milk. J. Dairy Res. 57:213–226.

Badal Tejedor, M., S. Pazesh, N. Nordgren, M. Schuleit, M.W. Rutland, G. Alderborn, and A. Millqvist-Fureby. 2018. Milling induced amorphisation and recrystallization of α-lactose monohydrate. Int. J. Pharm. 537:140–147.

Bhargava, A., and P. Jelen. 1996. Lactose Solubility and Crystal Growth as Affected by Mineral Impurities. J. Food Sci. 61:180–184.

Cahalane, G., and L.S. Ward. 2012. High-Protein Beverages Comprising Whey Protein. U.S. Classification 426/583; International Classification A23J3/08, A23J1/20; Cooperative Classification A23V2002/00, A23L33/19, A23L33/18; European Classification A23L1/305B, A23L1/305D, assignee. US Pat. No. US20120015092 A1.

Carpin, M., H. Bertelsen, J.K. Bech, R. Jeantet, J. Risbo, and P. Schuck. 2016. Caking of lactose: A critical review. Trends Food Sci. Technol. 53:1–12.

Carpin, M., H. Bertelsen, A. Dalberg, J.K. Bech, J. Risbo, P. Schuck, and R. Jeantet. 2017. How does particle size influence caking in lactose powder? J. Food Eng. 209:61–67.

Chandrapala, J., M.C. Duke, S.R. Gray, B. Zisu, M. Weeks, M. Palmer, and T. Vasiljevic. 2015. Properties of acid whey as a function of pH and temperature. J. Dairy Sci. 98:4352–4363.

Chandrapala, J., R. Wijayasinghe, and T. Vasiljevic. 2016. Lactose crystallization as affected by presence of lactic acid and calcium in model lactose systems. J. Food Eng. 178:181–189.

Chiou, D., T.A.G. Langrish, and R. Braham. 2008. The effect of temperature on the crystallinity of lactose powders produced by spray drying. J. Food Eng. 86:288–293.

Creamer, L.K., A. Bienvenue, H. Nilsson, M. Paulsson, M. van Wanroij, E.K. Lowe, S.G. Anema, M.J. Boland, and R. Jiménez-Flores. 2004. Heat-induced redistribution of disulfide bonds in milk proteins. 1. Bovine beta-lactoglobulin. J. Agric. Food Chem. 52:7660–7668.

Dalgleish, D.G. 1992. Sedimentation of Casein Micelles During the Storage of Ultra-High Temperature Milk Products—a Calculation. J. Dairy Sci. 75:371–379.

Dalgleish, D.G., and M. Corredig. 2012. The Structure of the Casein Micelle of Milk and Its Changes During Processing. Annu. Rev. Food Sci. Technol. 3:449–467.

Darcy, P., and G. Buckton. 1998. Crystallization of Bulk Samples of Partially Amorphous Spray-Dried Lactose. Pharm. Dev. Technol. 3:503–507.

Das, D., H.A. Husni, and T.A.G. Langrish. 2010. The effects of operating conditions on lactose crystallization in a pilot-scale spray dryer. J. Food Eng. 100:551–556.

Datta, N., and H.C. Deeth. 2001. Age Gelation of UHT Milk—A Review. Food Bioprod. Process. 79:197–210.

Drapier-Beche, N., J. Fanni, M. Parmentier, and M. Vilasi. 1997. Evaluation of Lactose Crystalline Forms by Nondestructive Analysis. J. Dairy Sci. 80:457–463.

Evans, J.W., and G.C. Young. 1982. Production of USP quality lactose. U.S. Classification 127/55, 127/58, 127/31; International Classification C13K5/00; Cooperative

Classification C13K5/00; European Classification C13K5/00, assignee. US Pat. No. US4316749 A.

Gänzle, M.G., G. Haase, and P. Jelen. 2008. Lactose: Crystallization, hydrolysis and value-added derivatives. Int. Dairy J. 18:685–694.

Garnier, S., S. Petit, and G. Coquerel. 2002. Influence of supersaturation and structurally related additives on the crystal growth of α-lactose monohydrate. J. Cryst. Growth 234:207–219.

Gernigon, G., F. Baillon, F. Espitalier, C. Le Floch-Fouéré, P. Schuck, and R. Jeantet. 2013. Effects of the addition of various minerals, proteins and salts of organic acids on the principal steps of α-lactose monohydrate crystallisation. Int. Dairy J. 30:88–95.

Gombas, A., P. Szabó-Révész, M. Kata, G. Regdon, and I. Er\Hos. 2002. Quantitative determination of crystallinity of α-lactose monohydrate by DSC. J. Therm. Anal. Calorim. 68:503–510.

Goulart, D.B., and R.W. Hartel. 2017. Lactose crystallization in milk protein concentrate and its effects on rheology. J. Food Eng. 212:97–107.

Grygorczyk, A. 2009. Biophysical studies of milk protein interactions in relation to storage defects in high protein beverages. MS Thesis. McGill Univ., MacDonald, Canada.

Guu, M.Y.K., and R.R. Zall. 1991. Lactose crystallization: effects of minerals and seeding. Process Biochem. 26:167–172.

Haque, M.K., and Y.H. Roos. 2004. Water Plasticization and Crystallization of Lactose in Spray-dried Lactose/Protein Mixtures. J. Food Sci. 69: FEP23–FEP29.

Hartel, R.W. 2013. Advances in Food Crystallization. Annu. Rev. Food Sci. Technol. 4:277–292.

Hourigan, J.A., E.V. Lifran, L.T. Vu, Y. Listiohadi, and R.W. Sleigh. 2013. Lactose: chemistry, processing, and utilization. Pages 21-41 in Advances in dairy ingredients. 1st. ed. John Wiley & Sons, Inc. Hoboken, NJ

Huang, J., G. Kaul, J. Utz, P. Hernandez, V. Wong, D. Bradley, A. Nagi, and D. O'Grady. 2010. A PAT approach to improve process understanding of high shear wet granulation through in-line particle measurement using FBRM C35. J. Pharm. Sci. 99:3205–3212.

Islam, M.I.U., and T.A.G. Langrish. 2010. An investigation into lactose crystallization under high temperature conditions during spray drying. Food Res. Int. 43:46–56.

Kaliappan, S., and J.A. Lucey. 2011. Influence of mixtures of calcium-chelating salts on the physicochemical properties of casein micelles. J. Dairy Sci. 94:4255–4263.

de Kort, E., M. Minor, T. Snoeren, T. van Hooijdonk, and E. van der Linden. 2011. Effect of calcium chelators on physical changes in casein micelles in concentrated micellar casein solutions. Int. Dairy J. 21:907–913.

de Kort, E., M. Minor, T. Snoeren, T. van Hooijdonk, and E. van der Linden. 2012. Effect of calcium chelators on heat coagulation and heat-induced changes of concentrated micellar casein solutions: The role of calcium-ion activity and micellar integrity. Int. Dairy J. 26:112–119.

Lagrange, V., D. Whitsett, and C. Burris. 2015. Global Market for Dairy Proteins. J. Food Sci. 80: A16–A22.

Lallukka, Y., and M.K. Heikonen. 1986. A process for preparing anhydrous lactose. Assignee US Pat. No. EP0196892A2.

Lifran, E.V., R.W. Sleigh, R.L. Johnson, R.J. Steele, J.A. Hourigan, and S.M. Dalziel. 2010. Method for Purification of Lactose. Google Patents.

Lifran, E.V., T.T.L. Vu, R.J. Durham, J.A. Hourigan, and R.W. Sleigh. 2007. Crystallisation kinetics of lactose in the presence of lactose phosphate. Powder Technol. 179:43–54.

Listiohadi, Y., J.A. Hourigan, R.W. Sleigh, and R.J. Steele. 2008. Moisture sorption, compressibility and caking of lactose polymorphs. Int. J. Pharm. 359:123–134.

Listiohadi, Y., J.A. Hourigan, R.W. Sleigh, and R.J. Steele. 2009. Thermal analysis of amorphous lactose and α-lactose monohydrate. Dairy Sci. Technol. 89:43–67.

Listiohadi, Y.D., J.A. Hourigan, R.W. Sleigh, and R.J. Steele. 2005a. Effect of milling on the caking behaviour of lactose. Aust. J. Dairy Technol. 60:214–224.

Listiohadi, Y.D., J.A. Hourigan, R.W. Sleigh, and R.J. Steele. 2005b. Role of amorphous lactose in the caking of [alpha]-lactose monohydrate powders. Aust. J. Dairy Technol. 60:19–32.

Lloyd, R.J., X. Dong Chen, and J.B. Hargreaves. 1996. Glass transition and caking of spray-dried lactose. Int. J. Food Sci. Technol. 31:305–311.

McLeod, J., A.H.J. Paterson, J.R. Jones, and J.E. Bronlund. 2011. Primary nucleation of alpha-lactose monohydrate: The effect of supersaturation and temperature. Int. Dairy J. 21:455–461.

McLeod, J.S., A.H.J. Paterson, J.E. Bronlund, and J.R. Jones. 2016. The effect of agitation on the nucleation of α-lactose monohydrate. Int. Dairy J. 61:114–119.

McSweeney, P., and P.F. Fox eds. 2009. Lactose: Chemistry and Properties. Solid and Liquid States of Lactose. Pages 1- 55 in Advanced Dairy Chemistry. Springer New York, New York, NY.

Mimouni, A., P. Schuck, and S. Bouhallab. 2005. Kinetics of lactose crystallization and crystal size as monitored by refractometry and laser light scattering: effect of proteins. Le Lait 85:253–260.

Mimouni, A., P. Schuck, and S. Bouhallab. 2009. Isothermal batch crystallization of alpha-lactose: A kinetic model combining mutarotation, nucleation and growth steps. Int. Dairy J. 19:129–136.

Modler, H.W., and L.P. Lefkovitch. 1986. Influence of pH, Casein, and Whey Protein Denaturation on the Composition, Crystal Size, and Yield of Lactose from Condensed Whey. J. Dairy Sci. 69:684–697.

Mullin, J.W. 2001. Crystallization. 4th ed. Butterworth-Heinemann, Oxford; Boston.

Nonnemacher, M.L. 2004. Effect of whey concentrate crystallization parameters on lactose crystal forms. MS Thesis Thesis. Oregon State University, Corvallis, OR.

Pandalaneni, K., and J.K. Amamcharla. 2016. Focused beam reflectance measurement as a tool for in situ monitoring of the lactose crystallization process. J. Dairy Sci. 99:5244–5253.

Panouillé, M., T. Nicolai, and D. Durand. 2004. Heat induced aggregation and gelation of casein submicelles. Int. Dairy J. 14:297–303.

Patel, S.R., and Z.V.P. Murthy. 2012. Lactose Recovery Processes from Whey: A Comparative Study Based on Sonocrystallization. Sep. Purif. Rev. 41:251–266.

Paterson, A.H.J. 2017. Lactose processing: From fundamental understanding to industrial application. Int. Dairy J. 67:80–90.

Paterson, A.H.J., G.F. Brooks, J.E. Bronlund, and K.D. Foster. 2005. Development of stickiness in amorphous lactose at constant T−Tg levels. Int. Dairy J. 5:513–519.

Phillips, G.O., and P.A. Williams. 2009. Cellulosics. 2nd Edition. Woodhead Pub; CRC.

Raghavan, S.L., R.I. Ristic, D.B. Sheen, and J.N. Sherwood. 2001. The bulk crystallization of α-lactose monohydrate from aqueous solution. J Pharm Sci. 90:823–832.

Robertson, G.L. 2009. Food Packaging and Shelf Life: A Practical Guide. CRC Press.

Roos, Y. rj., and M. arcu. Karel. 1992. Crystallization of Amorphous Lactose. J. Food Sci. 57:775–777.

Roos, Y.H. 2002. Importance of glass transition and water activity to spray drying and stability of dairy powders. Le Lait 82:475–484.

Saffari, M., and T. Langrish. 2014. Effect of lactic acid in-process crystallization of lactose/protein powders during spray drying. J. Food Eng. 137:88–94.

Saltmarch, M., and T.P. Labuza. 1980. Influence of Relative Humidity on the Physicochemical State of Lactose in Spray-Dried Sweet Whey Powders. J. Food Sci. 45:1231–1236.

Schuck, P. 2002. Spray drying of dairy products: state of the art. Le Lait 82:375–382.

Shakiba, S., S. Mansouri, C. Selomulya, and M.W. Woo. 2018. The role of the intermediate stage of drying on particle in-situ crystallization in spray dryers. Powder Technol. 323:357–366.

Shi, X., and Q. Zhong. 2014. Enhancing lactose crystallization in aqueous solutions by soluble soybean polysaccharide. Food Res. Int. 66:432–437.

Shi, X., and Q. Zhong. 2015. Crystallinity and quality of spray-dried lactose powder improved by soluble soybean polysaccharide. LWT - Food Sci. Technol. 62:89–96.

Singh, H. 2004. Heat stability of milk. Int. J. Dairy Technol. 57:111–119.

Singh, H., and P.F. Fox. 1987. Heat stability of milk: role of β-lactoglobulin in the pH-dependent dissociation of micellar κ-casein. J. Dairy Res. 54:509–521.

Smits, P., and J.H.V. Brouwershaven. 1980. Heat-induced association of β-lactoglobulin and casein micelles. J. Dairy Res. 47:313–325.

Thomas, M., J. Scher, and S. Desobry. 2005. Study of lactose / β -lactoglobulin interactions during storage. Le Lait 85:325–333.

Trasi, N.S., S.X.M. Boerrigter, and S.R. Byrn. 2010. Investigation of the milling-induced thermal behavior of crystalline and amorphous griseofulvin. Pharm. Res. 27:1377–1389.

Tsioulpas, A., M.J. Lewis, and A.S. Grandison. 2007. Effect of Minerals on Casein Micelle Stability of Cows' Milk. J. Dairy Res. 74:167–173.

Udabage, P., I.R. McKinnon, and M.A. Augustin. 2000. Mineral and casein equilibria in milk: effects of added salts and calcium-chelating agents. J. Dairy Res. 67:361–370.

Ulrich, J., and C. Strege. 2002. Some aspects of the importance of metastable zone width and nucleation in industrial crystallizers. J. Cryst. Growth 237–239, Part 3:2130–2135.

Vasbinder, A.J., and C.G. de Kruif. 2003. Casein–whey protein interactions in heated milk: the influence of pH. Int. Dairy J. 13:669–677.

Walstra, P., T.J. Geurts, A. Noomen, A. Jellema, and M.A.J.S. van Boekel. 1999. Dairy technology: principles of milk properties and processes. Marcel Dekker Inc. NY.

Wang, S., T. Langrish, and M. Leszczynski. 2010. The Effect of Casein as a Spray-Drying Additive on the Sorption and Crystallization Behavior of Lactose. Dry. Technol. 28:422–429.

Wijayasinghe, R., T. Vasiljevic, and J. Chandrapala. 2015. Water-lactose behavior as a function of concentration and presence of lactic acid in lactose model systems. J. Dairy Sci. 98:8505–8514.

Wong, S.Y., R.K. Bund, R.K. Connelly, and R.W. Hartel. 2011. Determination of the dynamic metastable limit for α-lactose monohydrate crystallization. Int. Dairy J. 21:839–847.

Wong, S.Y., R.K. Bund, R.K. Connelly, and R.W. Hartel. 2012. Designing a lactose crystallization process based on dynamic metastable limit. J. Food Eng. 111:642–654.

Wong, S.Y., and R.W. Hartel. 2014. Crystallization in Lactose Refining—A Review. J. Food Sci. 79: R257–R272.

Xun, A., T. Truong, and B. Bhandari. 2016. Effect of Carbonation of Supersaturated Lactose Solution on Crystallisation Behaviour of Alpha-Lactose Monohydrate. Food Biophys.

Yazdanpanah, N., and T.A. Langrish. 2011. Fast crystallization of lactose and milk powder in fluidized bed dryer/crystallizer. Dairy Sci. Technol. 91:323–340.

Yucel, U., and J.N. Coupland. 2011. Ultrasonic Characterization of Lactose Crystallization in Gelatin Gels. J. Food Sci. 76: E48–E54.

Zadow, J.G. 1984. Lactose: Properties and Uses. J. Dairy Sci. 67:2654–2679.

Zisu, B., M. Sciberras, V. Jayasena, M. Weeks, M. Palmer, and T.D. Dincer. 2014. Sonocrystallisation of lactose in concentrated whey. Ultrason. Sonochem. 21:2117–2121.

Chapter 3 - Focused Beam Reflectance Measurement (FBRM) as a Tool for *in situ* monitoring of Lactose Crystallization Process[†]

Abstract

Lactose accounts for about 75 and 85% of the solids in whey and deproteinized whey, respectively. Production of lactose is usually carried out by a process called crystallization. Several factors including rate of cooling, presence of impurities, and mixing speed influence the crystal size characteristics. In order to optimize the lactose crystallization process parameters to maximize the lactose yield, it is important to monitor the crystallization process. However, efficient *in-situ* tools to implement at concentrations relevant to the dairy industry are lacking. The objective of the present work was to use focused beam reflectance measurement (FBRM) system for *in situ* monitoring of lactose crystallization at supersaturated concentrations (w/w) 50%, 55%, and 60% at 20ºC and 30ºC. The FBRM data were compared with Brix readings collected using a refractometer during isothermal crystallization. Chord length distributions obtained from FBRM in the ranges of <50 µm (fine crystals) and 50–300 µm (coarse crystals) were recorded and evaluated in relation to the extent of crystallization and rate constants deduced from the refractometer measurements. Extent of crystallization and rate constants were increased, with increasing supersaturation concentration and temperature. The measured fine crystal counts from FBRM increased at higher supersaturated concentration and temperature during isothermal crystallization. On the other hand, coarse counts were observed to increase with decreasing supersaturated concentration and temperature. Square weighted chord length distribution obtained from FBRM showed that as concentration increased, there was a decrease in chord lengths at 20ºC and similar observations were made from microscopic images. The

[†]Pandalaneni, K. and J.K. Amamcharla. 2016. Focused Beam Reflectance Measurement (FBRM) as a Tool for in situ Monitoring of Lactose Crystallization Process. J. Dairy Sci. 99: 5244–5253. (Editor's Choice)

robustness of FBRM in understanding isothermal lactose crystallization at various concentrations and temperatures was successfully assessed in the study.

Introduction

Lactose is the most abundant carbohydrate present in milk. It is found in concentrations of 4.4 – 5.2% and is one of the major constituents in infant formulations, dried milk, and whey products. It is also used by the pharmaceutical industry as a filler in tableting and for dry powder inhalers (Lifran et al., 2010). Commercial production of lactose involves concentration of whey or whey permeate or milk permeate by evaporation under vacuum followed by batch crystallization (Zisu et al., 2014). As the temperature of supersaturated mixture is gradually reduced, the degree of supersaturation increases, leading to crystallization of lactose as tomahawk-shaped crystals. Crystal size distribution and total lactose yield are the two most important measures in monitoring the industrial crystallization of lactose. Crystallization of lactose is influenced by presence of denatured protein, pH (Modler and Lefkovitch, 1986), degree of supersaturation, presence of impurities (Garnier et al., 2002), agitator speed (Dhumal et al., 2008), and rate of cooling (McLeod et al., 2011; Wong et al., 2012).

Lactose crystallization is a technological operation which starts with nucleation, followed by crystal growth. Nucleation occurs as primary and secondary, where primary nucleation spontaneously occurs within the cooled supersaturated solution. On the other hand, secondary nucleation occurs from crystals already present in the solution (McLeod et al., 2011). The nucleation, crystal size, and lactose yield depend on the crystallizing conditions such as crystallizer design, degree of supersaturation and rate of cooling, which emphasizes the need to understand the effect of these parameters on crystallization (Raghavan et al., 2001).

The first step in controlling lactose crystallization is to use cost effective monitoring technologies to follow the process. Several reports have been published on the use of various technologies to monitor lactose crystallization. Amamcharla et al. (2012) utilized a commercial

ultrasound spectrometer in pulse-echo mode for *in situ* monitoring of isothermal lactose crystallization process and observed an increase in ultrasound attenuation during nucleation and crystal growth. Also, Yucel and Coupland (2011) used ultrasound spectroscopy to study crystallization of lactose in gelatin gels by comparing ultrasound data to turbidity measurements. Mimouni et al. (2005) monitored kinetics of lactose crystallization by using laser light scattering technique and compared with traditional refractometry. Kadam et al. (2010) studied solute concentration measurements by comparing attenuated total reflectance Fourier transform infrared (ATR-FTIR), and Fourier transform near infrared (FT-NIR) spectroscopy for batch crystallization of lactose and concluded that ATR-FTIR was more reliable because of less fouling of the probe. Arellano et al. (2004) compared refractive index measurements to digital video polarized light microscopy technique to monitor lactose crystallization. Digital imaging was found to be a useful technique to identify induction time but not sensitive enough to monitor crystal growth due to overlapping of crystals. Most of these techniques were carried out in lab scale setup and require extensive scale up experiments to implement at an industrial scale crystallization process. The dairy industry is still heavily dependent on traditional refractometer technique to follow lactose crystallization process. However, crystal size characteristics cannot be obtained from refractometer data.

Concentration is a time dependent phenomenon in lactose crystallization and monitoring crystallization step with non-invasive and online methods is essential in current manufacturing practices to meet the required CSD. Focused Beam Reflectance Measurement (FBRM) is a versatile technique for *in situ* monitoring of chord length distribution (CLD) and rate of change in crystal size. Figure 3.1 shows the working principle of FBRM and it is extensively reviewed by Huang et al. (2010). Ndoye and Alvarez (2015) successfully used FBRM technique to find

significant difference in recrystallization rates in stored ice creams with different stabilizers. Fang et al. (2010) utilized FBRM to characterize dissolution behavior of milk protein concentrates at different water temperatures. More importantly, Kail et al. (2008, 2009) presented a method to analyze dynamic processes such as crystallization and granulation using FBRM. They validated the developed models using α-lactose monohydrate as a case study. However, the lactose concentration used the study was around 38.7% (w/w), which was lower than the concentrations generally used in crystallization of lactose in the dairy industry. Generally, lactose crystallization process employed in the dairy industry involves concentration of whey in the range of 55 – 65% total solids (Bund and Pandit, 2007). Keeping this in view, the objective of the present study was to evaluate the effectiveness of FBRM at lactose concentrations relevant to the industrial scale crystallization of lactose.

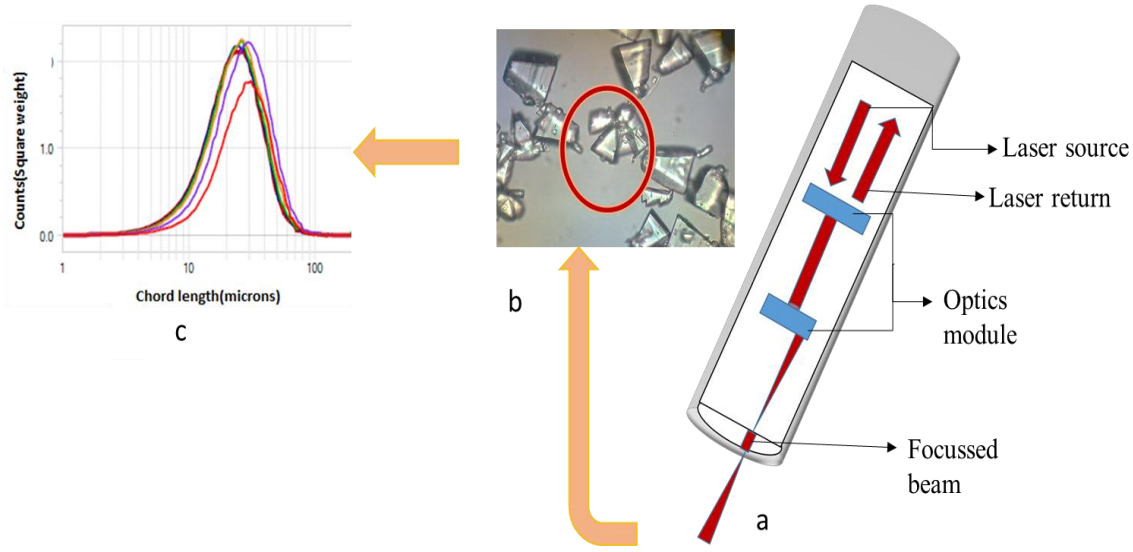

Figure 3.1.Working principle of FBRM (a) FBRM probe design, (b) detection of particles by probe using a laser moving at a constant velocity, and (c) chord length distribution graph obtained from crystal distribution.

Materials and methods

Experimental Design

For the purpose of generating wide differences in the lactose crystallization process, a 2 × 3 factorial design was used in the study, with temperature and lactose concentration as independent variables. Three levels of lactose concentrations (50%, 55%, and 60% w/w) and two levels of temperatures (20ºC and 30ºC) were incorporated into the experimental design. Isothermal lactose crystallization experiments were conducted in duplicate as per the experimental design.

Preparation of Supersaturated Lactose Solutions

Lactose solutions of desired concentration were prepared using 99.7% pure α-lactose (Davisco Foods International, Inc., Le Seuer, MN). Desired concentrations of lactose (w/w) were obtained by dissolving 250, 275, and 300 g of lactose in 250, 225, and 200 g of deionized water to prepare 50% (100 g of lactose/100 g of water), 55% (122.2 g of lactose/100 g of water), and 60% (150 g of lactose/100 g of water) supersaturated solutions, respectively. Supersaturated lactose solutions were prepared as described by Mimouni et al. (2005) with few modifications. The lactose and water mixture was heated on a hot plate to 87±3°C under continuous stirring to dissolve all the crystals. A lid was placed on the beaker to avoid moisture loss during heating. After ensuring the dissolution of all the crystals, the supersaturated lactose solution was cooled to the desired experimental temperature (20ºC or 30ºC) in a temperature-controlled water bath without agitation for 90 min. Supersaturated lactose solution devoid of any lactose crystals was then carefully transferred to a clean 600 mL batch crystallizer to carry out the isothermal crystallization of lactose.

Isothermal Crystallization of Lactose

Isothermal lactose crystallization was carried out in a purpose-built batch crystallizer (Figure 3.2) specially designed for this work. The FBRM probe (Particle Track E25, Mettler-Toledo AutoChem, Inc., Columbus, OH) was kept immersed in a batch crystallizer throughout the experiment for *in situ* monitoring of the crystallization process. The batch crystallizer was placed in a temperature-controlled water bath (Isotemp 202, Fisher Scientific, Waltham, MA) that was maintained at 20ºC or 30ºC. An overhead stirrer with a four-bladed propeller (Caframo, Georgian Bluffs, Ontario, Canada) was placed in the batch crystallizer to facilitate stirring. As shown in Figure 3.2, the propeller was maintained at 2.5 cm above the bottom of the beaker containing the supersaturated solution. The FBRM probe was mounted at a height of 5 cm from the bottom of the crystallizer. As suggested by Barrett and Glennon (1999), the FBRM probe was mounted at an angle of 30 ± 5° to the vertical axis to improve the efficiency of the probe.

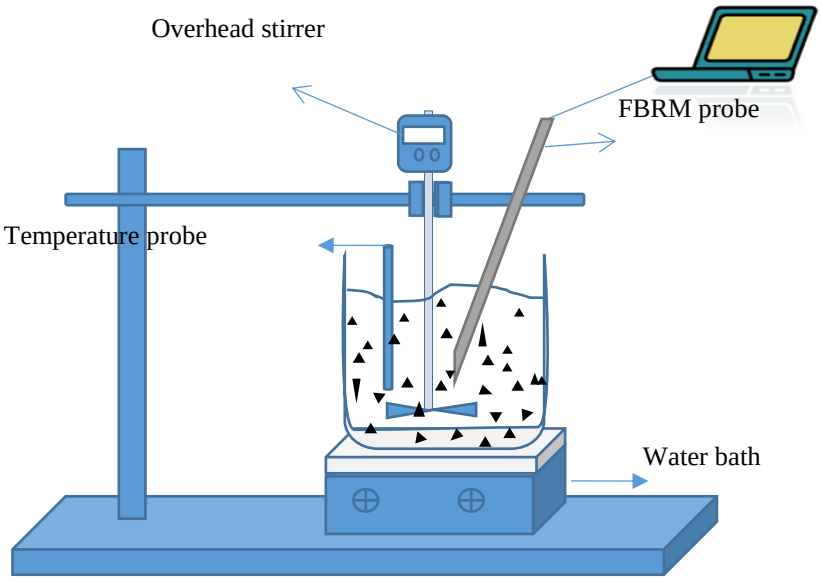

Figure 3.2. Experimental setup used for monitoring isothermal lactose crystallization using focused beam reflectance measurement (FBRM).

Determination of Extent of Crystallization and Rate Constant

During crystallization, approximately 1 mL of the crystal suspension was collected from the crystallizer using a dropper to measure the refractive index of the suspension. The refractive index, expressed in terms of °Brix, of lactose solution was measured using a digital refractometer (Reichert Technologies, Depew, NY). A previously generated calibration curve was used to convert the °Brix readings to the actual lactose concentration in solution. The refractometer readings were subsequently used to calculate the mass of crystals and extent of crystallization at any time *t* during isothermal crystallization process. Mass of crystals at any time *t* was calculated from the initial lactose concentration C(0) and lactose concentration C(*t*) at time *t* using Equation 1. Water was assumed to represent 5% of the total mass of lactose crystal (Mimouni et al., 2005).

$$M_{Crystal}(t) = \mathrm{M}_{\mathrm{H_2O}}(0).\frac{C(0) - \mathrm{C}(t)}{95 - 0.05.C(t)} \quad (1)$$

where $\mathrm{M}_{Crystal}(t)$ is mass of crystals at a given time *t*, $\mathrm{M}_{\mathrm{H_2O}}(0)$ represents 5% of the total mass of lactose crystal, C(0) is initial concentration, and C(*t*) is concentration at time *t.*

The extent of crystallization at time *t* was calculated using Equation 2 from the mass of crystals at time *t* obtained from Equation 1 and saturation concentration of lactose at temperature 20°C and 30°C (Mimouni et al., 2005).

$$\%Y(t) = \frac{M_{Crystal}(t)}{M_{Crystal}(t \to \infty)} X100 \quad (2)$$

where Y(*t*) is the percent extent of crystallization at time *t*, $\mathrm{M}_{Crystal}(t)$ is the mass of crystals obtained from Equation 1, and $\mathrm{M}_{Crystal}(t \to \infty)$ is the mass of crystals at lactose solubility at experimental temperature.

From the concentration difference ΔC, plotted against time *t*, it was observed that the curve shows best the first-order decay fit. The rate constant can be deduced from plotting Equation 3, the first-order decay equation, where $[A_0]$ is the initial concentration of lactose solution before crystallization and *k* is the rate constant. [A] is the concentration difference ΔC, at a given time *t*, where $\Delta C = C(t) - C(t \to \infty)$, with $C(t \to \infty)$ as lactose solubility value at the temperature of interest.

$$ln\left(\frac{[A]}{[A_0]}\right) = -kt \quad (3)$$

Crystallization Monitoring using FBRM

Before the start of each experiment, the FBRM probe was cleaned thoroughly with distilled water to avoid any interference from unwanted particles, as suggested by the manufacturer. The data from the FBRM probe were acquired using a computer through iC FBRM software (version 4.3.391, Mettler-Toledo, AutoChem Inc., MD). For simplicity, crystals sizes of lactose were acquired at every 3 min for the first 60 min and thereafter every 30 min for 570 min from pool of collected FBRM data. Three categories of crystal chord length ranges, <50 µm, 50–300 µm, and 300–2,000 µm, were monitored and were designated as fine, coarse, and large crystals, respectively.

Chord Length Distribution (CLD) of Lactose crystals. CLD were obtained from FBRM over different time periods of interest. Square weight function was applied to CLD to emphasize on a particular crystal size range. For example, having no weight emphasizes on the fine crystals, whereas square weight emphasizes on coarse crystals (Huang et al., 2010). Square weight distribution was applied to CLD in our study to compensate for fine chord lengths of crystals that outweigh coarse chord lengths during crystallization. Distributions at 120 min and

600 min were taken representing initial crystallization and towards the end, respectively. Auto scaled percent crystals was taken on Y-axis and chord lengths (µm) was taken on X-axis for easy comparison of chord length shift of crystals irrespective of crystal counts.

Microscopic Examination of Lactose Crystals

Crystal suspension of approximately 0.2 mL was collected at 120 and 600 min on a clean glass slide and immediately an image was acquired with 10X magnification. Microscopic images of lactose crystals were obtained using a compound microscope (American Optical, Depew, NY) connected to a digital camera (Ken-a-vision, Kansas City, MO).

Results and Discussion

Extent of Crystallization and Rate Constant from Refractometry

The average initial lactose concentrations were found to be 49.05%, 54.36%, 59.09% (w/w) for intended 50, 55, and 60% (w/w) lactose solutions. The extent of crystallization was determined during the isothermal crystallization of lactose for 50%, 55%, and 60% concentrations at 20ºC and 30ºC as plotted in Figure 3.3. From Figure 3.3, it was observed that the extent of crystallization was higher at 30ºC than at 20ºC for all concentrations of lactose. A maximum extent of crystallization was observed for 60% supersaturated solution followed by 55% and 50% lactose concentrations at 30ºC. The extent of crystallization at 20ºC also followed a similar trend. At 30°C, the time required to reach 90% extent of crystallization was found to be 300, 360, and 420 min for 60%, 55%, and 50% solutions, respectively. On the other hand, the extent of crystallization at 20ºC did not reach 90% even after 630 min for all the lactose concentrations studied. The extent of crystallization at 30ºC was calculated to be 93%, 95%, and 96% for 50%, 55%, and 60% solutions, respectively. The extent of crystallization at 20ºC was calculated to be 80%, 83%, and 86% for 50%, 55%, and 60% solutions, respectively. At a given

temperature, the extent of crystallization increased as the supersaturation concentration increased, which is the driving force for the crystallization.

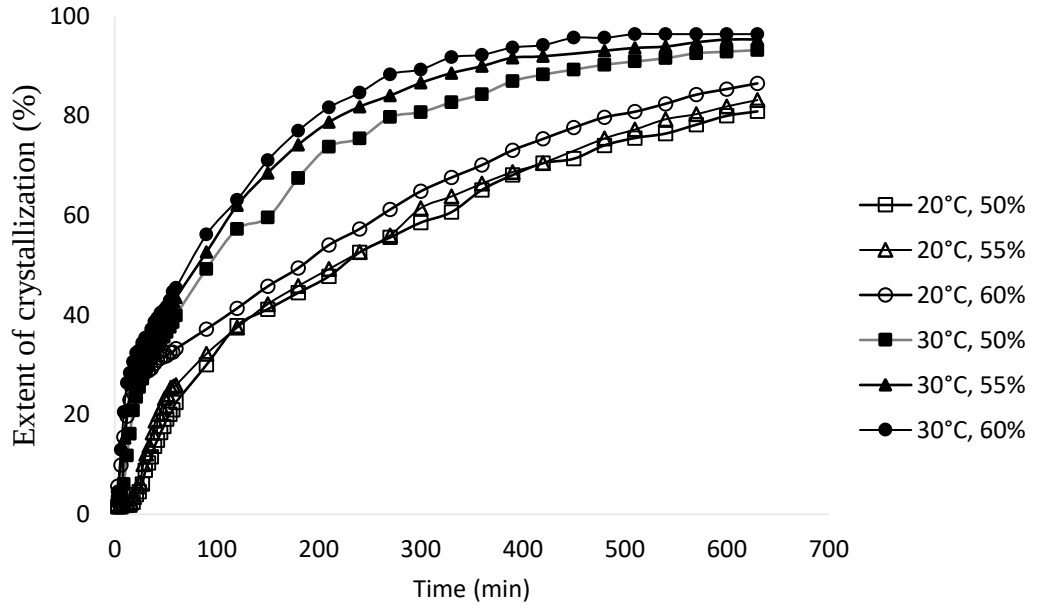

Figure 3.3. Extent of crystallization obtained during isothermal crystallization of lactose for lactose concentrations 50%, 55% and 60% (w/w) at 20ºC and 30ºC.

Rate constants for the isothermal crystallization of lactose at 20°C and 30°C were calculated using Equation 3. For the calculation purposes, it was assumed that the rate of mutarotation proceeded at a higher rate than crystallization of α-lactose. This assumption was based on the fact that mutarotation is not a limiting factor during unseeded crystallization of lactose (Raghavan et al., 2001). Calculated average overall rate constants at 20°C were 2.7×10^{-3}, 2.8×10^{-3}, and 2.8×10^{-3} min^{-1} for 50%, 55%, and 60% concentrations, respectively. On the other hand, the average overall rate constants of crystallization at 30°C were 4.3×10^{-3}, 4.9×10^{-3}, and 5.4×10^{-3} min^{-1} for 50%, 55%, and 60% concentrations, respectively. Previous studies on lactose crystallization kinetics available in literature were studied at much lower lactose concentrations

than supersaturation concentrations studied in this research. Mimouni et al. (2005) obtained a mean rate constant of 8.1×10^{-3} min^{-1} during isothermal crystallization of lactose at 30°C from an initial lactose concentration of 41.1% (w/w). Arellano et al. (2004) studied isothermal crystallization of lactose at concentrations 27.1%, 30.8%, and 37.5% (w/w) at 20°C and observed growth rates of 2.1, 4.1, and 8.8 µm/h, respectively. Similarly, average growth rates of 7.1, 9.8, and 25.8 µm/h were obtained for lactose concentrations 33.3%, 37.5%, and 44.6% (w/w) at 30°C. From the results presented by Arellano et al. (2004), it can be seen that there was an increase in single lactose crystal growth rates as the temperature increased from 20°C to 30°C as observed by digital video microscopy technique. In addition, Jelen and Coulter (1973) reported that an increase in crystallization temperature promoted nucleation rates and mass transfer rates of lactose during isothermal crystallization of lactose. The present study also found a higher crystallization rate constant at 30°C than at 20°C at a given supersaturation concentration.

Overall, refractometry was found to be a useful technique to calculate degree of crystallization at any point during lactose crystallization. In addition, the technique can be implemented easily at any commercial batch crystallizer regardless of crystallizer design. However, refractometer readings do not provide information on crystal size distribution. Refractometry is a traditional technique but insensitive to more specific information like crystal counts and CLD.

Evaluation of FBRM Data

Fine crystals in this study represented primary and secondary nucleation in terms of crystal chord lengths less than 50µm formed during isothermal lactose crystallization. FBRM's ability to measure the particles as small as 0.5µm makes it a sensitive tool to monitor fine crystal counts. Counts of fine and coarse crystals (50-300 µm) obtained from the FBRM during the

isothermal crystallization of lactose at experimental temperatures and concentrations against time were plotted in Figures 3.4 and 3.5, respectively. Fine crystal counts obtained for 50%, 55%, and 60% concentrations at 30°C can be explained in three phases: rapid, gradual, and plateaued phase. These were divided based on the increase in fine crystal counts at 30°C over 630 min of crystallization. Rapid increase in the fine crystal counts for first 100 min of lactose crystallization at 30°C was observed at all concentrations and can be attributed to primary nucleation. A gradual increase in the number of fine crystal counts in the later phase was influenced by secondary nucleation and disintegration of lactose crystals. The gradual increase in fine crystal counts can be explained by a reduction in primary nucleation and disintegration of coarse crystals. The disintegration of lactose crystals was caused by attrition and collisions of lactose crystals with other crystals, with the crystallizer walls, and also with propeller used for mixing. It was also noted that the possibility of secondary nucleation increased as counts of lactose crystals increased, which could be observed from fine crystal counts at 30ºC (Figure 3.4). Breakage of coarse crystals at concentrations 55% and 60% can be observed from Figure 3.5 as fluctuations in the coarse crystal counts staring around 300 min. The coarse crystal counts obtained at 55% and 60% were eventually lower than the coarse crystal counts observed for 50% lactose concentration. Third phase was plateaued phase, where increase in fine crystal counts plateaued after 300 min. A similar observation was made from extent of crystallization of all three concentrations at 30°C (Figure 3.3). Minimum increase in the number of fine crystals after 300 min when compared to phase 1 and phase 2 can be explained as decrease in the driving force of crystallization. Fine crystals formed in the earlier two phases restricted the further growth of fine crystals.

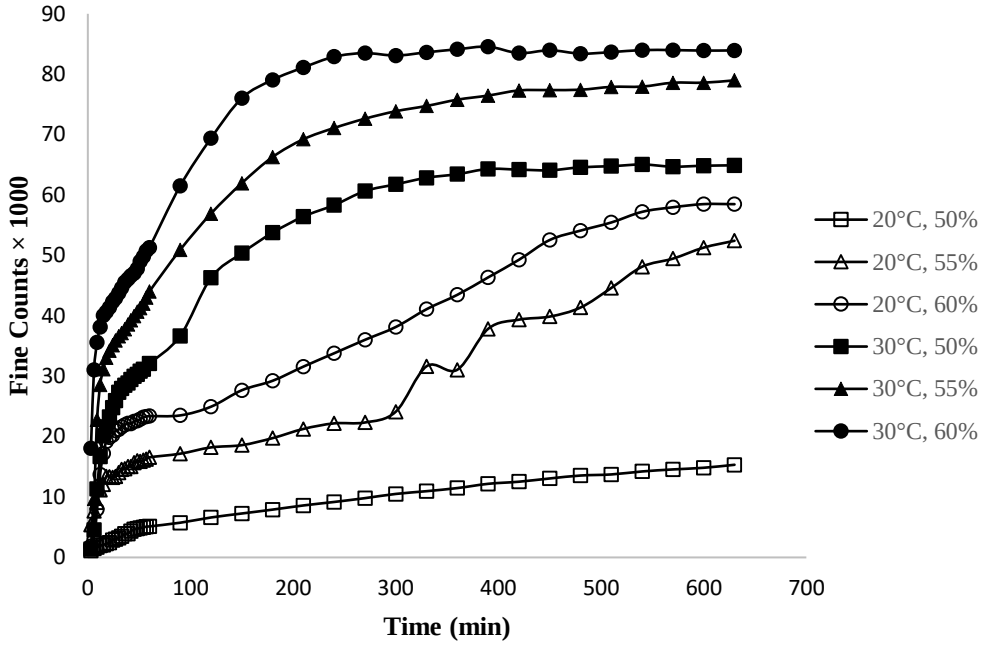

Figure 3.4. Counts of fine crystals (<50μm) for 50%, 55%, and 60% concentrations and at 20ºC and 30ºC obtained from focused beam reflectance measurement (FBRM).

Fine and coarse crystal counts at 20°C for supersaturation concentrations, 50%, 55%, and 60% were also plotted in Figures 3.4 and 3.5, respectively. Unlike the fine crystal counts at 30°C, there was a continuous increase in fine crystal counts at 20°C because supersaturation driving force was effective in causing continuous nucleation. However, supersaturation concentration had the similar effect on fine counts at both 20°C and 30°C: the higher the concentration, the greater the final fine crystal counts. There was a continuous increase of coarse crystal counts for 50% concentration at 20°C, whereas, 55% and 60% concentrations exhibited slow increase in coarse crystal counts, which later decreased after 300 min. Continuous increase in coarse crystal counts for 50% at 20°C was due to having a fewer number of crystals in the total volume of solution, where growth of lactose crystals was not restricted. In the case of 55% and 60% concentrations at 20°C, fluctuations in the coarse crystal counts after 300 min indicate the breakage of lactose crystals. The observations indicated that breakage of lactose crystals was

mainly due to crystal to crystal collision rather than breakage caused by speed of impeller. Impeller speed (400 rpm) maintained at this experiment was sufficient to keep crystals in suspension without causing any breakage. As the fine crystal counts increased, crystal density in the suspension increased, causing collisions between lactose crystals and leading to breakage.

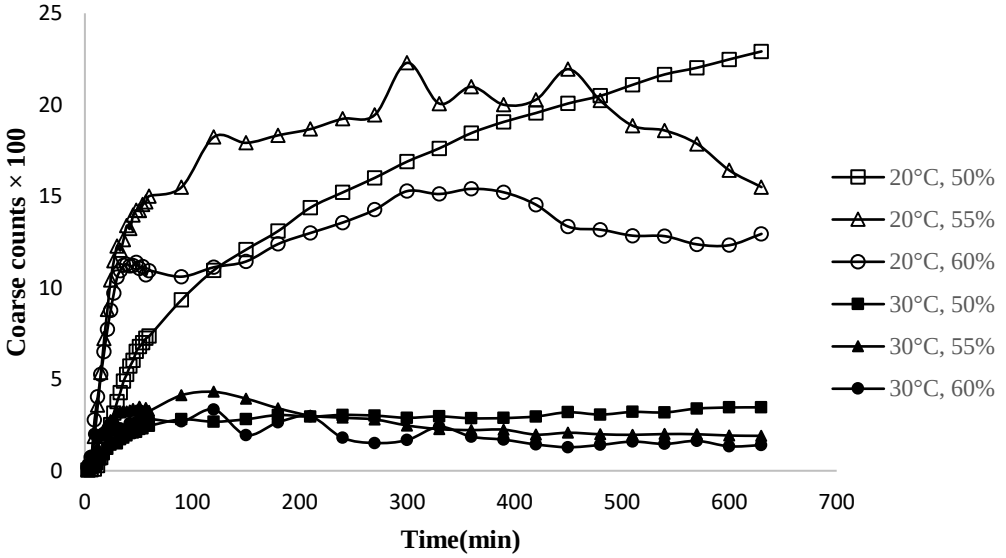

Figure 3.5. Count of coarse crystals (50–300µm) for 50%, 55%, and 60% concentrations and at 20ºC and 30ºC obtained from focused beam reflectance measurement (FBRM).

Number of coarse crystals increased as the temperature and supersaturation decreased. In other words, isothermal crystallization at 20°C for supersaturation concentration 50% w/w favored producing coarse crystals bigger than 50 µm; whereas, fine crystal counts increased as temperature and supersaturation increased. These results suggest that growth of crystals was favorable at low temperatures in isothermal lactose crystallization; whereas high temperature favored nucleation and formation of finer crystals. These results were also in agreement with rate constant observations, where nucleation was high at 30°C, implying formation of fine crystals was favored at high temperatures in isothermal lactose crystallization. In the present study, an

increase in fine crystal counts as observed by FBEM represented nucleation of lactose. On the other hand, an increase in coarse crystal counts represented lactose crystal growth. As the lactose supersaturation and crystallization temperature increased, nucleation increased as the driving force of lactose crystallization increased.

FBRM is capable of following particle chord lengths up to 2000 µm. However, counts of larger particles (300–1,200 µm) were found to be negligible and were excluded from further analysis.

Evaluation of Chord Length Distribution

Square weighted chord length distributions obtained from FBRM at 120 and 600 min of each treatment are shown in Figure 3.6. In order to compare the crystal growth at various supersaturations of lactose, CLD was obtained at 120 and 600 min during isothermal lactose crystallization. It is important to know that the CLD can be obtained at any instant during lactose crystallization using iC FBRM software. However, data at 120 and 600 min were shown to simplify the data. CLD of square weighted crystals for 50% concentration at both 20°C and 30°C were plotted in Figure 3.6a. It was evident from CLD that there was no change in the distribution at 120 and 600 min at both 20°C and 30°C. However, there was a difference in CLD as temperature changed. The mean chord lengths of lactose crystals for 50% concentration at 20°C and 30°C were 57.99 µm (120min), 58.10 µm (600 min), and 27.25 µm (120 min), 27.36 µm (600 min), respectively. Mean chord lengths of crystals at 20°C were higher than at 30°C, which implies that growth of crystals was higher at lower temperatures. Similar observations were also deduced from Figures 3.4 and 3.5. CLD of 55% and 60% lactose concentrations at 20°C and 30°C was plotted in Figures 3.6b and 3.6c, respectively. For 55% concentration at 600 min mean chord lengths at 20°C and 30°C were 41.06 µm and 24.66 µm, respectively. At 60%

concentration at 600 min, mean chord lengths at 20°C and 30°C were 39.12 µm and 23.31 µm, respectively. At 55% and 60% concentrations the CLD shifted towards lower mean chord lengths at 600 min at both the temperatures. As concentration increased, the difference in the mean chord length at 600 min between 20°C and 30°C decreased.

Though there was an increase in coarse crystal counts for all the three concentrations at 20°C, a shift in mean chord length to a smaller chord length was explained by an increase in fine crystals counts during isothermal crystallization of lactose. In addition, breakage of the crystals due to crystal-crystal and crystal-crystallizer wall collisions could lead to a decrease in coarse crystals and an increase in fine crystals. As the lactose crystal density (number crystals per unit volume) increased, the probability of FBRM detecting the particle width rather than particle length was high (Leyssens et al., 2011) and consequently produced a smaller mean chord length.

CLD data from FBRM was supported by microscopic images of lactose crystals taken at 120 and 600 min at experimental temperatures and three supersaturation concentrations are shown in Figure 3.7. As observed from Figures 3.7-A1 and A2 at 120 and 600 min respectively, for 50% supersaturated concentration at 20°C, there was no visible breakage of crystals. Similarly, from Figure 3.7- B1 and B2 representing 120 and 600 min observed for 50% concentration at 30°C, no visible breakage was observed. Broken crystals were more prominently visible at 55% and 60% concentrations at 600 min at both 20°C (Figure 3.7-C2-55%, E2-60%) and 30°C (Figure 3.7-D2-55%, F2-60%). Broken crystals were observed more at 30°C crystallization temperature for 55% and 60% concentrations. These microscopic images support the FBRM data observations made about breakage of crystals contributing to increase in fine crystal counts.

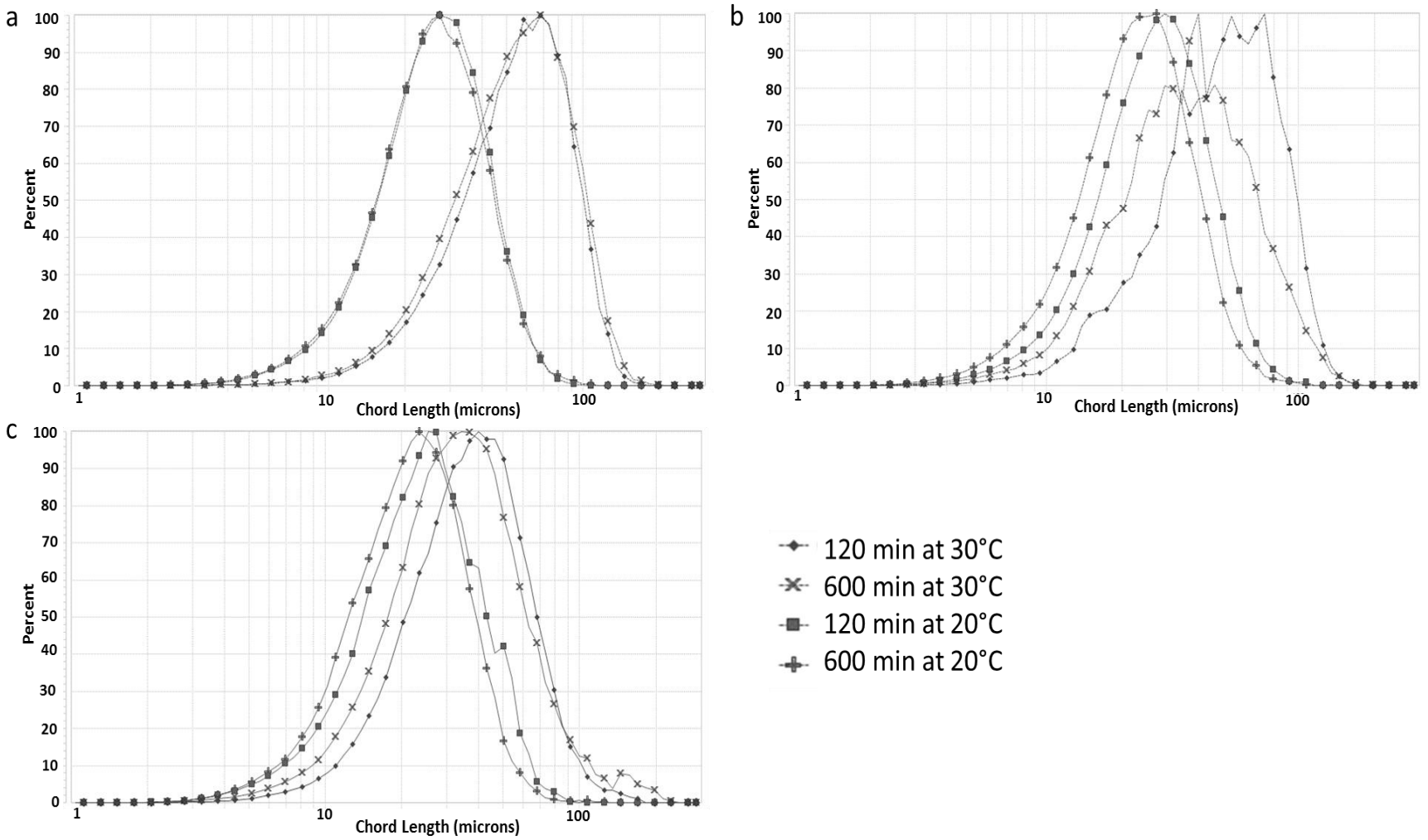

Figure 3.6. Square weighted, auto scaled percent chord length distributions of crystals obtained from focused beam reflectance measurement data at 120 and 600 min. (a) 20ºC, 50%; 30ºC, 50%; (b) 20ºC, 55%; 30ºC, 55%; (c) 20ºC, 60%; 30ºC, 60%.

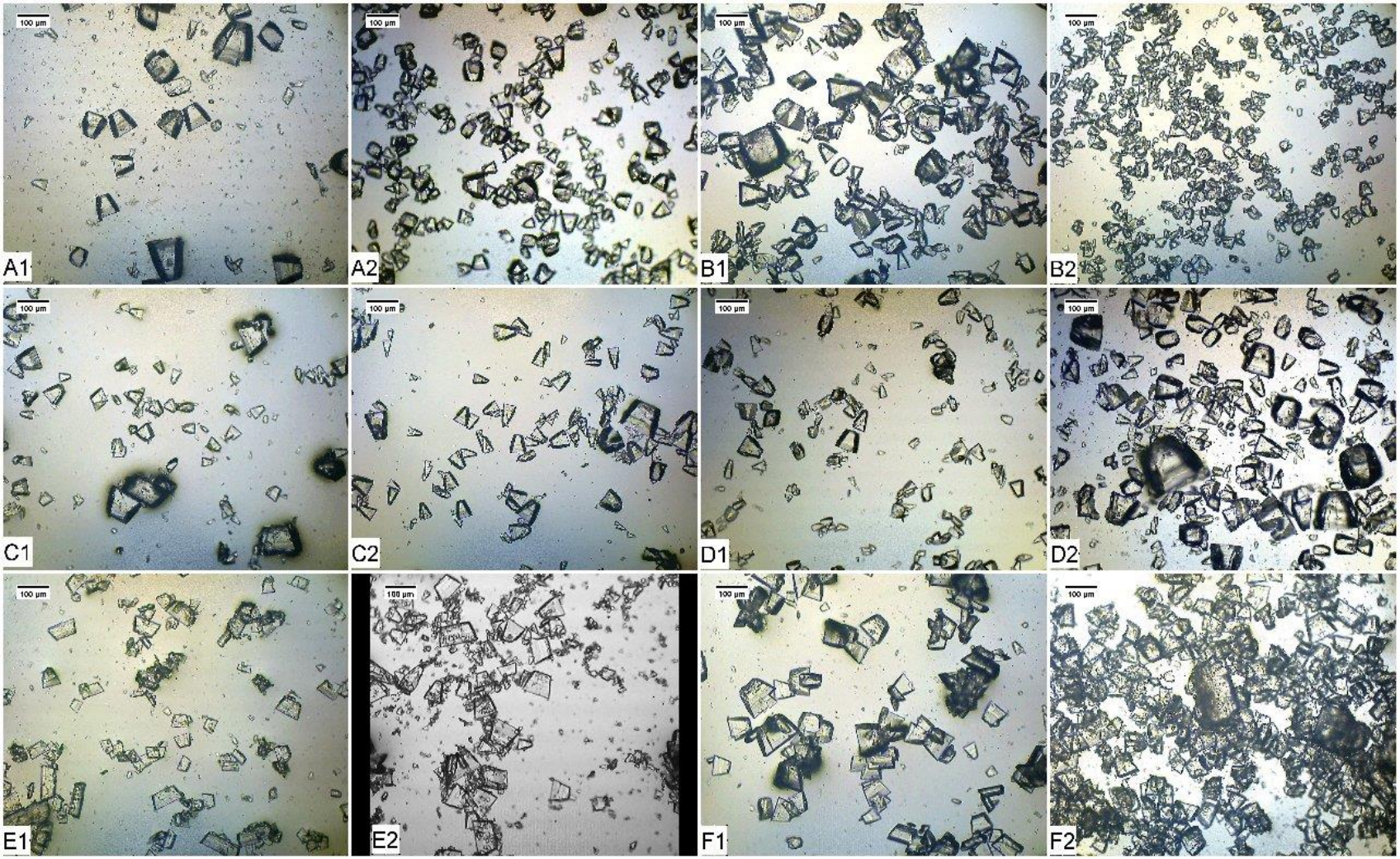

Figure 3.7. Microscopic images of lactose crystals, A. 20ºC, 50%; B. 30ºC, 50%; C. 20ºC, 55%; D. 30ºC, 55%; E. 20ºC, 60%; F. 30ºC, 60% at 1. 120 min and 2. 600 min during isothermal crystallization of lactose.

Conclusions

The efficiency of FBRM in studying the lactose crystallization with respect to operation parameters such as concentration and temperature was evaluated. FBRM is a powerful tool, and it can be used to follow nucleation, crystal growth, attrition, and breakage from chord length distribution and crystal size data. Lactose crystallization monitoring using FBRM in this study explained that as the lactose concentration and crystallization temperature increased, there was an increase in possible breakage of crystals along with increase in fine crystal counts. On the other hand, there was increased crystal growth at 20°C rather than at 30°C. Extent of crystallization obtained from refractive index data supported the FBRM observations. The results of this study imply that changes in concentration and temperature were well understood in terms of crystal size and counts over time using FBRM. The data obtained from FBRM supplements and strengthens refractive index data. Ideally, coarse crystals were preferred to fine crystals to avoid loss of lactose crystal yield during post crystallization process. Overall, FBRM technique shows potential to be a part of process analytical technology to monitor and control the lactose crystallization process.

Acknowledgements

We thank Midwest Dairy Foods Research Center (St. Paul, MN) for their financial support. Kansas State Research and Extension contribution number 16-088-J.

References

Agrawal, S.G., J. Mcleod, A.H.J. Paterson, J.R. Jones. 2011. Secondary nucleation studies on lactose: A mechanistic understanding. Pages 677-687 in Chemeca 2011- Engineering a better world, Sydney, Australia.

Amamcharla, J. K., L. E. Metzger, and R. Tweedie. 2012. Application of ultrasound spectroscopy to monitor lactose crystallization. J. Dairy Sci. 94(Suppl. 1): 653.

Arellano, M.P., J.M. Aguilera, and P. Bouchon. 2004. Development of a digital video-microscopy technique to study lactose crystallisation kinetics in situ. Carbohydr. Res. 339:2721–2730.

Barrett, P., and B. Glennon. 1999. In-line FBRM monitoring of particle size in dilute agitated suspensions. Part. Part. Syst. Charact. 16:207–211.

Bund, R.K., and A.B. Pandit. 2007. Sonocrystallization: Effect on lactose recovery and crystal habit. Ultrason Sonochem.14:143–152.

Dhumal, R.S., S.V. Biradar, A.R. Paradkar, and P. York. 2008. Ultrasound assisted engineering of lactose crystals. Pharm Res. 25:2835–2844.

Fang, Y., C. Selomulya, and X.D. Chen. 2010. Characterization of milk protein concentrate solubility using focused beam reflectance measurement. Dairy Sci Technol. 90:253–270.

Garnier, S., S. Petit, and G. Coquerel. 2002. Influence of supersaturation and structurally related additives on the crystal growth of α-lactose monohydrate. J Cryst Growth. 234:207–219.

Huang, J., G. Kaul, J. Utz, P. Hernandez, V. Wong, D. Bradley, A. Nagi, and D. O'Grady. 2010. A PAT approach to improve process understanding of high shear wet granulation through in-line particle measurement using FBRM C35. J. Pharm. Sci. 99:3205–3212.

Jelen, P., and S. T Coulter. 1973. Effects of supersaturation and temperature on the growth of lactose crystals. J Food Sci. 38:1182–1185.

Kadam, S.S., E. van der Windt, P.J. Daudey, and H.J.M. Kramer. 2010. A comparative study of ATR-FTIR and FT-NIR spectroscopy for in-situ concentration monitoring during batch cooling crystallization processes. Cryst Growth Des. 10:2629–2640.

Kail, N., W. Marquardt, and H. Briesen. 2009. Process analysis by means of focused beam reflectance measurements. Ind and Eng Chem Res. 48:2936–2946.

Kail, N., H. Briesen, and W. Marquardt. 2008. Analysis of FBRM measurements by means of a 3D optical model. Powder Technol. 185:211–222.

Lifran, E.V., R.W. Sleigh, R.L. Johnson, R.J. Steele, J.A. Hourigan, and S.M. Dalziel. 2010. Enhancing purity of lactose via demineralization and alcohol precipitation; infant dairy product; veterinary medicine. Dairy Australia Limited, assignee. US Pat. No. 7754876 B2.

Leyssens, T., C. Baudry, and M.L. Escudero Hernandez. 2011. Optimization of a crystallization by online FBRM analysis of needle-shaped crystals. Org. Process Res. Dev. 15:413–426.

McLeod, J., A.H.J. Paterson, J.R. Jones, and J.E. Bronlund. 2011. Primary nucleation of alpha-lactose monohydrate: The effect of supersaturation and temperature. Int Dairy J. 21:455–461.

Mimouni, A., P. Schuck, and S. Bouhallab. 2005. Kinetics of lactose crystallization and crystal size as monitored by refractometry and laser light scattering: effect of proteins. Le Lait. 85:253–260.

Modler, H.W., and L.P. Lefkovitch. 1986. Influence of pH, casein, and whey protein denaturation on the composition, crystal size, and yield of lactose from condensed whey. J Dairy Sci. 69:684–697.

Ndoye, F.T., and G. Alvarez. 2015. Characterization of ice recrystallization in ice cream during storage using the focused beam reflectance measurement. J Food Eng. 148:24–34.

Raghavan, S.L., R.I. Ristic, D.B. Sheen, and J.N. Sherwood. 2001. The bulk crystallization of α-lactose monohydrate from aqueous solution. J Pharm Sci 90:823–832.

Wong, S.Y., R.K. Bund, R.K. Connelly, and R.W. Hartel. 2012. Designing a lactose crystallization process based on dynamic metastable limit. J Food Eng. 111:642–654.

Yucel, U., and J.N. Coupland. 2011. Ultrasonic characterization of lactose crystallization in gelatin gels. J Food Sci. 76:E48–E54.

Zisu, B., M. Sciberras, V. Jayasena, M. Weeks, M. Palmer, and T.D. Dincer. 2014. Sonocrystallisation of lactose in concentrated whey. Ultrason Sonochem. 21:2117–2121.

Chapter 4 - Crystallization of Lactose from Milk and Whey Permeates at Different Cooling Rates

Abstract

The cooling rate of supersaturated lactose solution is one of the important parameters determining the yield and size distribution of lactose crystals. Influence of increasing cooling rate on lactose crystallization and quality of lactose crystals was evaluated in concentrated solutions prepared from deproteinized whey (DPW) powder and milk permeate powder (MPP). Concentrated permeates (DPW and MPP) with 60% (w/w) total solids were prepared by reconstituting permeate powders in water at 80°C for 2 h for lactose dissolution. Three cooling rates, 0.04°C/ min (slow), 0.06°C/ min (medium), and 0.08°C/ min (fast) were studied in duplicate. A common rapid cooling step (80°C to 60°C at 0.5°C/ min) followed by slow, medium, and fast cooling rates were applied as per the experimental design from 60°C to 20°C. After crystallization, the crystal slurry was centrifuged, washed with cold water, and dried. The dried lactose crystals were weighed to calculate the lactose yield. Final mean particle chord lengths were measured at the end of crystallization using focused beam reflectance measurement for slow, medium, and fast cooling rates and observed to be not significantly different ($P>0.05$) for DPW (27-33 µm) and MPP (31-34 µm) concentrates. Similarly, the lactose yield for slow, medium and fast cooling rates in the DPW and MPP concentrates were in the range of 71-73 % and 76-81%, respectively, and found no significant difference between the 3 cooling rates. Qualitative analysis of dried lactose crystals exhibited no noticeable differences in the crystal purity with increasing cooling rate. This study evaluated the possibility of reducing the crystallization times by 8 h compared to current industrial practice without compromising the crystal yield and quality.

Introduction

The growing demand for high-protein dairy ingredients led to fractionation of sweet whey and skim milk into a protein-rich fraction and protein-depleted fraction often referred to as permeate. Milk permeate powder (MPP) and deproteinized whey (DPW) are the permeate fractions obtained during manufacturing of milk protein concentrate (MPC) and whey protein concentrates (WPC), respectively using ultrafiltration and subsequent spray drying. Lactose is one of the major constituents in DPW and MPP along with a small fraction of soluble minerals and proteins. DPW is composed of 76-85% lactose, 11-16% of proteins and minerals, whereas, MPP is composed of higher lactose content of 78-88%, with 11-16% of proteins and minerals (US Dairy Export Council, 2015).

Lactose is used as an ingredient in infant formulations, food products, and pharmaceutical industry and it is manufactured using crystallization process from whey and milk permeates. The aim of crystallization is to recover lactose in the most stable and non-hygroscopic α-lactose monohydrate form and consequently prevent the storage defects like agglomeration and caking (Carpin et al., 2017). A typical lactose production at an industrial scale involves: concentration of permeate to 60-65 % total solids, followed by a gradual cooling, decantation, washing, and drying (Wong and Hartel, 2014). For an economical industrial production of lactose, maximum crystal yield is preferred. Lactose yield is reduced due to loss of smaller crystals during decantation and washing processes and it is suggested to produce bigger lactose crystals during crystallization to maximize the yield (Pandalaneni and Amamcharla, 2016).

Quality and yield of lactose is dependent on factors like presence of impurities (Modler and Lefkovitch, 1986; Lifran et al., 2007; Chandrapala et al., 2016), agitation, cooling rate during crystallization, crystallizer design (Wong et al., 2012), and degree of supersaturation

(McLeod et al., 2011). Crystallization is considered the most important step in lactose recovery that includes approximately 6 h to fill the crystallization tanks and 14-18 h of crystallization process accounting for a total of 20-24 h process (Wong et al., 2012). As the supersaturated solution is gradually cooled, lactose solubility decreases and increasing the supersaturation drive. The supersaturation driving force is required for the formation of lactose crystals (McLeod et al., 2011). When supersaturated lactose solution is rapidly cooled, nucleation is dominant and risk of obtaining lactose crystals with smaller particle size is high. On the other hand, when cooled slowly, lactose crystal nucleation and growth occur simultaneously, resulting in bigger lactose crystals (McLeod, 2007).

During crystallization, if nucleation is spontaneously induced by supersaturated lactose, then it is referred to as homogeneous nucleation. On the other hand, if nucleation is induced by a foreign substance, it is called the heterogeneous nucleation. Heterogeneous nucleation is also dependent on the solubility of impurities present in the solution (Mullin, 2001). During crystallization, along with lactose, impurities also settle on the lactose crystal lattice (Lifran et al., 2007). Impurities settled over the lactose crystals are removed during crystal washing step, but impurities settled in the crystal lattice can affect the quality of lactose crystals. Hence, understanding the effect of cooling rate on the lactose crystallization, in presence of impurities is critical.

Because there is a lack of information on the lactose crystallization in whey permeate and milk permeate at concentrations used in industrial practice, this study was focused on characterizing the lactose crystallization and quality of lactose crystals at different cooling rates in concentrated permeates. Influence of cooling rate and naturally present impurities in the concentrated permeates on lactose crystallization and quality was evaluated in this study.

Materials and Methods

Experimental Design

The effect of cooling rate during lactose crystallization in concentrated DPW and MPP solutions was studied at 3 levels: slow (0.04°C/min), medium (0.06°C/min), and fast (0.08°C/min). All the experiments were conducted randomly and in duplicates. One of the 3 cooling rates, slow, medium, and fast was applied during cooling from 60°C to 20°C, accounting for the total crystallization period of 1040, 706, and 540 min, respectively.

Preparation of Supersaturated Lactose Solution from Permeates

DPW powder with 78.3% (db) lactose and MPP with 86.6% (db) lactose were acquired from Davisco Foods International, Inc., (Le Seuer, MN) and Idaho Milk Products (Jerome, ID), respectively. Concentrated DPW solution of 900 g with 60% (w/w) total solids was prepared by gradually reconstituting 540 g of DPW into 360 g of deionized water at 80°C for 2 hours under constant stirring. Complete dissolution of lactose was confirmed by microscopic examination. Concentrated MPP solution with 60% total solids was also prepared following the same procedure as described for concentrated DPW. Fully solubilized permeate solution was then transferred into a crystallizer maintained at 80 °C and one of the 3 cooling rates was used to crystallize the lactose in permeate system. No lactose seeds were added during the crystallization in this study.

Experimental Setup and Lactose Crystallization

Lactose crystallization was carried out in a custom built double-jacketed crystallizer attached to a programmable water bath (Polystat Standard, Cole-Parmer, Court Vernon Hills, IL) as shown in Figure 4.1. A custom-made four-blade anchor propeller was attached to an overhead stirrer (Caframo, Georgian Bluffs, Ontario, Canada) to facilitate the agitation. From preliminary

experiments (data not reported), agitation speed of 140 rpm was selected to keep the crystals in suspension with minimal secondary nucleation due to breakage of crystals. A temperature probe connected to a data logger (HOBO, Bourne, MA) was used to acquire the crystallizer temperature every 10 s. The crystallizer was covered with a lid to avoid any water loss. Three cooling rates were studied with a same initial flash cooling from 80°C to 60°C at 0.5°C/ min. For in-situ monitoring of lactose crystallization, focused beam reflectance measurement (**FBRM**) (Particle Track E25, Mettler-Toledo AutoChem, Inc., Columbus, OH) was installed in the crystallizer at 30 ± 5° angle as described by Pandalaneni and Amamcharla (2016).

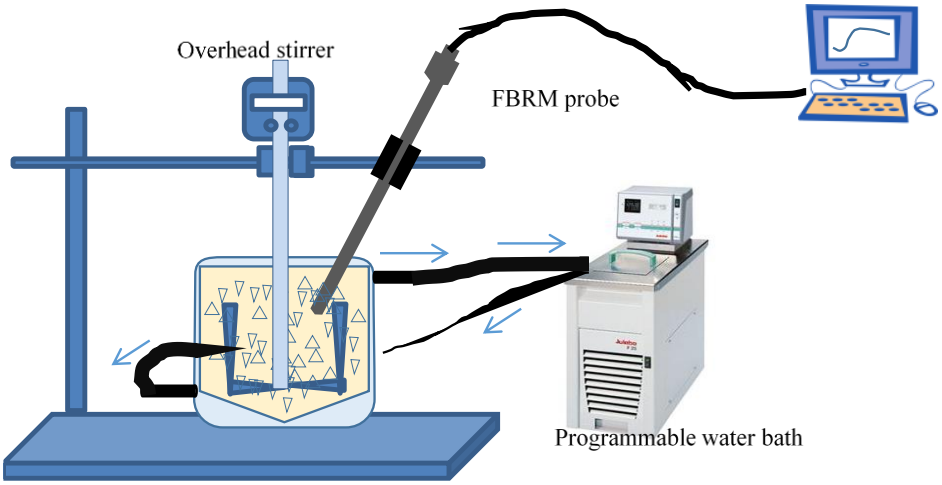

Figure 4.1. Experimental Setup used in the study for controlled cooling of lactose solutions.

Monitoring of Lactose Crystallization using FBRM. FBRM was used an in-situ monitoring tool during lactose crystallization in concentrated permeates. Cleaning of FBRM probe window and data acquisition was done following manufacturer's instructions. During crystallization, FBRM data was acquired for every 3°C temperature drop from the pool of collected data. Particle chord lengths obtained from FBRM were categorized into <50 µm and

50-150 µm and were referred to as fine and large particle counts, respectively. Particle chord length distribution (**PCLD**) was obtained at the end of lactose crystallization as described as Pandalaneni and Amamcharla (2016).

Determination of Lactose Concentration

A representative sample (1 mL) was withdrawn from the crystallizer at the beginning of crystallization (80°C) and at 60°C. Subsequently, a representative sample was also collected from the crystallizer at every 5°C temperature drop between 60°C to 20°C. The sample was diluted with 4 mL of chilled water (5°C) and centrifuged at 3000 × g for 3 min. The supernatant (~1 mL) was further diluted with 7 mL of water to determine the lactose concentration using HPLC (Agilent, Palo Alto, CA). Considering the dilution factor, lactose concentration in the diluted sample was determined using the method described by Amamcharla and Metzger (2011) with some modifications. Lactose was separated using a 300 × 7.80 mm ion exclusion column (ROA-Organic acid, Phenomenex, Rezex, Phenomenex Inc., CA) maintained at 50°C using filtered distilled water as a mobile phase at a flow rate of 0.6 mL/min. Lactose concentration was measured using refractive index detector (1047A, Agilent, Palo Alto, CA) maintained at 50°C.

Degree of Crystallization. Lactose concentrations obtained from HPLC were used to calculate the mass of crystals and extent of crystallization during the lactose crystallization following the same method as Pandalaneni and Amamcharla (2016).

Lactose Crystal Morphology. A sample volume of 1 mL was collected at every 5°C interval to determine crystal morphology. Sample was gently spread over a microscopic glass slide and images were acquired using a camera (Ken-a-vision, Kansas City, MO) attached to a compound microscope (American Optical, Depew, NY) at 10X magnification. The visual comparison was done to evaluate the influence of different cooling rates on the crystal growth

and morphology. The glass slide was equilibrated to the crystallizer temperature to avoid rapid nucleation on the glass surface.

Crystal Yield (%)

At the end of crystallization, crystal slurry was transferred into 250 mL centrifuge tubes and centrifuged (Beckman, J2-21, Indianapolis, IN) at 9820 × g at 10°C for 10 min. After centrifugation, mother liquor was separated from crystals and 200 g of wash water at 5°C was added into the centrifuge tubes. Crystal slurry was thoroughly mixed and again centrifuged at 9820 × g for 5 min. This washing process was repeated 3 times to obtain washed lactose crystals. Washed lactose crystals were dried in a force draft oven (Isotemp Oven, Fisher Scientific, Pittsburgh, PA) at 60°C for 14 h. Dried lactose crystals weight was recorded and percentage yield of lactose was calculated using the Equation 1 (Chandrapala et al., 2016).

$$Lactose\ crystal\ yield\ (\%) = \frac{0.95 \times Mass\ of\ dried\ crystals\ obtained}{Maximum\ theoritical\ crystal\ yield} \times 100 \qquad [1]$$

Compositional Analysis

Total solids percentage was determined using oven drying method (AOAC International, 2016; method 990.20). Total nitrogen was determined following IDF Standard 185 (IDF, 2002) by the combustion method for Nitrogen/Protein determination. Ash content was determined after ignition of sample at 550 °C (AOAC International, 2002; method 954.46). Trace minerals in dried lactose crystals were determined in the filtrate obtained by acid digestion (6 N HCl) of ash. Filtrate was analyzed for Ca, K, P, Na, and Mg at wavelengths 220, 766, 820, 589, and 383 nm, respectively with Inductive-coupled Plasma (ICP) Spectrophotometry (720-ES, Varian Australia Pvt. Ltd, Mulgrave, Australia) (Chandrapala et al., 2015).

Characterization of Dried Lactose Crystals

Dried lactose crystals were characterized for crystal purity using a series of qualitative analysis including microscopic analysis, thermal analysis, and Fourier Transform Infrared Spectroscopy (**FTIR**).

Crystal Purity. Impurities embedded in the lactose crystals were qualitatively analyzed using a method adapted from Butler (1998) with few modifications. Approximately 4 mg of dried lactose crystals were suspended in 3 drops of refractive index solution on a microscopic slide and observed under an compound microscope. The refractive index solution with the same refractive index as lactose crystals (1.55) was custom ordered from Cargille Labs, NJ. Due to the same refractive index, lactose crystals appear translucent and any other impurities on the lactose crystals appear black spots in the microscopic images.

Differential Scanning Calorimetry (DSC). Thermal analysis of dried lactose crystals was conducted using a DSC model Q2000 (TA Instruments, New Castle, DE). Approximately 5 mg of the sample was weighed and sealed in hermetic aluminum pans and heated from temperatures 30 to 180 °C at the rate of 10 °C/min (Shi and Zhong, 2014).

Fourier Transform Infrared Spectroscopy (FTIR). FTIR spectra of dried lactose crystals were obtained in the 400 to 4000 cm^{-1} at a resolution of 4 cm^{-1} using spectrometer (Cary 630, Agilent, Santa Clara, CA) with Micro Lab PC software. Absorbance mode was used for the analysis after subtracting the background spectra. Each spectrum was an average of 32 scans and all measurements were done in duplicate (Chandrapala et al., 2016). FTIR spectra of pure lactose (99.8% purity) obtained from Hilmar Ingredient (Turlock, CA), DPW and MPP powders were also acquired and compared with the dried lactose crystals recovered from the respective sources.

Statistical Analysis

Statistical analysis was performed using SAS software (v 9.1). One-way ANOVA and Tukey's test were conducted to compare the significant differences in parameters measured between cooling rates and were declared significant if $P \leq 0.05$.

Results and Discussion

Anomers of lactose, α-lactose and β-lactose, exist in equilibrium in lactose solutions. When a supersaturated lactose solution is gradually cooled during crystallization, α-lactose diffuses into the solid phase due to its low solubility compared to β-lactose and supersaturation driving force. As a result, the equilibrium between α and β forms of lactose in solution is disturbed, resulting in mutarotation of β-lactose to α-lactose. This sequence of transformation of α-lactose to α-lactose monohydrate followed by mutarotation of β-lactose to α-lactose occurs until there is an equilibrium established (Gänzle et al., 2008). However, α-lactose does not readily form nuclei at supersaturated lactose concentrations as it needs an external force like agitation or addition of lactose seed crystals to initiate nucleation (McLeod et al., 2011). The time required for a supersaturated solution to form nuclei of detectable size is called induction time (Mullin 2001). The nucleation phenomenon during the induction time was explained by Mullin (2001) in 3 stages: relaxation time (time required to form clusters of nuclei from the imposed supersaturation), followed by nucleation time (time required to form a stable nucleus), and growth time (time required to grow to a detectable size). During lactose crystallization, desupersaturation of lactose continues to occur during nucleation followed by crystal growth until the lactose concentration reaches the equilibrium at the end of crystallization process.

Effect of Cooling Rate on Desupersaturation of Lactose

This section summarizes the effect of slow, medium, and fast cooling rates on the rate at which desupersaturation progressed in concentrated permeates.

Table 4.1. Mean ± standard deviation of total solids, protein, and ash from 60% deproteinized whey (DPW) and milk permeate powder (MPP) concentrates used for crystallization of lactose at different cooling rates.

		Total solids (%)	Lactose (%)	Protein (%)	Ash (%)
DPW	0.04 °C/min	57.55±0.25^{a}	47.28±0.10^{a}	3.53±0.02^{a}	5.43±0.09^{a}
	0.06 °C/min	57.23±0.15^{a}	48.26±0.65^{a}	3.50±0.02^{a}	5.35±0.09^{a}
	0.08 °C/min	58.06±1.10^{a}	48.55±0.42^{a}	3.56±0.03^{a}	5.30±0.13^{a}
MPP	0.04 °C/min	58.25±1.01^{A}	51.71±0.43^{A}	2.22±0.32^{A}	4.80±0.12^{A}
	0.06 °C/min	57.93±0.04^{A}	51.77±0.53^{A}	2.30±0.31^{A}	4.79±0.08^{A}
	0.08 °C/min	57.24±0.10^{A}	52.07±0.21^{A}	2.35±0.37^{A}	4.66±0.00^{A}

Values with the same superscript are not significantly different (P>0.05); n=2
Values are compared within DPW and MPP concentrates, and within a column
a, b, c superscripts were used to compare values from lactose crystallization experiments in DPW concentrate
A, B, C superscripts were used to compare values from lactose crystallization experiments in MPP concentrate

DPW Concentrate. The initial mean concentration of lactose in 60% DPW concentrates were in the range of 47.28-48.55% as shown in Table 4.1. Desupersaturation curve of lactose during crystallization in DPW exhibited a similar trend as observed in the literature (Mullin, 2001; Goulart and Hartel, 2017) with an initial induction period, followed by a rapid decrease in the lactose concentration, and reached a steady decrease towards the end of crystallization as shown in Figure 4.2A. During the initial common cooling phase from 80 to 60°C, lactose concentration decreased from an average concentration of 47.26% to 44.8% across the 3 cooling rates studied. The induction period was followed by a rapid desupersaturation of lactose from 60

to 50°C with an average decrease in lactose concentration from 43.8% to 26.42% for the 3 cooling rates studied. The time taken for slow, medium, and fast cooling rates to reach the same extent of desupersaturation (from 43.8% to 26.42%) was 227, 148, and 106 min, respectively. This implies that irrespective of the cooling rate used for lactose crystallization, the extent of desupersaturation was similar in DPW concentrates. A slow but steady decrease in lactose supersaturation was observed from 50 to 20°C because of the reduced supersaturation driving force as the lactose concentration approached a phase equilibrium (Goulart and Hartel, 2017). The decrease in lactose concentration observed was from 26.42% at 50 °C to an average of 22.50% at 20 °C for the 3 cooling rates studied. The degree of crystallization at the end of the crystallization in DPW permeates using 3 cooling rates studied was not significantly different ($P>0.05$) as shown in Table 4.2. It was evident from the Figure 4.2A and degree of crystallization (Table 4.2) that desupersaturation of lactose was not influenced by the cooling rates during lactose crystallization in DPW concentrate.

MPP Concentrate. The initial mean concentration of lactose in 60% MPP concentrate has in the range of 51.71-52.07% as shown in Table 4.1. The desupersaturation curve of lactose during crystallization in MPP concentrates (Figure 4.2B) also exhibited a similar behavior as desupersaturation curve of DPW concentrates (Figure 4.2A). Desupersaturation curve of MPP concentrates also exhibited an induction period, rapid decrease in lactose concentration, followed by a slow and steady decrease toward the end of crystallization. As the cooling progressed from 80 to 60°C during lactose crystallization, the average drop in lactose concentration during 3 cooling rate studies was observed from 51.13% to 48.87%. As the cooling rates started from 60 to 20°C, a rapid decrease in the lactose concentration was observed from 60 to 40°C. The average decrease in the lactose concentration was from 48.87% to 25.8% across all the cooling

rates. It is noteworthy to mention that time accounted for slow, medium, and fast cooling rates to reach the same extent of desupersaturation (48.87% to 25.8%) was 507, 298, and 228 min, respectively. The desupersaturation curve exhibited a slow and steady decrease towards the end of crystallization from 40 to 20°C because of the decrease in the supersaturation drive as the phase equilibrium is reached. Thus, the average decease in lactose concentration observed was from 25.8% to 21.99%. The degree of crystallization obtained at the end of the crystallization as shown in Table 4.2 was not significantly different between 3 cooling studies studied. The overall observation made from Figure 4.2B and the degree of crystallization (Table 4.2) was that the desupersaturation was not influenced by the slow, medium, and fast cooling rates during lactose crystallization.

When desupersaturation curves of DPW and MPP concentrates were compared (Figures 4.2A and 4.2B), a noteworthy difference in decrease in lactose concentration was observed during 60 to 50°C cooling, irrespective of cooling rates. A rapid decrease in lactose concentration from 43.8% to 26.42% was observed in DPW concentrates, whereas, a decrease from 48.87% to 34.69% was observed in MPP concentrates. This rapid desupersaturation in DPW concentrates can be attributed to the presence of higher percentage of proteins and minerals when compared to MPP concentrates as shown in Table 4.1. Presence of proteins contributed to increase the nucleation in supersaturated lactose solutions due to their hydrophilic properties, consequently increasing the rate of lactose crystallization (Mimouni et al., 2005). Along with proteins, minerals also contributed to improve the lactose crystal growth rate during lactose crystallization (Bhargava and Jelen, 1996). When degree of crystallization was compared (Table 4.2), it was evident that 3 cooling rate studies of MPP concentrates has higher degree of crystallization than of DPW concentrates. This can be attributed to the higher initial lactose

concentration in MPP concentrates which increased the supersaturation drive and thereby increasing the degree of crystallization.

Table 4.2. Mean ± standard deviation of degree of crystallization, final mean particle chord length (PCL), and the lactose crystal yield at the end of lactose crystallization from deproteinized whey (DPW) and milk permeate powder (MPP) concentrates at different cooling rates.

Values with the same superscript are not significantly different (P>0.05); n=2

		Total crystallization time (min)	Degree of Crystallization (%)	Final mean PCL (µm)	Lactose Yield (%)
DPW	0.04 °C/min	1008	82.0±0.80 [a]	33.2±2.43 [a]	73.7±0.28 [a]
	0.06 °C/min	691	81.4±1.55 [a]	30.3±5.13 [a]	71.4±3.75 [a]
	0.08 °C/min	521	83.9±1.99 [a]	27.1±3.04 [a]	72.7±1.13 [a]
MPP	0.04 °C/min	1010	98.4±0.44 [A]	32.1±0.12 [A]	79.7±2.44 [A]
	0.06 °C/min	684	98.6±0.35 [A]	31.9±5.73 [A]	81.4±4.10 [A]
	0.08 °C/min	529	96.3±0.09 [A]	34.6±0.59 [A]	76.8±0.24 [A]

Values are compared within DPW and MPP concentrate and within a column
a, b, c superscripts were used to compare values from lactose crystallization experiments in DPW concentrate
A, B, C superscripts were used to compare values from lactose crystallization experiments in MPP concentrate

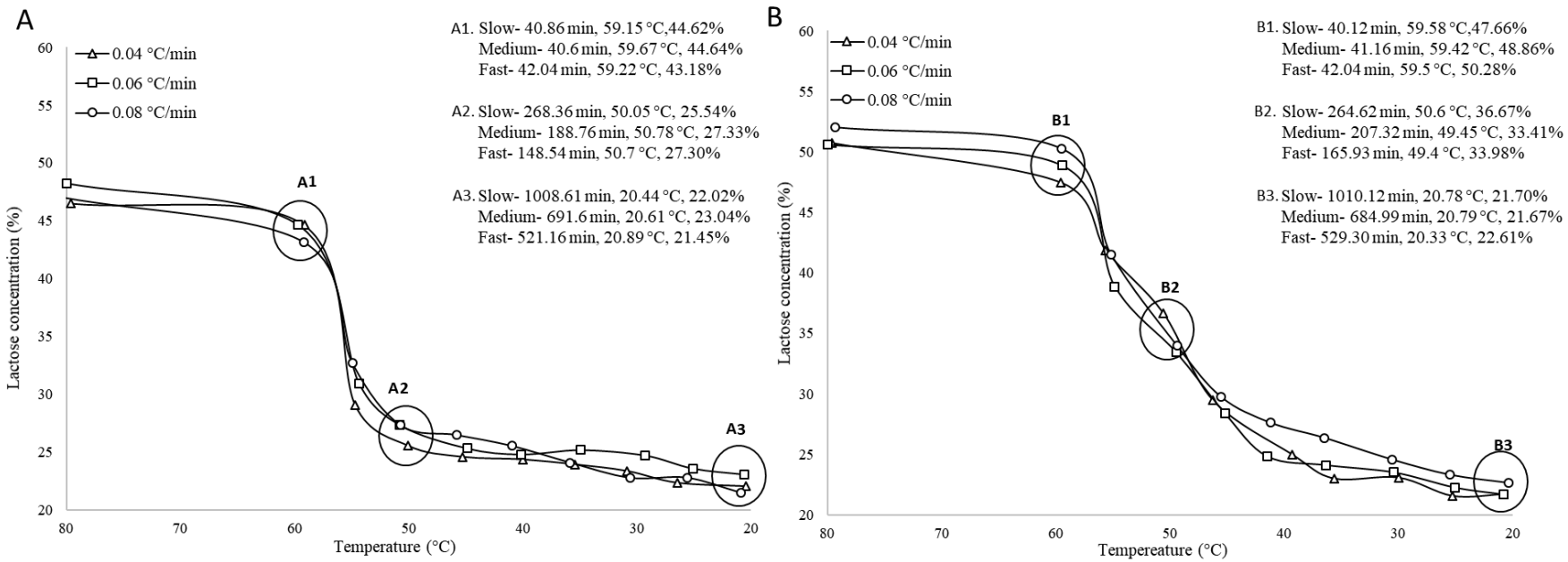

Figure 4.2. Desupersaturation of lactose during lactose crystallization in A. Deproteinized whey (DPW) and B. Milk permeate powder (MPP) concentrates using 0.04 °C/min (slow), 0.06 °C/min (medium), and 0.08 °C/min (fast) cooling rate. Time, temperature, and lactose concentration in during crystallization in DPW (circles A1, A2, and A3) and MPP (circles B1, B2, and B3) concentrates.

Evaluation of FBRM Data

In this study, the progress of lactose crystallization in the concentrated DPW and MPP solutions was evaluated using FBRM. FBRM is an efficient in-situ monitoring tool for monitoring changes in particle counts and growth during lactose crystallization (Pandalaneni and Amamcharla, 2016). However, it cannot differentiate between lactose crystals and other impurities present in suspension. Hence, the results were interpreted as particle counts in contrary to crystal counts in previous study (Pandalaneni and Amamcharla, 2016). During 3 cooling rates, particle sizes were grouped into fine (<50 µm) and large (50-150 µm) to evaluate the changes in particle sizes and counts during lactose crystallization.

Particle counts in DPW. In DPW concentrate, any particle counts at the beginning of the experiment at 80°C was due to the presence of air bubbles and calcium phosphate precipitates at higher temperatures as shown in Figure 4.3A. Butler (1998) also observed calcium phosphate residual lumps in concentrated permeates because of its lower solubility in aqueous solution. The protein fraction in DPW concentrates also precipitated at higher temperatures along with calcium phosphate (Chandrapala et al., 2015) contributing to large particle counts. This phenomenon was supported by the microscopic images confirming the absence of lactose nuclei or crystals in DPW concentrates at the beginning at 80°C. A typical microscopic image observed at the beginning of crystallization during 3 cooling rates was shown in Figure 4.4A.

As shown in Figures 4.3A and 4.3B, during the common cooling step (80-60°C), fine particle counts steadily increased while large particle counts decreased. These changes in the fine and large particle counts can be attributed to the solubilization and breakage of mineral precipitates due to agitation and cooling. With the decrease in temperature, the solubility of lactose also decreased and resulting in the increased supersaturation driving force. Increase in

supersaturation driving force and agitation promoted the lactose nucleation contributing to increase in fine particle counts. At 60°C, small clusters of nuclei were observed in the microscopic images (Figure 4.4B) because of the diffusion of lactose from the liquid phase to solid phase; however, lactose nuclei clusters were in relaxation phase of induction time during the common cooling step of lactose crystallization (Mullin, 2001). Sequence of microscopic images shown in Figure 4.4 illustrates the nucleation and growth behavior of lactose. From the image at 60°C (Figure 4.4B), the nuclei clusters and few stable tomahawk shaped nuclei can be observed along with some air bubbles.

As the cooling progressed during the lactose crystallization, fine particle counts rapidly increased and reached a local peak at approximately 26,000 counts in the temperature range of 57-55°C in all the 3 cooling rates studied. This rapid increase was followed by a drastic decrease in fine particle counts to approximately 20,000 during the temperature range of 55-51°C. The local peaks of fine particle counts can be attributed to rapid nucleation (Figure 4.3A), and the following decrease was because of the growth of formed lactose nuclei (Figure 4.3B). Lactose crystal growth was also evident from increased large particle counts during temperature range of 55-54°C. A sudden desupersaturation of lactose (Figure 4.2A) in the temperature range of 57-50°C suggested that the diffusion of lactose from liquid phase to the solid phase was rapid, supporting the particle count results observed from FBRM data. These rapid changes can be better explained using the classical nucleation theory (McLeod et al., 2011). According to this theory, the diffused lactose from the liquid phase is more prone to settle down on the available crystal surface than form a new nuclei. Due to the presence of impurities, diffused lactose used impurity precipitates as a seed to form nuclei referring to it as heterogenous nucleation. Heterogeneous nucleation is easier to occur because of the reduced energy barrier required for

the creation of new solid-liquid interface (McLeod et al., 2011). The 3 cooling rates did not show any influence on rapid nucleation, as evident from fine particle counts and the desupersaturation of lactose (Figure 4.2A). However, variation in the increase of large particle counts suggested that the lactose crystal growth changed depending on the cooling rate used during the lactose crystallization. There was an increase of 1200, 1035, and 651 large particle counts during cooling from 57-48°C when slow, medium, and fast cooling rates were used, respectively.

Increased large particle counts during 57-48°C led to an increased population density of lactose crystals resulting in the breakage of crystals either by collision into walls of the crystallizer or the impeller. As a result, the increase in fine particle counts and decrease in large particle counts was observed simultaneously as shown in Figures 4.3A and 4.3B. The attrition and breakage of crystals further promoted secondary nucleation and allowed lactose to diffuse on to the already formed crystal lattice (McLeod et al., 2011). The progressive increase in the fine particle counts as the cooling progressed was more prominent in the fast cooling rate compared to the medium and slow cooling rates. In large particle counts, slow and medium cooling rates were in the same range and had approximately 200 counts more than the fast cooling rate. These observations summarize that the nucleation was not influenced by the 3 cooling rates studied. However, the lactose crystal growth was favored by the slow cooling rate in the DPW concentrate.

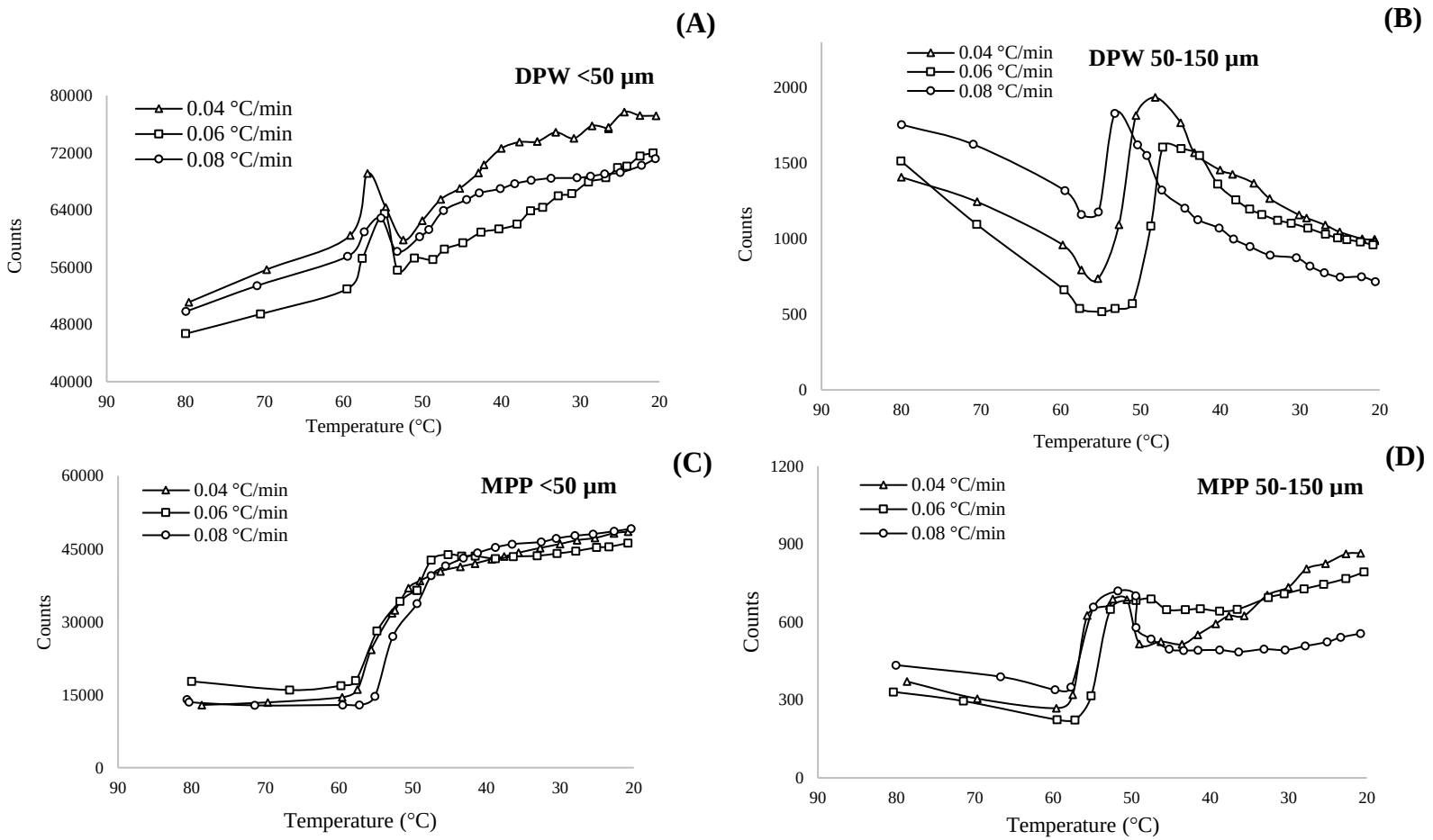

Figure 4.3. Fine (<50 µm) (A,C) and Large (50-150 µm) (B,D) particle counts data obtained from Focused beam reflectance measurement (FBRM) during lactose crystallization in Deproteinized whey (DPW) and Milk permeate powder (MPP) concentrates using 0.04 °C/min (slow), 0.06 °C/min (medium), and 0.08 °C/min (fast) cooling rates.

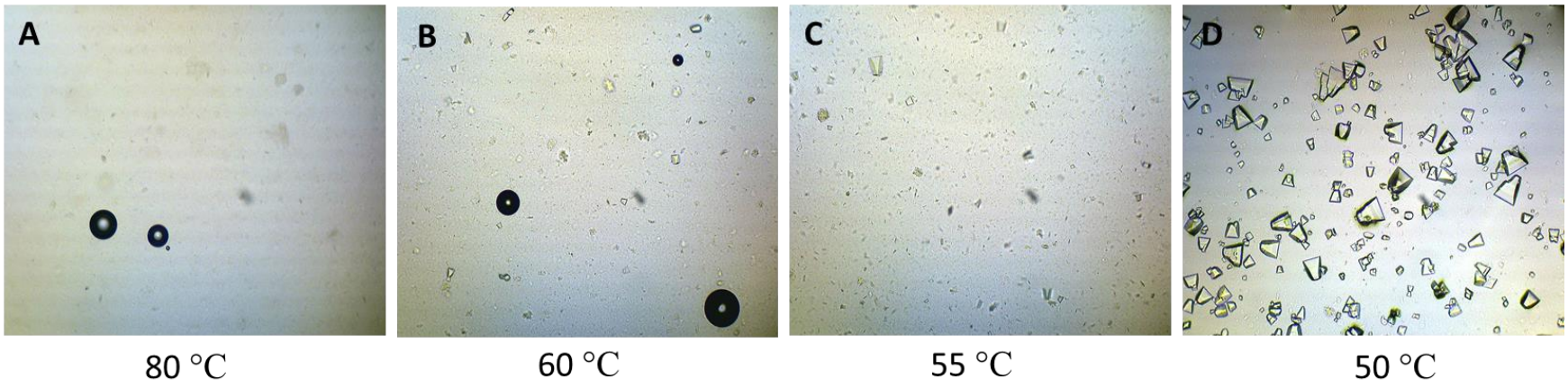

Figure 4.4. Typical representative microscopic images acquired at 80, 60, 55, and 50 °C to represent the changes occurred in the particle counts of Focused beam reflectance measurement (FBRM) during lactose crystallization in concentrated DPW/MPP.

Particle counts in MPP. In the MPP concentrate, the absence of lactose nuclei at the beginning of crystallization at 80°C was confirmed with the microscopic images as well. But there was a contrasting behavior of particle counts compared to the DPW concentrates. There were fewer fine and large particle counts observed in the MPP concentrate at 80°C compared to DPW concentrate. Lower ash and protein content in MPP concentrates compared to the DPW concentrates (Table 4.1) reduced the influence of mineral and protein precipitates on large particle counts at 80°C. In concentrated DPW solutions with 60% total solids, average protein and mineral percentages were 3.5 and 5.3%, respectively. Whereas, in concentrated MPP solutions with 60% total solids, measured protein and mineral percentages were in the range of 2.3 and 4.7%, respectively. As the cooling progressed, fine particle counts in the MPP concentrate exhibited a slight increase in number, but large particle counts decreased because of the mineral solubilization and breakage. As the MPP concentrate was cooled from 80°C to 60°C, lactose nuclei clusters were observed in the MPP concentrate similar to crystals shown in Figure 4.4B, along with a decrease in lactose concentration. The particle counts of the concentrated DPW and MPP solutions strengthened the assumption that the presence of impurities and their solubilization properties were dominant as the concentrates were cooled. Both DPW and MPP concentrates were in induction time until temperature reached to approximately 60°C as evident from the desupersaturation curve (Figure 4.2) and the FBRM counts (Figures 4.3C and 4.3D).

The particle counts of the MPP concentrate followed a different trend, compared to the DPW concentrate after the 80 to 60°C cooling (common cooling step). There was no intermediate peak or a drastic drop in fine and large particle counts at all the cooling rates studied. The change in the behavior of the lactose crystal nucleation and growth can be attributed to the minimum heterogenous nucleation due to low impurity content, compared to the DPW

concentrate. The ratio of lactose to protein and ash percentage in DPW and MPP concentrates at 60% total solids was approximately 5.4 and 7.4, respectively (Table 4.1). The continuous increase of fine and large particle counts at approximately 57°C imply that lactose crystal nucleation and crystal growth occurred simultaneously irrespective of the cooling rate studied. Due to the higher lactose concentration in the MPP concentrate (~52%) at the 60% total solids, the supersaturation drive was high resulting in both nucleation and crystal growth to occur simultaneously. A steady decrease in the lactose concentration from 48.8% at 60°C to 25.8% at 40°C was observed in MPP concentrate (Figure 4.2B) in contrast to the rapid decrease in DPW concentrate (Figure 4.2A). This observation also supported the hypothesis that rapid nucleation was absent in the MPP concentrates at 3 cooling rates.

After an increase in particle counts by nucleation and crystal growth, a steady increase in the fine and coarse counts was observed from approximately 48°C representing the primary nucleation and secondary nucleation at all the 3 cooling rates. However, the decrease in the large particle counts was not as prominent as in the DPW concentrate, implying that crystal growth was more dominant along with some secondary nucleation that occurred due to the crystal attrition and breakage. Only large particle counts were influenced by the slow, medium, and the fast cooling rates thereafter.

Evaluation of PCLD and Microscopic Analysis

FBRM is a helpful tool to determine the PCLD of the total particle population present in the crystallizer without any sample preparation. The final mean of particle counts obtained during the 3 cooling rates from PCLD was compared in DPW and MPP concentrates at the end of crystallization. Final mean of particle counts in the DPW concentrate for slow, medium, and fast cooling rates were 33.22, 30.29, and 27.05 µm, respectively (Table 4.2). Whereas, the final

mean of particle counts in the MPP concentrate for slow, medium, and fast cooling rates were 32.08, 31.91, and 34.61 µm, respectively. There was no significant difference ($P>0.05$) between the final mean of particle counts when slow, medium, and fast cooling rates were applied during the crystallization in DPW and MPP concentrates. Chord length distribution of lactose crystals obtained after 10 h of isothermal crystallization (20°C) in 50, 55, and 60% of pure lactose was reported as 58.10, 41.66, and 39.12 µm, respectively (Pandalaneni and Amamcharla, 2016). The difference in the final chord length of distribution in pure lactose system and in permeates system can be attributed to presence of impurities that hinder the rate of crystal growth (Bhargava and Jelen, 1996; Mimouni et al., 2005).

PCLD of 3 cooling rates obtained for DPW and MPP concentrates was shown in Figure 4.5. PCLD was obtained using FBRM at the end of crystallization to demonstrate the influence of cooling rates on the particle distribution in the crystallizer. From Figure 4.5, it was evident that the PCLD of slow, medium, and fast cooling rates had similar distribution at the end of crystallization. PCLD data was further supported by the microscopic images of lactose crystals taken at the end of lactose crystallization as shown in Figure 4.6. It is evident that the lactose crystals did not show any noticeable size differences during the 3 cooling rates and exhibited a similar size distribution.

Evaluating the Lactose Yield. Lactose crystal slurry obtained at the end of crystallization was dried and weighed to calculate the lactose yield (%) using Equation 1. The lactose yield obtained using the 3 cooling rates were in the range of 71-73% and 76-81% in DPW and MPP concentrates, respectively, as shown in Table 4.2. The lactose yields obtained in 3 cooling rates were not significantly different ($P>0.05$) in both the permeate concentrates.

Relatively higher lactose yield in the MPP concentrates was due to the increased supersaturation driving force compared to the DPW concentrate (Table 4.1).

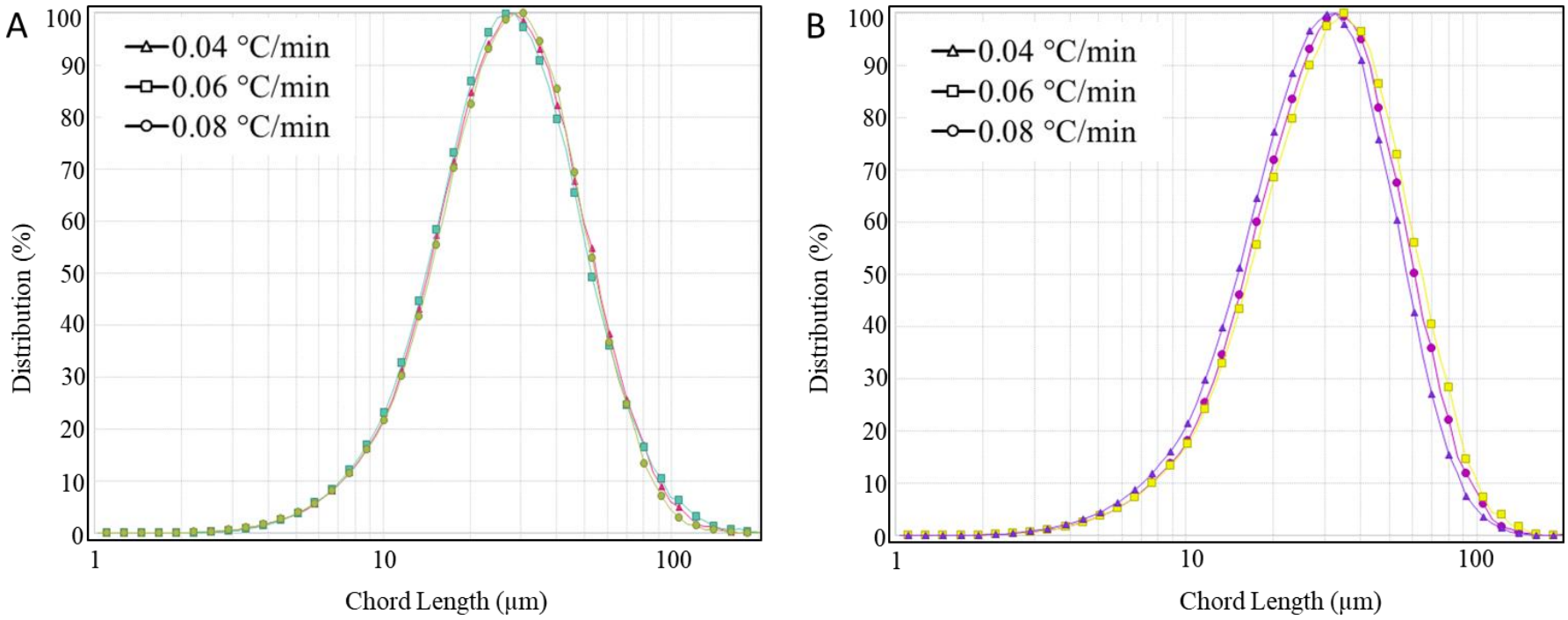

Figure 4.5. Particle chord length distribution (PCLD) data obtained from Focused beam reflectance measurement (FBRM) at the end of lactose crystallization in A. Deproteinized whey (DPW) and B. Milk permeate powder (MPP) concentrates using 0.04 °C/min (slow), 0.06 °C/min (medium), and 0.08 °C/min (fast) cooling rates.

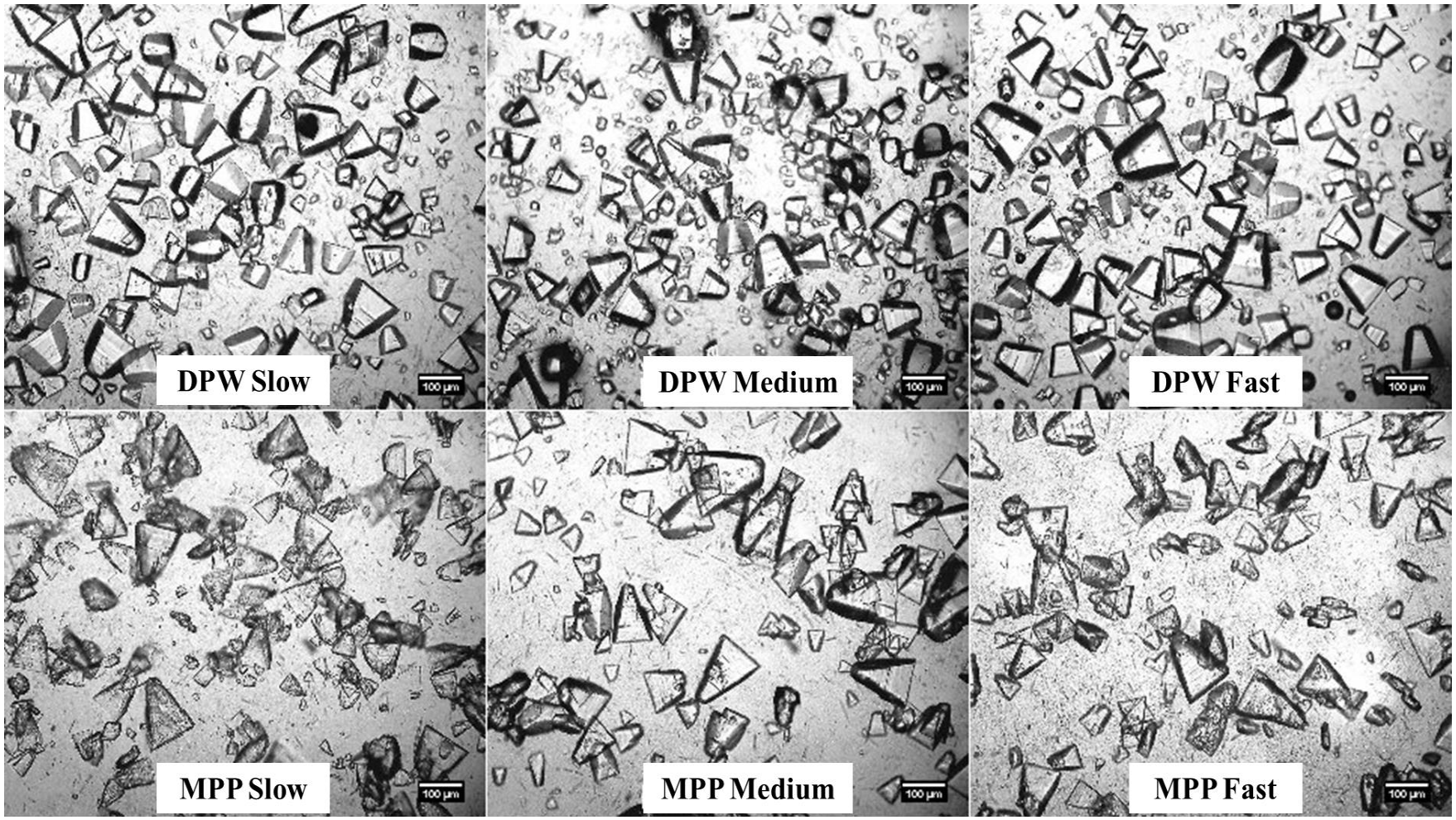

Figure 4.6. Microscope images of lactose crystals obtained at the end of lactose crystallization in Deproteinized whey (DPW) and Milk permeate powder (MPP) concentrates using 0.04 °C/min (slow), 0.06 °C/min (medium), and 0.08 °C/min (fast) cooling rates.

Characterization of Dried Lactose Crystals

This section was focused to describe the influence of the slow, medium, and fast cooling rates on the quality of lactose crystals recovered from concentrated permeate after crystallization. Production of lactose crystals with minimum or no impurities is critical for an economical industrial production to avoid further refining steps. Some of the impurities often present in whey and milk permeates are calcium phosphate, lactose phosphate, riboflavin, and potassium chloride (Lifran et al., 2007). Riboflavin tends to accumulate on the surface of lactose crystals and can be removed during the washing process. However, calcium phosphate and lactose phosphate are the impurities embeded into the crystalline lattice and cannot be washed off easily (Butler, 1988; Lifran et al., 2007). Hence, evaluating the extent of impurity deposition in the lactose crystals during different cooling rates is important for an efficient crystallization process.

Compositional Analysis. The protein and ash content in the lactose crystals recovered after crystallization and washing using the slow, medium, and fast cooling rates in the DPW concentrate were in the range of 0.66-0.78% and 1.35-1.46%, respectively as shown in Table 4.3. Although, there was a trend observed with percentage impurity decreased as the cooling rate increased, there was no significant difference ($P>0.05$) in protein and ash content in 3 cooling rates.

On the other hand, ash content in lactose crystals recovered from the MPP concentrate was in the range of 2.46-2.52% with no significant difference observed between the 3 cooling rates. However, protein percentage was significantly high (1.71%) in lactose crystals recovered after the crystallization using slow cooling rate. There was no significant difference in the protein content in lactose crystals recovered from the crystallization using medium and fast cooling rates. The absence of rapid nucleation in MPP but the presence of high impurities in

crystal mass imply that the deposition of impurities occurred during the lactose crystal growth. The MPP concentrates exhibited an early lactose crystal growth compared to the DPW concentrates as evident from large particle counts observed from FBRM data (Figures 4.4B and 4.4D). According to Mackintosh and White (1974) and Butler (1988), the amount of impurities inclusion in the crystal depends on the crystal growth rate and perfection of lactose crystal. With the increased crystal growth, the possibility of impurity inclusion in lactose crystal can be high resulting in the increased K, Ca, and P as impurities.

Crystal Purity. The microscopic analysis of lactose crystals to visualize the impurities was focused to interpret the location of impurities in the lactose crystal lattice and to identify if the impurity presence affected the tomahawk morphology. Calcium phosphate and lactose phosphate are the major impurities in the permeates that contribute towards major fraction of impurities (Butler, 1998; Lifran et al., 2007). Lifran et al. (2007) observed changes to the tomahawk shaped lactose crystals when the impurities such as lactose phosphate were incorporated at higher concentrations. Similar morphologies were observed in all the washed and dried lactose crystals recovered from both DPW and MPP concentrates at 3 cooling rates. From Figure 4.7, it is evident that the lactose crystals were in tomahawk shape and darker impurity region was mostly observed on the apex of tomahawk shaped lactose crystals. The impurities, especially calcium phosphate, precipitated at 80°C and acted as a seed for heterogeneous nucleation. As the crystallization continued, crystal growth occurred towards the base region leaving the impurities at the apex of tomahawk shaped crystal. Mineral content (Table 4.3) observed in the dried lactose crystals recovered from concentrated permeates also confirmed the theory of major impurity entrapped in the lactose crystal was composed of calcium and phosphate. These observations also supported the theory that higher large particle counts in

FBRM data (Figures 4.4B and 4.4D) were contributed by mineral precipitates during common cooling of the concentrated permeates. Along with impurity inclusion at the apex, there were few darker spots on the walls of crystals attributing to impurity inclusions during the crystal growth as well. Mother liquor and impurities tend to accumulate on the irregular sides of crystal walls and get trapped during crystal growth resulting in impurity inclusion in the crystal on the sides of lactose crystal (Mackintosh and White, 1974 and Butler, 1988). The microscopic image analysis of lactose crystals in Figure 4.7 also confirmed that tomahawk shape was not disturbed by the extent of impurities trapped in the lactose crystal. This observation showed that reducing the crystallization time in this study did not influence the shape of lactose.

Table 4.3. Mean ± standard deviation of dry basis protein, ash, and mineral analysis of dried lactose crystals on dry basis recovered from deproteinized whey (DPW) and milk permeate powder (MPP) concentrates.

		Total crystallization time required (min)	Protein (%)	Ash (%)	Calcium (%)	Magnesium (%)	Sodium (%)	Potassium (%)	Phosphate (%)
DPW	0.04 °C/min	1008	0.78±0.05 ^{a}	1.46±0.07 ^{a}	0.53±0.02 ^{a}	0.06±0.01 ^{a}	0.05±0.01 ^{a}	0.09±0.02 ^{a}	0.23±0.01 ^{a}
	0.06 °C/min	691	0.73±0.00 ^{a}	1.35±0.19 ^{a}	0.55±0.04 ^{a}	0.07±0.02 ^{a}	0.06±0.00 ^{a}	0.09±0.01 ^{a}	0.24±0.05 ^{a}
	0.08 °C/min	521	0.66±0.03 ^{a}	1.35±0.02 ^{a}	0.51±0.00 ^{a}	0.06±0.01 ^{a}	0.07±0.02 ^{a}	0.10±0.03 ^{a}	0.23±0.02 ^{a}
MPP	0.04 °C/min	1010	1.71±0.08 ^{B}	2.52±0.01 ^{A}	0.79±0.05 ^{A}	0.08±0.02 ^{A}	0.08±0.01 ^{A}	0.26±0.01 ^{A}	0.41±0.03 ^{A}
	0.06 °C/min	684	1.54±0.08 ^{A}	2.49±0.03 ^{A}	0.74±0.05 ^{A}	0.06±0.00 ^{A}	0.10±0.00 ^{A}	0.28±0.00 ^{A}	0.42±0.04 ^{A}
	0.08 °C/min	529	1.25±0.02 ^{A}	2.46±0.00 ^{A}	0.79±0.01 ^{A}	0.07±0.01 ^{A}	0.09±0.01 ^{A}	0.28±0.04 ^{A}	0.45±0.00 ^{A}

Values with the same superscript are not significantly different (P>0.05); n=2
Values are compared within DPW and MPP concentrate and within column
a, b, c superscripts were used to compare values from lactose crystallization experiments in DPW concentrate
A, B, C superscripts were used to compare values from lactose crystallization experiments in MPP concentrate

DSC. Thermal analysis of lactose crystals using calorimetry as shown in Figure 4.8, provided an information about the presence of amorphous or crystalline lactose in the sample (Listiohadi et al., 2009). The absence of exothermic peaks in dried lactose crystals recovered from permeate concentrates using 3 cooling rates, suggested the absence of amorphous lactose. Distinct endothermic peaks were observed in all the lactose crystals at 147-148°C, which were attributed to the loss of crystalline water as the temperature increased. This observation further confirmed that 100% crystalline lactose was present in the lactose crystals recovered from concentrated permeates using the 3 cooling rates studied (Gombas et al., 2002).

FTIR. To identify the extent of lactose crystal purity, FTIR spectra of dried lactose crystals were compared with spectra of commercial lactose, DPW, and MPP powders as shown in Figure 4.8. A less intense but broad peak at 1650 cm^{-1} accompanied by a peak at 1590 cm^{-1} was observed in lactose crystals recovered from both the DPW concentrates for the 3 cooling rates studied. The presence of a clear symmetric peak in commercial lactose at 1650 cm^{-1} is associated with bending vibration of O-H groups of water associated with lactose crystal (Nikanishi, 1962). Chandrapala et al. (2016) explained in a study related to addition to lactic acid and calcium to lactose model system that the intensity of these peaks was higher in presence of calcium and lactic acid when compared to peak of pure lactose systems. They justified that the higher intensity of peaks at 1590 and 1650 cm^{-1} was due to restricted mobility of water molecules in the presence of calcium and lactic acid. FTIR spectra of lactose crystals recovered from DPW concentrate using 3 cooling rates had no distinct differences in the peaks at 1590 cm^{-1} and 1650 cm^{-1}. A similar observation was made from the lactose crystals recovered from the MPP concentrate at 3 cooling rates studied as well. Presence of these two peaks in DPW, MPP and dried lactose crystals recovered from the concentrated permeates suggested that it is associated

with the presence of impurities restricting the vibration of O-H groups. Broad and intense peaks were observed in DPW and MPP spectra as compared to the clean symmetric peak at 1650 cm^{-1} in commercial lactose. This observation strengthens the theory that presence of impurities that restrict the O-H groups had influence in the peaks of 1590 cm^{-1} and 1650 cm^{-1} wavenumber. This observation confirmed the fact that the recovered lactose crystals had fewer impurities compared to DPW and MPP powders but the entrapped impurities in the crystals resulted in distorted peaks at 1590 cm^{-1} and 1650 cm^{-1} wavenumber.

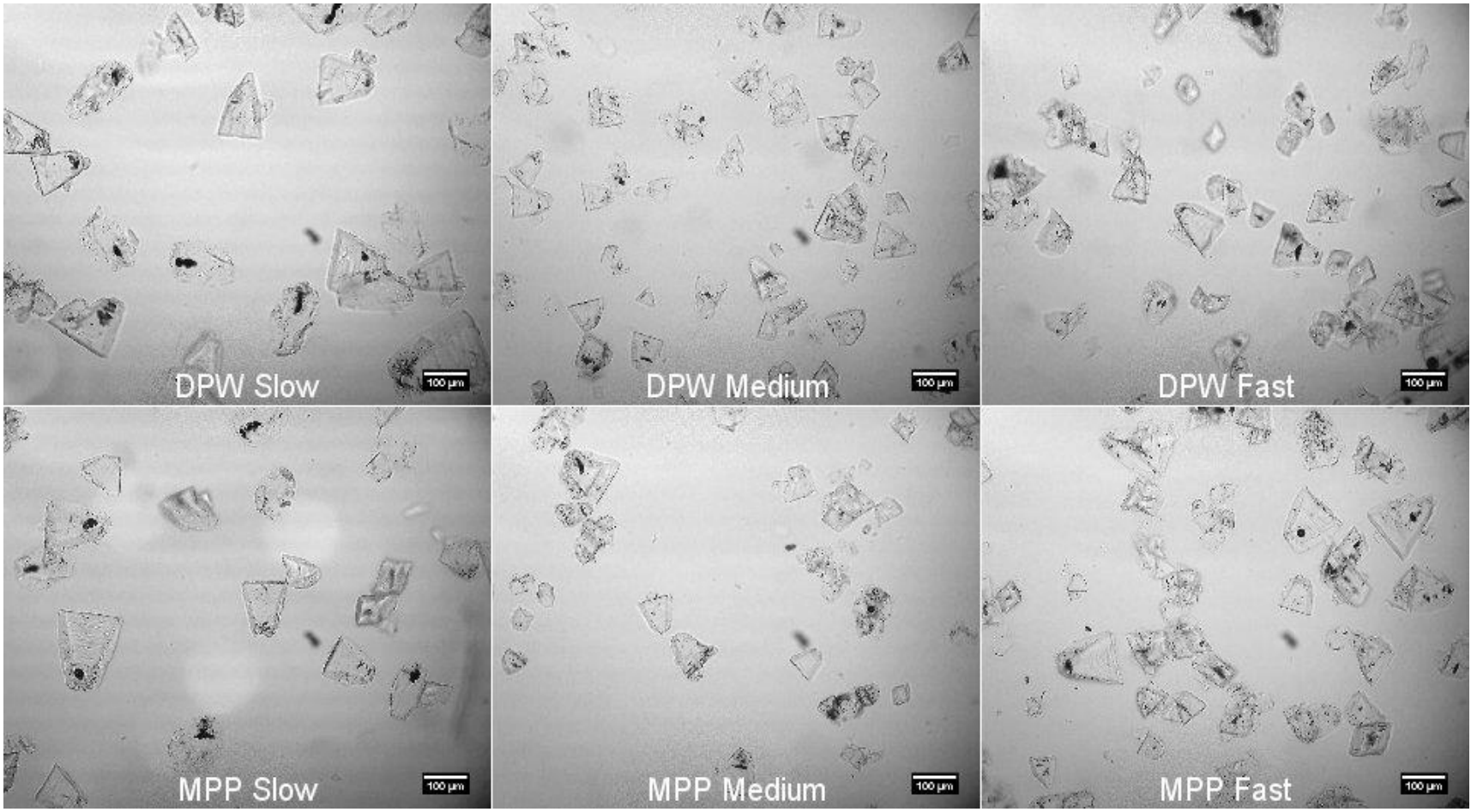

Figure 4.7. Lactose crystal purity images of dried lactose crystals recovered from lactose crystallization in Deproteinized whey (DPW) and Milk permeate powder (MPP) concentrates using 0.04 °C/min (slow), 0.06 °C/min (medium), and 0.08 °C/min (fast) cooling rates.

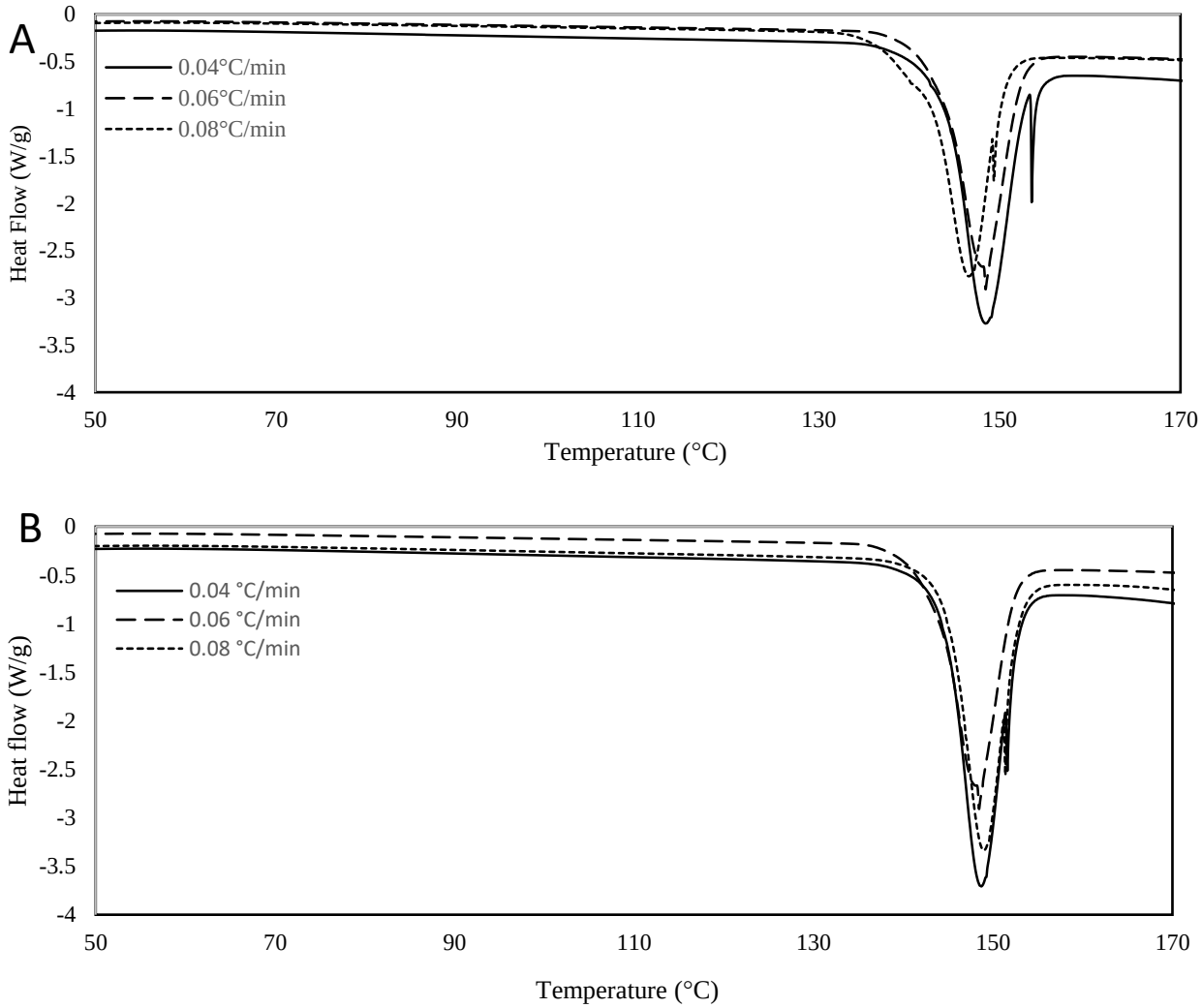

Figure 4.8. DSC thermograms obtained from dried lactose crystals recovered from lactose crystallization in A. Deproteinized whey (DPW) and B. Milk permeate powder (MPP) concentrates using 0.04 °C/min (slow), 0.06 °C/min (medium), and 0.08 °C/min (fast) cooling rates.

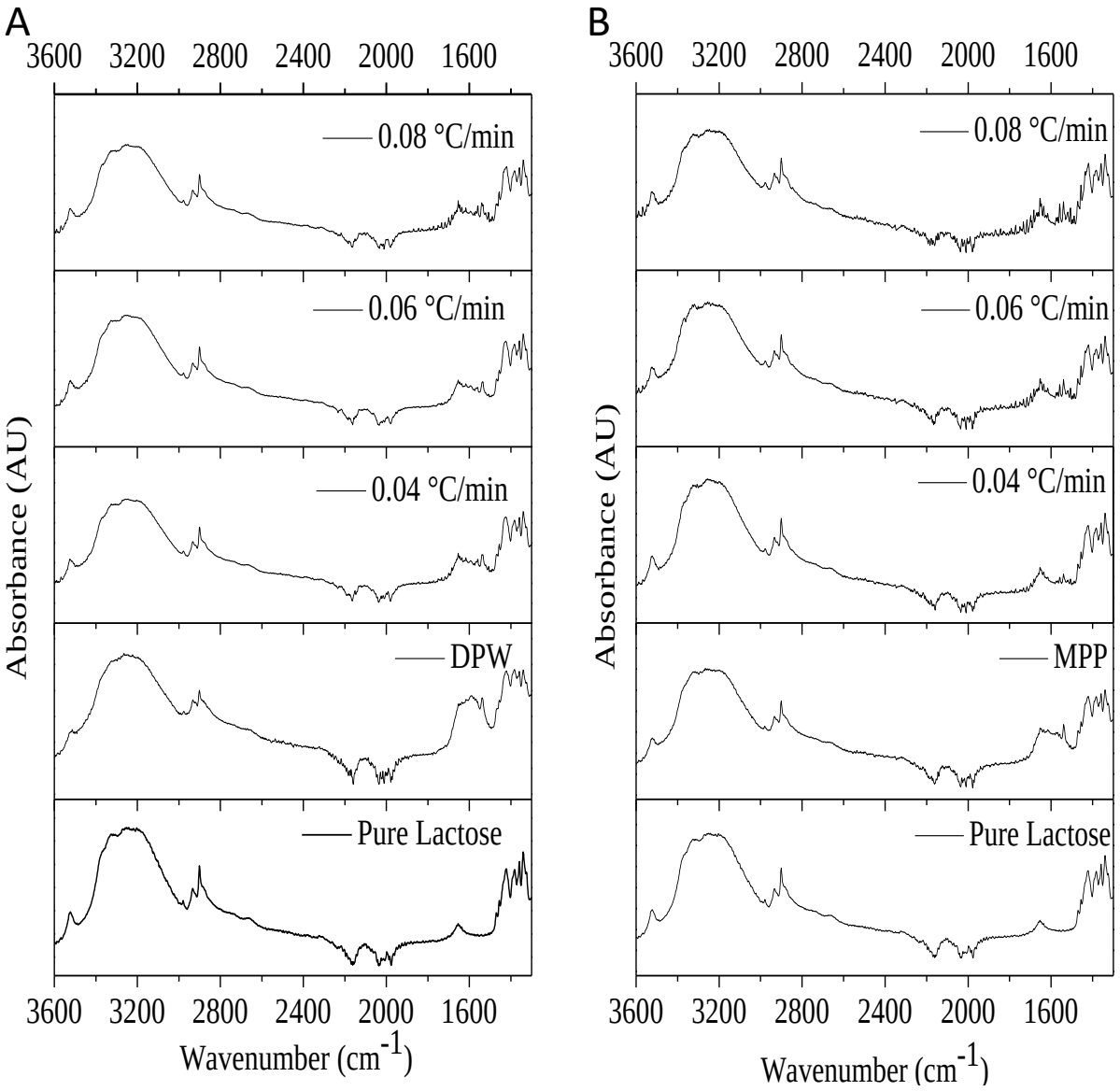

Figure 4.9. FTIR spectra acquired from dried lactose crystals recovered from lactose crystallization in A. Deproteinized whey (DPW) and B. Milk permeate powder (MPP) concentrates using 0.04 °C/min (slow), 0.06 °C/min (medium), and 0.08 °C/min (fast) cooling rates. FTIR spectra of Pure lactose, DPW, and MPP powder to compare the peaks with dried lactose crystals recovered.

Conclusion

The effect of cooling rate during the crystallization process, by measuring particle chord length data using FBRM and lactose yield was investigated. Increasing the cooling rate from 0.04 °C/min to 0.06 °C/min and 0.08 °C/min had no significant difference in lactose yield and mean chord lengths of particles at the end of crystallization. Qualitative analysis of lactose confirmed that the purity of crystals was not affected by increasing the cooling rate from slow to medium or fast in concentrated permeates. Using medium or fast cooling rates, could save the power and resources needed to run the crystallizer for 8 additional more hours during crystallization of lactose in DPW and MPP concentrated permeates. As evident from the results so far, reducing the crystallization time by increasing the cooling rate within the range studied had no effect on quality of lactose crystals recovered from the DPW and MPP concentrates with an exception of significantly higher protein content in dried lactose crystals recovered after MPP concentrate crystallized with slow cooling rate.

Ackowledgements

This project is funded by Kansas State Research and Extension with contribution number 18-363-J.

References

Amamcharla, J.K., and L.E. Metzger. 2011. Development of a rapid method for the measurement of lactose in milk using a blood glucose biosensor. J. Dairy Sci. 94:4800–4809.

AOAC International. (2016). Official methods of analysis. (20th ed.). Association of Analytical Communities, Rockville, MD.

Butler, B. 1998. Modelling Industrial lactose crystallization. PhD Thesis. Department of Chemical Engineering, The University of Queensland, Australia.

Carpin, M., H. Bertelsen, A. Dalberg, C. Roiland, J. Risbo, P. Schuck, and R. Jeantet. 2017. Impurities enhance caking in lactose powder. J. Food Eng. 198:91–97.

Chandrapala, J., M.C. Duke, S.R. Gray, M. Weeks, M. Palmer, and T. Vasiljevic. 2016. Nanofiltration and nanodiafiltration of acid whey as a function of pH and temperature. Sep. Purif. Technol. 160:18–27.

Chandrapala, J., M.C. Duke, S.R. Gray, B. Zisu, M. Weeks, M. Palmer, and T. Vasiljevic. 2015. Properties of acid whey as a function of pH and temperature. J. Dairy Sci. 98:4352–4363.

Chandrapala, J., R. Wijayasinghe, and T. Vasiljevic. Lactose crystallization as affected by presence of lactic acid and calcium in model lactose systems. J. Food Eng. 178:181–189.

Gänzle, M.G., G. Haase, and P. Jelen. 2008. Lactose: Crystallization, hydrolysis and value-added derivatives. Int. Dairy J. 18:685–694.

Gombas, A., P. Szabó-Révész, M. Kata, G. Regdon, and I. Er\Hos. 2002. Quantitative determination of crystallinity of α-lactose monohydrate by DSC. J. Therm. Anal. Calorim. 68:503–510.

Goulart, D.B., and R.W. Hartel. 2017. Lactose crystallization in milk protein concentrate and its effects on rheology. J. Food Eng. 212:97–107.

IDF. (2002). Milk and milk products; Determination of nitrogen content—Routine method using combustion according to the Dumas principle. Standard No. 185. International Dairy Federation, Brussels, Belgium.

Bhargava, A., and P. Jelen. 1996. Lactose Solubility and Crystal Growth as Affected by Mineral Impurities. J. Food Sci. 61:180–184.

Lifran, E.V., T.T.L. Vu, R.J. Durham, J.A. Hourigan, and R.W. Sleigh. 2007. Crystallisation kinetics of lactose in the presence of lactose phosphate. Powder Technol. 179:43–54.

Listiohadi, Y., J.A. Hourigan, R.W. Sleigh, and R.J. Steele. 2009. Thermal analysis of amorphous lactose and α-lactose monohydrate. Dairy Sci. Technol. 89:43–67.

Mackintosh, D., and E. White. 1974. The formation of inclusions in sugar crystals. AIChE Symposium Series. 72:11–20.

McLeod, J. 2007. Nucleation and growth of alpha lactose monohydrate thesis.pdf. PhD Thesis Thesis. Massey University, New Zealand.

McLeod, J., A.H.J. Paterson, J.R. Jones, and J.E. Bronlund. 2011. Primary nucleation of alpha-lactose monohydrate: The effect of supersaturation and temperature. Int. Dairy J. 21:455–461.

Mimouni, A., P. Schuck, and S. Bouhallab. 2005. Kinetics of lactose crystallization and crystal size as monitored by refractometry and laser light scattering: effect of proteins. Le Lait 85:253–260.

Modler, H.W., and L.P. Lefkovitch. 1986. Influence of pH, Casein, and Whey Protein Denaturation on the Composition, Crystal Size, and Yield of Lactose from Condensed Whey. J. Dairy Sci. 69:684–697.

Mullin, J.W. 2001. Crystallization. 4th ed. Butterworth-Heinemann, Boston, MA.

Pandalaneni, K., and J.K. Amamcharla. 2016. Focused beam reflectance measurement as a tool for in situ monitoring of the lactose crystallization process. J. Dairy Sci. 99:5244–5253.

Shi, X., and Q. Zhong. 2014. Enhancing lactose crystallization in aqueous solutions by soluble soybean polysaccharide. Food Res. Int. 66:432–437.

U.S Whey and Milk Permeate. 2015. U.S. Dairy Export Council. Dairy Management Inc., Arlington, VA.

Wehr, H.M., and J.F. Frank. 2004. Standard Methods for the Examination of Dairy Products. American Public Health Association.

Wong, S.Y., R.K. Bund, R.K. Connelly, and R.W. Hartel. 2012. Designing a lactose crystallization process based on dynamic metastable limit. J. Food Eng. 111:642–654.

Chapter 5 - Influence of milk protein concentrates with modified calcium content on the dairy beverage formulation: Physico-chemical properties

Abstract

Milk protein concentrates (MPCs) are the highly preferred ingredients in high dairy protein ready-to-drink (RTD) and nutrition beverages. Calcium-mediated aggregation of proteins during storage is one of the main reasons for the loss of storage stability of these beverages. Control and calcium-reduced MPCs (20% calcium-reduced (MPC-20), and 30% calcium-reduced (MPC-30)) were used to evaluate the physicochemical properties in this study. This study was conducted in 2 phases. In phase I, 8% protein solutions were prepared by reconstituting the MPCs followed by adjusting the pH to 7. This solution was divided into 3 equal parts and 0, 0.15, and 0.25% sodium hexametaphosphate (SHMP) was added and homogenized. In phase II, a dairy beverage formulation (5.19 % of a mixture of gums, maltodextrin, and sugar) containing MPC was evaluated following the same procedure as phase I. In both phase I and II, heat stability, apparent viscosity, and particle size were compared before and after heat treatment at 140°C for 15 s. In the absence of SHMP, MPC-20 and MPC-30 exhibited the highest heat coagulation time (HCT) at 30.9 and 32.8 min, respectively, compared to control (20.9 min). In phase II, without any addition of SHMP, MPC-20 exhibited the highest HCT of 9.3 min compared to 7.1 min for control and 6.2 min for MPC-30. An increase in apparent viscosity and a decrease in particle size of reconstituted MPC solutions in phase I and II with an increase in SHMP concentration were attributed to casein micelle dissociation because of

the calcium chelation. This study presents a potential for application of calcium-reduced MPCs in dairy-based ready-to-drink and nutrition beverage formulations to improve their heat stability.

Introduction

Milk protein concentrates (MPCs) are one of the most widely used dairy ingredients in the food industry because of their protein content (50-85%) and the presence of casein and whey proteins in the same ratio as milk. MPCs are used as a major ingredient in protein beverages such as sports nutrition and shake-type products (Lagrange et al., 2015). MPCs are the preferred source of protein in high-protein ready-to-drink and nutrition formulas as they score high on protein quality. The storage stability and shelf-life of these products is dependent on the composition and quality of ingredients used. It has been theorized that MPC solubility, protein-protein interactions during processing, and solubility changes during storage are influenced by the calcium content of the MPC (Marella et al., 2015). Additionally, issues during processing and storage of dairy beverages have been attributed to protein-protein and protein-mineral interactions (Augustin, 2000; Anema et al., 2006), leading to age gelation and phase separation in the dairy beverages.

Several studies have been carried out that reduced the calcium-ion activity in MPC either by addition of calcium chelators or by partial demineralization during ultrafiltration. Crowley et al. (2014) investigated the influence of pH and the addition of lactose and urea in the serum phase of reconstituted MPC solutions on heat stability. It was observed that adding urea increased the heat stability, whereas the addition of lactose and maltodextrin reduced the heat stability when pH > 6.9. Also, Fang et al. (2012) observed that the solubility of MPC powders was improved by reducing the inlet temperature during spray drying of MPC. Marella et al. (2015) also worked on improving the functionality of MPC by injecting carbon dioxide (CO_2) in skim milk before and during ultrafiltration. By injecting the CO_2, pH of the milk was reduced and consequently solubilizing the micellar calcium and phosphate resulting in reduced mineral

content in the retentate fraction. As a result, manufactured calcium-reduced MPC was reported to have better cold-water solubility. In another study to improve the functionality of MPC, Xu et al. (2016) partially removed calcium in skim milk by ion-exchange treatment. It was observed that at 83.6% decalcification, colloidal calcium phosphate (CCP) nanoclusters were completely dissociated. Ramchandran et al. (2017) improved the heat stability and emulsion capacity of MPC powders by pre-treating the skim milk with calcium chelating agents during ultrafiltration. This reduced the calcium in retentate and casein micelle size, thereby improving the MPC properties.

Due to improved heat stability and functional properties of MPCs as the calcium percent was reduced, this study was designed to evaluate their application in dairy beverage formulation. MPCs with different levels of reduced calcium along with varying levels of calcium chelating salt were used to study changes in physiochemical properties of protein solutions.

Materials and Methods

Experimental Design

Two batches of 0 (control), 20 (MPC-20), and 30% (MPC-30) calcium-reduced MPC85 were obtained from Idaho Milk Products, Jerome, ID with the composition shown in Table 5.1. MPC-20 is a commercially available calcium-reduced MPC known as IdaPlus 1085. Calcium-reduced MPCs were manufactured by injecting CO_2 into pasteurized skim milk before ultrafiltration as per the method provided by Marella et al. (2015). In this study, a split-plot design with 3 types of MPC (control, MPC-20, and MPC-30) with 85% protein content on dry basis (MPC85) and 2 replicates are considered as a whole plot. Three levels of sodium hexametaphosphate (SHMP) (0, 0.15, and 0.25% (w/w)) were considered in sub-plot. The influence of SHMP and calcium-reduced MPCs on heat stability, apparent viscosity, and particle

size was studied in 2 phases and in duplicate. In phase I, reconstituted solutions were prepared using only MPCs with 3 levels of calcium. In phase II, an nutrition dairy formulation containing MPC was evaluated (Table 5.2).

Table 5.1. Compositions of the MPC powders used to formulate a high-protein dairy beverage. Total solids, protein, and calcium percent are given as mean ± standard deviation.

MPC	Total solids (%)	Protein (%)	Calcium (%)	Calcium Reduction (%)
Control	94.73±0.18	80.77±0.02	2.21±0.04	-
20% Ca reduced	95.13±0.89	80.77±0.55	1.73±0.02	21.7
30% Ca reduced	94.70±0.17	80.02±0.14	1.47±0.02	33.5

Table 5.2. Dairy beverage formulation used in preparation of phase II formulations.

Ingredients	Percent	Sources
MPC85	9.76	Idaho Milk Products, Jerome, ID
Corn Maltodextrin	2.90	Maltrin M100, GPC, Muscatine, IO
Sugar (sucrose)	1.21	C&H Sugar, Crockett, CA
Canola Oil	0.68	Crisco, Orrville, OH
Potassium citrate	0.12	Sigma Aldrich, St. Louis, MO
Cellulose Gum	0.12	TICACEL-700 MCC, TIC Gums, Inc., White Marsh, MD
Carrageenan	0.02	Ticaloid 100, TIC Gums, Inc., White Marsh, MD
Cellulose Gel	0.02	TICACEL-700 MCC, TIC Gums, Inc., White Marsh, MD
Gellan Gum	0.12	Ticagel Gellan DPB, TIC Gums, Inc., White Marsh, MD
Deionized Water	85.05	
Total	100.00	

Phase I

Control and calcium-reduced MPCs were reconstituted in distilled water to make 8% (w/w) protein in the final solution. The reconstitution was carried out at approximately 45°C and the solution was maintained at 45°C under constant stirring for 30 min using a magnetic stirrer. The pH of the reconstituted MPCs was adjusted to 7.0 using 0.5 N NaOH for the solutions when pH < 7.0 and no pH adjustments were done for solutions when pH > 7.0. The pH adjusted solutions were divided into 3 equal parts and were mixed with 0, 0.15, and 0.25% SHMP under constant stirring for additional 10 min. Subsequently, the samples were homogenized using a hand-held homogenizer (Polytron PT 2500 E, Luzern, Switzerland) at 5000 rpm for 30 s. Homogenized MPC solutions were further divided into 2 equal parts. One part was filled in 6 mL glass vials and brought to 140°C in an oil bath for 15 s and immediately transferred to an ice bath to cool down. Time required to bring the solution in 6 mL vial at 140°C was determined during preliminary experiments. Subsequently glass vials were used to measure the apparent viscosity, particle size, and color to determine the effect of heat treatment. The other unheated portion was used to measure the heat coagulation time (HCT), apparent viscosity, particle size, and color.

Phase II

A dairy-based beverage was formulated using control and calcium-reduced MPCs to prepare 8% (w/w) protein in the final formulation. The other ingredients in the formulation included corn maltodextrin, sugar (sucrose), canola oil, potassium citrate, and gums. The composition of the formulation used in phase II is shown in Table 5.2. The pH of the formulations was adjusted to 7.0 when the pH <7.0, following the same procedure as phase I. Further division into 3 equal parts and subsequent addition of SHMP, homogenization, and

analysis of physical properties of heated and unheated samples was followed as described in phase I.

Apparent Viscosity

The apparent viscosity of the heated and unheated solutions from phase I and II was measured using controlled stress rheometer (ATS RheoSystems, NJ) using a bob and cup set up with 13 mL of sample volume. Apparent viscosity was measured at 20°C at a shear rate of $100s^{-1}$ and compared statistically.

Particle Size

The particle size of the heated and unheated solutions from phase I and II solutions was measured using Dynamic Light Scattering (DLS) technique with a Zetasizer Nano ZSP (Malvern instruments Ltd., Malvern, UK) using a method adapted from Silva et al. (2001). Samples were diluted 50 times in calcium imidazole buffer to avoid rapid dilution of samples and transferred into a disposable cuvette for analysis. This system is equipped with a helium/neon laser at 633 nm wavelength and at a backscattering angle of 173° at 10mW. The particle size was measured at 25°C at 20 s intervals for 2 repeated measurements. The autocorrelation function of the intensity scattering from the particles calculated the mean hydrodynamic diameter (Z-average mean).

Color

L*, a*, and b* values of heated and unheated MPC solutions in Phase I and II were measured using colorimeter (HunterLab, Miniscan XE, Reston, VA). L* corresponds to whiteness, a* corresponds to green to red on the positive-to-negative scale, respectively, and b* corresponds to blue to yellow on the positive-to-negative scale, respectively. The colorimeter was calibrated against white and green standards provided (Nasirpour et al., 2006).

Heat Stability

A sample volume of 3 mL was transferred into glass tubes and capped securely before immersion in the oil bath (Narang Scientific Works Pvt. Ltd., New Delhi, India). Tubes were placed on the rocking frame and placed in an oil bath at 140°C to observe HCT. HCT is defined as the time required for the visual coagulation of the sample after it was placed in an oil bath at the given temperature (Singh, 2004).

Statistical Analysis

Statistical analysis of replicates was performed using SAS (version 9.1, SAS Institute Inc., Cary, NC). The experiment followed a split-plot design with MPC type and replicate as whole plot factors and concentration of SHMP as sub-plot factors. PROC GLIMMIX procedure was used for the analysis and Tukey's test was used to determine the significant differences between treatments and were declared significant when $P \leq 0.05$.

Results and Discussion

Casein micelles are composed of submicelles consisting of casein proteins bound together by hydrophobic interactions and CCP (Chandrapala, 2009). In a stable milk system, there exists a mineral equilibrium between colloidal and serum phases which determines the casein micelle integrity. However, when a chelating agent is added to the milk system, the chelating agent binds to ionic calcium and consequently disturbing the mineral equilibrium between the colloidal and serum phases. As a result, additional calcium migrates from the colloidal phase to the serum phase. At this stage, the casein micelle is still intact due to hydrophobic interactions. On chelation of calcium above a critical level, casein micelles destabilize and dissociate as submicelles (Panouillé et al., 2004) as shown in mechanism I of Figure 5.1. According to Pitkowski et al. (2008), the extent of dissociation depends on the

concentration of casein and concentration and type of chelating salt. They also suggested that dissociation of casein micelles was a cooperative process, i.e., casein micelles were either fully dissociated or remained intact until critical level calcium was chelated. Pitkowski et al. (2008) and Griffin et al. (1988) suggested that calcium can be chelated from the casein micelle in lower amounts without disturbing the integrity of casein micelles. However, casein micelle dissociates completely at higher concentrations of chelating agents such as SHMP.

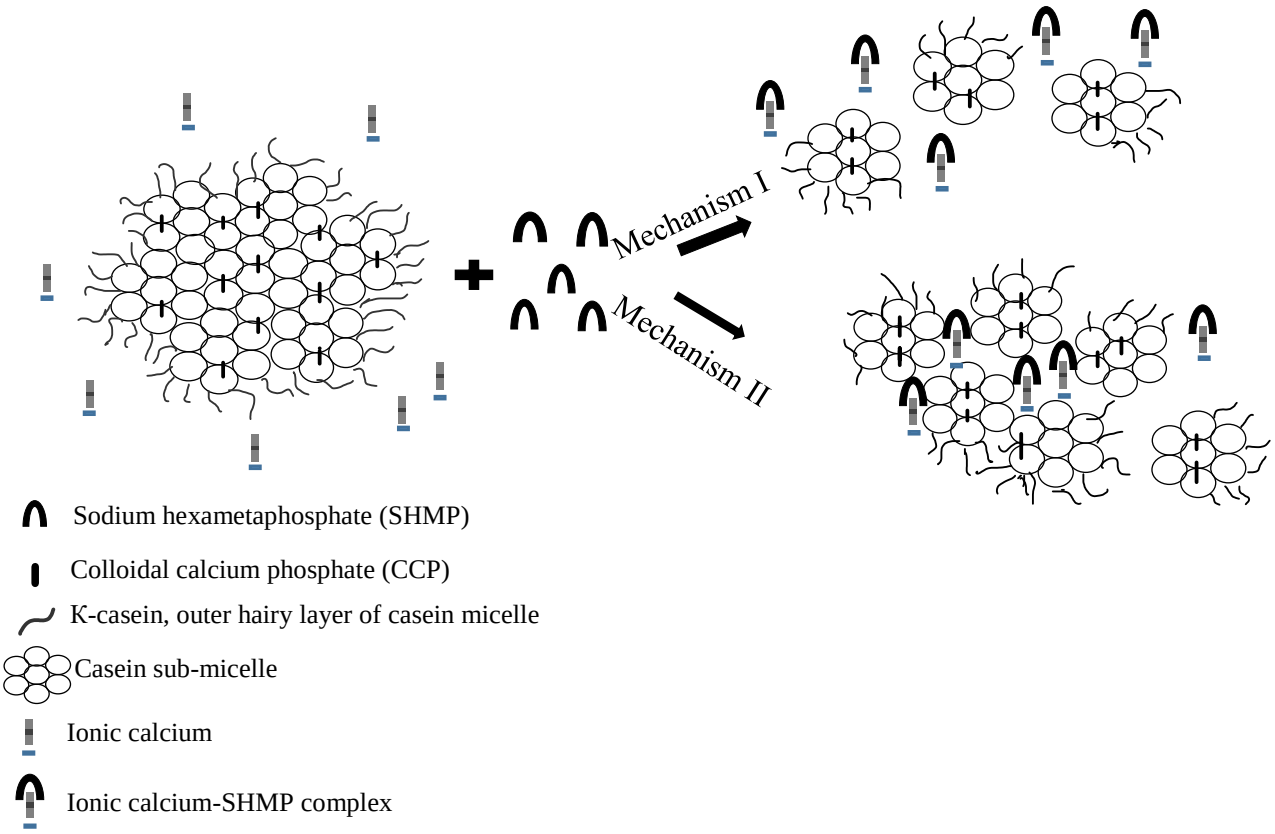

Figure 5.1. Illustration of interaction between casein micelles and sodium hexametaphosphate (SHMP). Mechanism I: Dissociation of casein micelles by addition of SHMP. Mechanism II: Formation of calcium-casein phosphate complexes in excess SHMP.

In addition to calcium chelation, SHMP can crosslink with casein proteins due to its 6 negative charges and homogenous charge distribution. When SHMP is present in higher concentrations, it also forms calcium-casein phosphate complexes in the presence of calcium (McCarthy et al., 2017) as shown in Figure 5.1 (mechanism II). Understanding the role of calcium, caseins, and SHMP as a chelator can help understand the changes in the physical and functional properties of high-protein dairy beverages.

Phase I

Apparent Viscosity. ***Unheated MPC Solutions.*** The apparent viscosity of the heated and unheated MPC solutions is shown in Table 5.3. Reconstituted MPC solutions of the control exhibited no significant difference in apparent viscosity between 0% SHMP (6.62 cP) and 0.15% SHMP but a significant increase in apparent viscosity as the SHMP concentration increased to 0.25% (56.54 cP). Similarly, in MPC-20, solutions had no significant change as SHMP concentration increased from 0 to 0.15%. However, an increase from 5.04 to 29.70 cP was observed when SHMP concentration increased from 0 to 0.25%. Increase in apparent viscosity of control and MPC-20 solutions occurred because of the diffusion of caseins into serum phase due to dissociation of casein micelles after addition of SHMP. McCarthy et al. (2017) also observed that, after the addition of SHMP to 5% MPC solutions, apparent viscosity increased because of the calcium chelation and casein cross-links formed *via* calcium-casein phosphate complexes in the serum phase. The calcium-SHMP complex formation prevents calcium interaction with caseins and avoids aggregation. On the other hand, MPC-30 had viscosities in the range of 7.30 to 12.53 cP, with no significant difference at all levels of SHMP studied because of the lower calcium levels, leading to easy dissociation of casein micelles. Similarly, in the absence in SHMP, there was no significant difference in the viscosities of control, MPC-20, and MPC-30.

Apparent viscosity of solutions did not significantly increase as SHMP concentration increased from 0 to 0.15% in control, MPC-20, and MPC-30. This implies that the extent of casein micelles dissociation was the same in control, MPC-20, and MPC-30 at 0.15% SHMP. However, when 0.25% SHMP was added, apparent viscosity of control increased by 9-fold, whereas MPC-20 had an increase of only 6-fold. On the other hand, there was no significant increase in apparent viscosity in MPC-30 at all the 3 levels of SHMP studied. The higher extent of increase in apparent viscosity of control was assumed to be due to the presence of higher calcium than MPC-20 and MPC-30. We theorize that the presence of higher calcium in control results in calcium-casein phosphate complexes as the SHMP concentration increased to 0.25%, resulting in higher increase in apparent viscosity, as described in mechanism II of Figure 5.1. de Kort et al. (2011) and McCarthy et al. (2017) also observed a strong affinity of SHMP not just towards the calcium but also towards caseins. As calcium decreased in MPC-20 and MPC-30, dissociation of casein micelles occurred easily along with minimum formation of calcium-casein phosphate complexes as shown in mechanism I from Figure 5.1. This reduced the increase in apparent viscosity at 0.25% SHMP in MPC-20 compared to control and had no significant difference in MPC-30.

Heated MPC Solutions. Heated MPC solutions showed no significant interaction effect between main effects, i.e., calcium concentration in MPC and SHMP concentration. And there was no significant difference in the viscosities of the MPC solutions and they were in the range of 2.89-3.88 cP in control, 3.74 to 5.34 cP in MPC-20, and 3.65 to 4.86 cP in MPC-30. Hence, these results were not further discussed. It is assumed that the reduced calcium in MPC and addition of strong chelating agent like SHMP dissocaited casein micelles to a greater extent that

interaction among denatured whey proteins and reaggregation of casein micelles did not infleunce the viscosity.

Table 5.3. Apparent viscosity (cP) of the unheated and heated solutions at $100s^{-1}$ shear rate in phase I given as mean ± standard deviation from excel.

MPC	SHMP (%)	Unheated	Heated
Control	0	6.62 ± 0.07^{c}	2.89 ± 0.11^{NS}
	0.15	15.85 ± 0.64^{bc}	3.12 ± 0.49^{NS}
	0.25	56.54 ± 8.71^{a}	3.88 ± 0.05^{NS}
20% Ca reduced	0	5.04 ± 0.43^{c}	3.74 ± 0.27^{NS}
	0.15	16.69 ± 3.05^{bc}	5.60 ± 0.98^{NS}
	0.25	29.70 ± 0.07^{b}	5.34 ± 0.81^{NS}
30% Ca reduced	0	7.30 ± 1.61^{c}	3.65 ± 0.74^{NS}
	0.15	11.71 ± 0.33^{c}	4.65 ± 1.27^{NS}
	0.25	12.53 ± 2.47^{c}	4.86 ± 0.67^{NS}

Sodium hexametaphosphate (SHMP)
NS- No significant interaction effect between main effects
Apparent viscosity was compared within a column
Values with the same superscript in a column are not significantly different (P>0.05)

Particle Size. ***Unheated MPC Solutions.*** Particle size of heated and unheated MPC solutions are given in Table 5.4. A significant decrease in the particle size was observed in control as the concentration of the SHMP increased. Particle size decreased from 192 to 90 nm when 0.15% SHMP was added to the solutions, but only decreased to 82 nm on further addition of SHMP in 0.25%. This observed decrease in particle size was because of the dissociation of casein micelles into submicelles and non-micellar casein proteins as the calcium was chelated by SHMP (Panouillé et al., 2004; Mizuno and Lucey, 2005; de Kort et al., 2011; Kaliappan and Lucey, 2011). Similarly, in MPC-20 there was a decrease from 186 to 87 nm on 0.15% SHMP addition and decreased further to 76 nm on 0.25% SHMP addition. However, in the case of

MPC-30, there was a significant decrease in particle size when SHMP was added in 0.15% from 108 to 83 nm with no further significant decrease as concentration increased to 0.25%. Particle size decreases in control, MPC-20, and MPC-30 with increasing SHMP concentration support the apparent viscosity results discussed in an earlier section. It is evident from apparent viscosity and particle size data that calcium percentage in MPCs influenced the extent of casein micelle dissociation, confirming that the lower the calcium percent, the higher the dissociated casein micelles. These observations also support the findings in apparent viscosity that the presence of larger particle size in the control are attributed to CCP keeping micelles intact, whereas in MPC-20 and MPC-30 they dissociated faster due to reduced calcium, even in the absence of SHMP. Although significant dissociation of casein micelles was observed in absence of SHMP, it did not influence the apparent viscosity of the MPC solutions.

Heated MPC Solutions. Particle size in MPC solutions increased after heat treatment due to the heat-induced interactions between proteins. The increase in particle size is attributed to reaggregation of dissociated casein micelles among themselves and with denatured whey proteins (Singh and Fox, 1987). The increase in particle size was also the result of deposition of precipitated calcium phosphate on the casein micelles (Chen and O'Mahony, 2016). When reconstituted MPC solutions were heated in phase I, there was a significant increase in the particle size of control as SHMP concentration increased from 0 to 0.15% and then decreased on further addition to 0.25%. A similar trend followed in MPC-20 and MPC-30 as well, where particle size increased on addition of 0.15% SHMP because of initial swelling caused by calcium chelation. Particle size decreased upon addition of 0.25% SHMP due to casein micelle dissociation. On the other hand, in the absence of SHMP, there was no significant difference in the particle size in control (229.04 nm), MPC-20 (235.47 nm), and MPC-30 (229.16 nm). This

suggests that in the absence of SHMP, the reduced calcium percent in the MPCs had no influence on the particle size.

Table 5.4. Particle size (nm) of the unheated and heated solutions in phase I given as mean ± standard deviation.

MPC	SHMP (%)	Unheated	Heated
Control	0	192.14±0.59^{a}	229.04±8.25^{d}
	0.15	90.71±0.77^{d}	380.24±2.64^{a}
	0.25	82.13±1.05^{f}	337.12±1.77^{b}
20% Ca reduced	0	186.61±1.07^{b}	235.47±4.24^{d}
	0.15	87.52±0.49^{de}	270.29±5.71^{c}
	0.25	76.65±2.66^{g}	223.45±5.27^{d}
30% Ca reduced	0	108.53±0.81^{c}	229.16±7.34^{d}
	0.15	83.56±1.21^{ef}	268.40±8.84^{c}
	0.25	65.56±0.08^{h}	246.25±3.74^{cd}

Sodium hexametaphosphate (SHMP)
Particle size was compared within a same column
Values with the same superscript in a column are not significantly different (P>0.05)

Color. ***Unheated MPC Solutions.*** To emphasize on the change in lightness of MPC solutions only L* values were discussed.

Measured L* values of the unheated and heated MPC solutions in phase I are given in Table 5.5. Whiteness and turbidity of the milk are attributed to the polydisperse casein micelles. Hence, dissociation of casein micelles decreases both whiteness and turbidity, and reduces the L* values as well (Kaliappan and Lucey, 2011; McCarthy et al., 2017). There was no significant difference in L* of control solutions at all levels of SHMP studied and L* were reported in the range of 73-75. Similar observation was made in MPC-20 as well, where no significant difference was observed in L* values with SHMP levels studied. However, in MPC-30, 0 and

0.15%, SHMP has no significantly different L* values. However, on addition of 0.25% SHMP, a significant difference was observed with a lowest L* of 58. This is due to of the reduced opacity of the solution on dissociation of casein micelles due to calcium chelation.

Table 5.5. L* of the unheated and heated solutions in phase I given as mean ± standard deviation.

MPC	SHMP (%)	Unheated	Heated
Control	0	74.38 ± 0.00^{b}	76.77 ± 2.31^{a}
	0.15	75.35 ± 0.01^{b}	72.58 ± 0.60^{a}
	0.25	73.15 ± 1.29^{b}	64.22 ± 1.05^{b}
20% Ca reduced	0	79.05 ± 1.56^{a}	73.79 ± 1.76^{a}
	0.15	77.93 ± 2.66^{ab}	55.34 ± 1.22^{c}
	0.25	74.02 ± 0.28^{b}	41.99 ± 0.64^{d}
30% Ca reduced	0	74.64 ± 0.33^{b}	71.01 ± 2.11^{a}
	0.15	75.72 ± 1.51^{b}	58.25 ± 1.61^{bc}
	0.25	58.41 ± 1.63^{c}	45.23 ± 1.32^{d}

Sodium hexametaphosphate (SHMP)
Lightness (L*) was compared within the column
Values with same superscript in a column are not significantly different (P>0.05)

Heated MPC Solutions. L* of control solutions had no significant change observed when SHMP concentration increased from 0 to 0.15% but decreased significantly from 76 to 64 with increase in SHMP concentration from 0% to 0.25%. In the case of MPC-20, L* decreased as SHMP concentration increased from 0 to 0.15% and further to 0.25%. A similar observation was made in MPC-30 heated solutions as well. The decrease in L* is attributed to the translucency of the solutions due to casein micelle dispersion as the SHMP concentration increased, resulting in low whiteness values (Crudden et al., 2005). In the absence of SHMP, there was no significant difference between control, MPC-20, and MPC-30, though there was evidence of casein micelle dissociation from particle size results.

Heat Stability. Heat stability is one of the important attributes considered when estimating the processing parameters and stability of proteins in milk systems. When milk is heated to high temperatures (120 -140°C), changes in mineral equilibria between serum and colloidal phase along with dissociation of κ-casein from casein micelle surface can lead to steric destabilization of casein micelles. At pH >6.9, heat-induced coagulation is sensitive to calcium-ion concentration in κ-casein depleted casein micelles (Singh, 2004). Calcium-ion concentration, pH, and protein concentration are a few important factors that determine the heat stability in milk systems. At pH > 6.7, Crowley et al. (2014) observed a significant decrease in HCT at 140°C by approximately 20 min in 3.5 % reconstituted solutions prepared from MPCs in the range of MPC 35-MPC 90. This decreased HCT was due to increase in calcium-ion activity along with heat-induced dissociation of κ-casein. To improve the heat stability of the milk systems, especially in dairy beverages, calcium chelators are added to reduce the free calcium-ion concentration and susceptibility of ultra-high temperatures during processing (Kaliappan and Lucey, 2011).

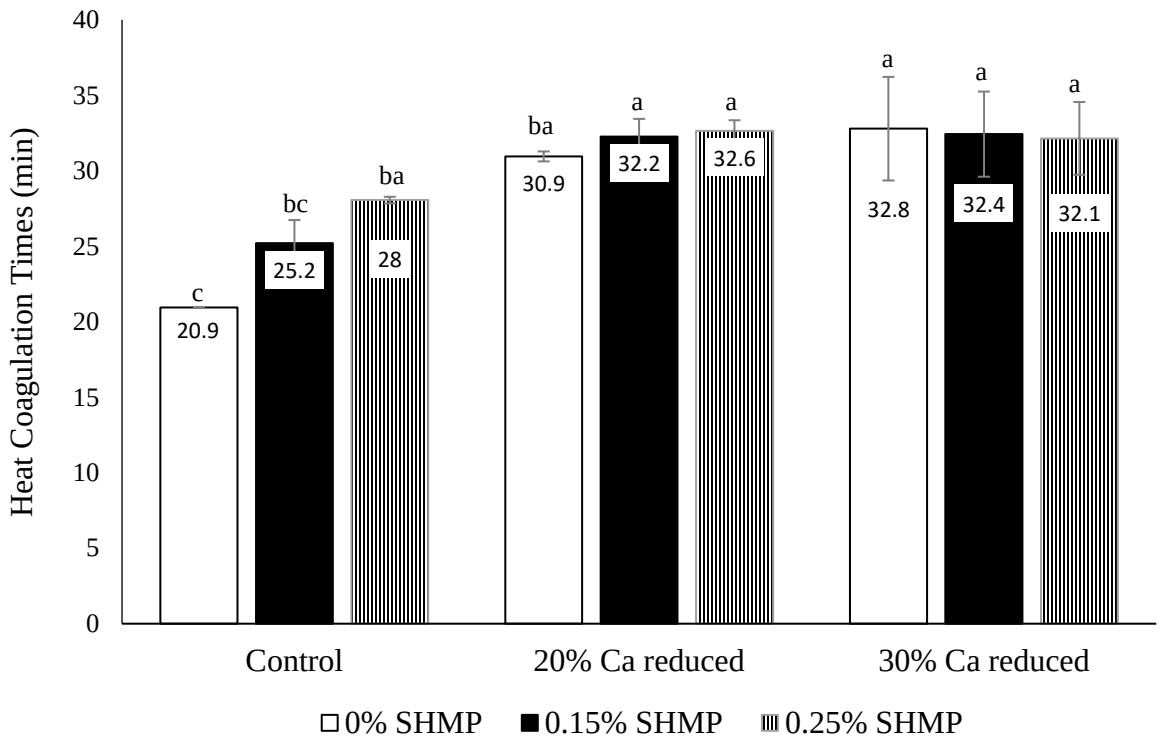

Figure 5.2. Heat Coagulation Time (HCT) of the solutions prepared using control, 20% calcium-reduced MPC (MPC-20), and 30% calcium-reduced MPC (MPC-30) in 8% protein MPC solutions of phase I with sodium hexametaphosphate (SHMP) at different levels. Values with same superscript are not significantly different (P>0.05).

In this study, dominating factors that could change mineral equilibria include the concentration of calcium in the MPC and SHMP. HCTs of the MPC solutions in phase I are shown in Figure 5.2. In control, the significant increase in HCT was only observed when SHMP concentration increased from 0 (20.9 min) to 0.25% (28 min). Calcium chelating salts like SHMP decrease the availability of the free calcium-ions in the serum phase, and thereby reducing the calcium-mediated aggregation of caseins (Augustin and Clarke, 1990). Whereas, there was no significant difference in HCT of MPC-20 at different levels of SHMP and measured HCTs were in the range of 30-32 min. This is because of the disruption of casein micellar structure integrity as SHMP concentration increased, resulting in rapid coagulation. de Kort et al.

(2012) also observed that HCT of the 9% (w/v) micellar casein isolate solution at pH 7.0 decreased as the SHMP concentration increased. As the concentration above 7.5mmol/L (0.45% w/v) was used, calcium was completely chelated, resulting in complete dissociation of casein micelle and leading to a faster coagulation and lower HCT. Similar observation was found in MPC-30 as well, where HCTs were approximately 32 min for all levels of SHMP studied.

In the absence of SHMP, HCT increased by 10 and 12 min in MPC-20 and MPC-30, respectively, when compared to control. This significant increase in HCT can be attributed to the reduced calcium content in the MPCs, which increased the casein micelle stability at higher temperatures. These results support the fact that the calcium concentration in MPC plays a key role in determining the HCT of the reconstituted MPC solutions. Faka et al. (2009) observed an increase in heat stability during in-can sterilization of 25% reconstituted low-heat skim milk when the calcium-ion concentration was reduced. It was also concluded that calcium-ion concentration played a more important role than the pH in improving the heat stability during in-can sterilization of reconstituted skim milk. These results suggest that heat stability of the reconstituted MPC solutions can be significantly improved by using calcium-reduced MPCs rather than with the addition of chelating salts like SHMP.

Phase II

Apparent Viscosity. ***Unheated Formulations.*** Phase II formulations had an increase in apparent viscosity of control and MPC-20 as the SHMP concentration increased, following the same trend as phase I and shown in Table 5.6. MPC formulations in control showed a significant increase from 85.61 to 194.27 cP as the SHMP increased to 0.15%. The highest apparent viscosity of 426.53 cP was observed in control formulation with 0.25% SHMP. As described in

mechanism II of Figure 5.1, the extremely high apparent viscosity in 0.25% SHMP of control was due to the cross-linking ability of SHMP (McCarthy et al., 2017).

MPC-20 had a significant increase from 30.54 to 105.52 cP as SHMP was added in 0.15%, and further increased to 164.95 cP on addition of 0.25% SHMP. In MPC-30, there was no significant difference in apparent viscosity at all SHMP concentrations studied. However, in case of phase II formulations, higher viscosities compared to phase I were contributed by the gums present in the formulations, giving a thickening effect (Lal et al., 2006). As discussed earlier, apparent viscosity increase was also caused by SHMP and citrate by dissociating casein micelles into serum phase.

Increase in apparent viscosity was more prominent in control as the concentration of SHMP increased from 0% to 0.25% when compared to apparent viscosity increase in MPC-20 formulations. As explained in phase I, this is the result of varying calcium concentrations which could change the extent of casein micelle dissociation and formation of calcium-casein phosphate complexes on addition of SHMP as illustrated in Figure 5.1. There was no significant difference in apparent viscosity of control, MPC-20, and MPC-30 in the absence of SHMP in phase II as well.

Heated Formulations. Heated formulations of phase II have higher apparent viscosities when compared to heated solutions of phase I. On heating, components of formulation like gums tend to react with κ-caseins and form a network. This network binds to the water molecules, increasing the apparent viscosity and also hydrating the proteins and stabilizing them (Lal et al., 2006). Increased total solids and the presence of carbohydrates also increased the protein hydrodynamic volume after heat treatment and consequently the viscostities of formulations (Gao et al., 2010; Chen and O'Mahony, 2016).

Table 5.6. Apparent viscosity (cP) of unheated and heated solutions at 100s^{-1} shear rate in phase II given as mean ± standard deviation.

MPC	SHMP (%)	Unheated	Heated
Control	0	85.61±1.41^{cd}	124.66±0.48^{bc}
	0.15	194.27±1.03^{b}	235.61±0.86^{a}
	0.25	426.53±26.20^{a}	224.35±1.91^{a}
20% Ca reduced	0	39.54±7.98^{d}	97.88±6.36^{c}
	0.15	105.52±10.72^{c}	100.78±23.38^{bc}
	0.25	164.95±5.44^{b}	237.75±21.07^{a}
30% Ca reduced	0	53.23±9.19^{cd}	186.38±1.94^{ab}
	0.15	79.54±9.82^{cd}	168.50±49.07^{ab}
	0.25	78.09±16.19^{cd}	176.04±25.69^{ab}

Sodium hexametaphosphate (SHMP)
Apparent viscosity was compared within the column irrespective of the phase
Values with the same superscript in a column are not significantly different (P>0.05)

Formulations of control exhibited a significant increase in apparent viscosity from 124 cP at 0% SHMP to 235 cP as SHMP was added in 0.15%, and had no significant change on increasing the concentration to 0.25%. In the case of MPC-20, lowest apparent viscosities of 97 and 100 cP were observed at 0 and 0.15% SHMP addition, respectively. A significant increase of apparent viscosity was observed only at 0.25% SHMP addition. Apparent viscosity increased from 97 cP at 0% SHMP to 237 cP at 0.25% of SHMP. This reported increase in the viscosities with added SHMP in phase II was due to the exposure of phosphoserine residues, leading to increased electrostatic repulsions as the calcium was chelated. These repulsions caused dissociation of caseins from casein micelles, increasing the apparent viscosity. Whereas, MPC-30 showed no significant difference at all levels of SHMP studied and observed viscosities were in the range of 168 to 186 cP. These relatively higher viscosites and the different trend in MPC-30 compared to unheated MPC-30 formulations was due to the aggregation of casein

submicelles. Dissociated casein submicelles form aggregates on heating and are reported to continue growing in number and size until they form a gel, resulting in increase in apparent viscosity (Panouillé et al., 2004).

Particle Size. ***Unheated Formulations.*** Particle size of phase II unheated formulations is given in Table 5.7, and the same trend as phase I was observed. Particle size significantly decreased in control from 236 to 176 nm, with an increase in SHMP concentration from 0 to 0.15%. A further decrease to 123 nm was observed on the addition of 0.25% SHMP. A similar observation was made in MPC-20 as well, but particle size only decreased significantly from 163 to 148 nm on the addition of 0.15% and further down to 126 nm at 0.25% SHMP. In the case of MPC-30, particle size decreased from 135 nm at 0% SHMP to 112 nm at 0.15% with no significant change with increase in SHMP concentration. As described in the apparent viscosity section of unheated formulations, dissociation of casein micelles was caused by both SHMP and citrate in this phase II. Control has significantly higher particle size, followed by MPC-20 and MPC-30 in absence of SHMP. Like phase I solutions, casein micelle dissociation did not influence the apparent viscosity of the formulations in this case.

Heated Formulations. In case of heated formulations, a significant decrease in particle size from 263 to 246 nm was only observed as the concentration increased from 0 to 0.25% in control. Similarly, MPC-20 had a significant decrease in particle size from 252 to 214 nm as SHMP concentration increased from 0 to 0.25%. This reported decrease in particle size as SHMP concentration increased is due to the casein micelle dissociation by SHMP and citrate in the formulation. However, in MPC-30, the particle size increased from 315 to 331 nm as the SHMP concentration increased from 0 to 0.15% and decreased to 303 nm on further increase to 0.25%. These observations correlated well with apparent viscosity data explained for phase II. Particle

size increase in MPC-30 in the absence of SHMP was attributed to the interaction between dispersed casein aggregates and denatured whey proteins. The addition of 0.15% SHMP caused more swelling, resulting in increased particle size, and further addition of SHMP caused casein micelle dissociation. In the absence of SHMP, particle size was not significantly different between control and MPC-20, but there was a reported an increase in MPC-30 because of the casein micelle aggregation.

Table 5.7. Particle size (nm) of unheated and heated solutions in phase II given as mean ± standard deviation.

MPC	SHMP (%)	Unheated	Heated
Control	0	236.08 ± 1.98^{a}	263.45 ± 1.52^{c}
	0.15	176.35 ± 4.84^{b}	259.28 ± 5.80^{cd}
	0.25	123.00 ± 1.03^{f}	246.44 ± 4.61^{d}
20% Ca reduced	0	163.09 ± 1.01^{c}	252.86 ± 1.57^{cd}
	0.15	148.43 ± 1.24^{d}	225.26 ± 3.38^{e}
	0.25	126.18 ± 3.91^{ef}	214.69 ± 1.71^{e}
30% Ca reduced	0	135.64 ± 1.50^{e}	315.26 ± 5.25^{b}
	0.15	112.28 ± 1.55^{g}	331.46 ± 4.34^{a}
	0.25	105.35 ± 2.44^{g}	303.81 ± 2.17^{b}

Sodium hexametaphosphate (SHMP)
Particle size was compared within a same column
Values with the same superscript in a column are not significantly different (P>0.05)

Color. ***Unheated MPC Formulations.*** There is no significant difference in L* of control formulations at all levels of SHMP studied. L* was in the range of 69 to 75 in control formulations. In case of MPC-20, L* significantly decreased to 62 on addition of 0.25% SHMP and had no significant change between 0 and 0.15% SHMP. This decrease was due to the casein micelle dissociation which caused reduced opacity in the formulations. In MPC-30, there was no

significant change in the L* of formulations at all levels of SHMP studied, and L* were in the range of 62-67. In the absence of SHMP, there was no significant difference between L* values of control, MPC-20, and MPC-30.

Heated MPC Formulations. There was no significant interaction effect between calcium concentration of MPC and SHMP concentration main effects in a*, b*, and L* of heated formulations. There were no significant differences in the main effects as well, implying that the color was not influenced by either SHMP concentration or calcium percent in MPCs. On heating the formulations, formation of brown pigments from the Maillard reaction was similar in all the treatment levels studied.

Table 5.8. L* of unheated and heated solutions in phase II given as mean ± standard deviation.

MPC	SHMP (%)	Unheated	Heated
Control	0	69.01 ± 2.03^{abc}	70.16 ± 3.33^{NS}
	0.15	75.02 ± 3.81^{ab}	65.27 ± 0.12^{NS}
	0.25	72.27 ± 1.84^{ab}	58.72 ± 1.42^{NS}
20% Ca reduced	0	76.28 ± 1.57^{a}	64.24 ± 1.39^{NS}
	0.15	72.64 ± 2.22^{ab}	54.62 ± 1.20^{NS}
	0.25	62.43 ± 2.05^{c}	50.76 ± 0.77^{NS}
30% Ca reduced	0	67.88 ± 1.99^{bc}	58.54 ± 4.72^{NS}
	0.15	63.98 ± 0.04^{c}	52.51 ± 0.89^{NS}
	0.25	62.05 ± 2.06^{c}	52.00 ± 0.17^{NS}

Sodium hexametaphosphate (SHMP)
Lightness (L*) was compared within a same column
NS- No significant interaction effect between main effects
Values with same superscript in a column are not significantly different (P>0.05)

Heat Stability. HCTs of phase II formulations are shown in Figure 5.3 and are considerably less as compared to phase I MPC solutions. Although there was the same protein percent in phase I and II, the presence of other ingredients influenced the heat stability of phase II formulations. The presence of carbohydrates like maltodextrin and sucrose have been reported to negatively influence the heat stability of dairy beverage formulations, reducing the overall HCTs in phase II (Chen and O'Mahony, 2016). Gao et al. (2010) also found that after the addition of 10% sucrose, calcium ion activity increased in skim milk due to the combination of protein hydration and volume exclusion. These changes in calcium ion activity caused by the composition of the formulation resulted in the lower HCTs in phase II as compared to phase I.

There was a significant decrease in the HCT of control as the SHMP concentration increased from 0 (7.1 min) to 0.25% (3.8 min). This is because of the potassium citrate in formulation, which also acted as a calcium chelating agent (Le Ray et al., 1998; Kaliappan and Lucey, 2011) along with the increasing concentration of SHMP. When calcium was chelated beyond its threshold limit, it destabilized the casein micelles, inducing dissociation, causing aggregation, and decreasing heat stability (de Kort et al., 2012).

In the case of MPC-20, HCT significantly decreased as SHMP was added at 0.15 and 0.25%. Highest HCT was reported in MPC-20 with 0% SHMP with 9.3 min, where as in 0.15 and 0.25% of SHMP it was in the range of 4-6 min. In MPC-30, HCT was not significantly different at 0 and 0.15% SHMP with 6.2 min and decreased significantly to 5.2 min on 0.25% SHMP addition.

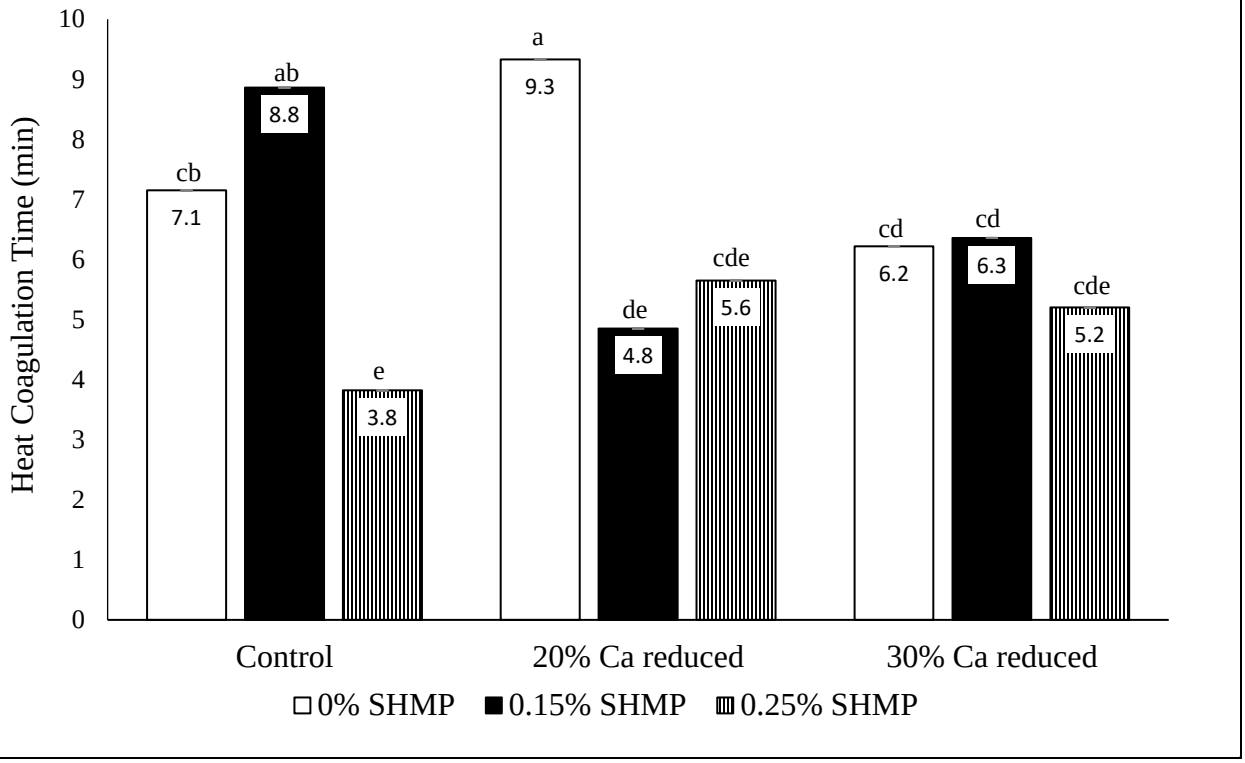

Figure 5.3. Heat Coagulation Time (HCT) of the dairy beverage formulations prepared using control, 20% calcium-reduced MPC (MPC-20), and 30% calcium-reduced MPC (MPC-30) in phase II with sodium hexametaphosphate (SHMP) at different levels. Values with same superscript are not significantly different (P>0.05).

In the absence of SHMP, MPC-20 has ~2 min of higher HCT compared to control and MPC-30. This is because of the calcium chelation in formulations within the threshold limit to keep the casein micelle stabilized. Whereas, on the addition of 0.15% SHMP, control has significantly higher HCT compared to MPC-20 and MPC-30. The addition of 0.15% SHMP chelated calcium beyond threshold destabilized the casein micelles. These results illustrate the importance of calcium percentage and amounts to be chelated to attain optimum heat stability in the dairy beverage formulations. This observation also opens an opportunity to use calcium-reduced MPC to improve the heat stability without the addition of SHMP as an ingredient in the dairy beverage formulations.

Conclusions

In phase I MPC solutions, HCT increased as calcium was chelated by SHMP in the control and resulted in no change in MPC-20 and MPC-30. Whereas in phase II, due to the presence of other ingredients, there was a different trend observed. In phase II, MPC-20 with no added SHMP showed highest heat stability. However, the addition of SHMP negatively influenced HCT of MPC-20 and MPC-30. In phase I and II, increased apparent viscosity with addition of SHMP is attributed to casein micelle dissociation because of calcium chelation. Particle-size data supported the observations regarding casein micelle dissociation on SHMP addition. Easier dissociation of casein micelles, even in absence of SHMP, was observed in MPC-20 and MPC-30 because of reduced calcium percentage, with the lowest apparent viscosity in MPC-20. These results suggest application of calcium-reduced MPCs would improve the heat stability even in presence of other ingredients of formulation. Application of calcium-reduced MPCs also eliminates the addition of chelating salts, contributing to a consumer-friendly label and saving processing and formulation costs. Dairy beverages should be evaluated on storage stability when calcium-reduced MPCs are used as a main ingredient.

Acknowledgements

This project is Kansas State Research and Extension contribution number 18-270-J. Idaho Milk Products, Jerome, ID for their generous donation of MPC powders is greatly appreciated. Use of names and names of ingredients is only for scientific clarity and does not constitute any endorsement of product by the authors or Kansas State University. We thank Dr. Chenchaiah Marella and Dr. Lloyd Metzger for their support during this research.

References

Anema, S.G., D.N. Pinder, R.J. Hunter, and Y. Hemar. 2006. Effects of storage temperature on the solubility of milk protein concentrate (MPC85). Food Hydrocoll. 20:386–393.

Augustin, M.A. 2000. Mineral salts and their effect on milk functionality. Aust J. Dairy Technol. 55:61–64.

Augustin, M.-A., and P.T. Clarke. 1990. Effects of added salts on the heat stability of recombined concentrated milk. J. Dairy Res. 57:213–226.

Chandrapala, J.J.S. 2009. Effect of concentration, pH and added chelating agents on the colloidal properties of heated reconstituted skim milk. PhD Thesis. Monash Univ., Australia.

Chen, B., and J.A. O'Mahony. 2016. Impact of glucose polymer chain length on heat and physical stability of milk protein-carbohydrate nutritional beverages. Food Chem. 211:474–482.

Crowley, S.V., M. Megemont, I. Gazi, A.L. Kelly, T. Huppertz, and J.A. O'Mahony. 2014. Heat stability of reconstituted milk protein concentrate powders. Int. Dairy J. 37:104–110.

Crudden, A., D. Afoufa-Bastien, P.F. Fox, G. Brisson, and A.L. Kelly. 2005. Effect of hydrolysis of casein by plasmin on the heat stability of milk. Int. Dairy J. 15:1017–1025.

Datta, N., and H.C. Deeth. 2001. Age Gelation of UHT Milk—A Review. Food Bioprod. Process. 79:197–210.

Faka, M., M.J. Lewis, A.S. Grandison, and H. Deeth. 2009. The effect of free Ca2+ on the heat stability and other characteristics of low-heat skim milk powder. Int. Dairy J. 19:386–392.

Fang, Y., S. Rogers, C. Selomulya, and X.D. Chen. 2012. Functionality of milk protein concentrate: Effect of spray drying temperature. Biochem. Eng. J. 62:101–105.

Gao, R., H.P. van Leeuwen, E.J. Temminghoff, H.J. van Valenberg, M.D. Eisner, and M.A. van Boekel. 2010. Effect of disaccharides on ion properties in milk-based systems. J. Agric. Food Chem. 58:6449–6457.

Griffin, M.C.A., R.L.J. Lyster, and J.C. Price. 1988. The disaggregation of calcium-depleted casein micelles. European Journal of Biochemistry 174:339–343.

Kaliappan, S., and J.A. Lucey. 2011. Influence of mixtures of calcium-chelating salts on the physicochemical properties of casein micelles. J. Dairy Sci. 94:4255–4263.

de Kort, E., M. Minor, T. Snoeren, T. van Hooijdonk, and E. van der Linden. 2011. Effect of calcium chelators on physical changes in casein micelles in concentrated micellar casein solutions. Int. Dairy J. 21:907–913.

de Kort, E., M. Minor, T. Snoeren, T. van Hooijdonk, and E. van der Linden. 2012. Effect of calcium chelators on heat coagulation and heat-induced changes of concentrated micellar casein solutions: The role of calcium-ion activity and micellar integrity. Int. Dairy J. 26:112–119.

Lagrange, V., D. Whitsett, and C. Burris. 2015. Global Market for Dairy Proteins. J. Food Sci. 80: A16–A22.

Lal, S.N.D., C.J. O'Connor, and L. Eyres. 2006. Application of emulsifiers/stabilizers in dairy products of high rheology. Adv. Colloid Interface Sci. 123–126:433–437.

Le Ray, C., J.-L. Maubois, F. Gaucheron, G. Brulé, P. Pronnier, and F. Garnier. 1998. Heat stability of reconstituted casein micelle dispersions: changes induced by salt addition. Le Lait 78:375–390.

Marella, C., P. Salunke, A.C. Biswas, A. Kommineni, and L.E. Metzger. 2015. Manufacture of modified milk protein concentrate utilizing injection of carbon dioxide. J. Dairy Sci. 98:3577–3589.

McCarthy, N.A., O. Power, H.B. Wijayanti, P.M. Kelly, L. Mao, and M.A. Fenelon. 2017. Effects of calcium chelating agents on the solubility of milk protein concentrate. Int. J. Dairy Technol. 70:415–423.

Mizuno, R., and J.A. Lucey. 2005. Effects of Emulsifying salts on the turbidity and calcium-phosphate–protein interactions in casein micelles. J. Dairy Sci. 88:3070–3078.

Nasirpour, A., J. Scher, M. Linder, and S. Desobry. 2006. Modeling of lactose crystallization and color changes in model infant foods. J. Dairy Sci. 89:2365–2373.

Panouillé, M., T. Nicolai, and D. Durand. 2004. Heat induced aggregation and gelation of casein submicelles. Int. Dairy J. 14:297–303.

Petersen, B., and L.S. Ward, inventors. 2014. Method for improving viscosity, solubility, and particle size of milk protein concentrates. U.S. Classification 426/42, 426/657, assignee. US Pat. No. US20140199436 A1.

Pitkowski, A., T. Nicolai, and D. Durand. 2008. Scattering and Turbidity Study of the Dissociation of Casein by Calcium Chelation. Biomacromolecules 9:369–375.

Ramchandran, L., X. Luo, and T. Vasiljevic. 2017. Effect of chelators on functionality of milk protein concentrates obtained by ultrafiltration at a constant pH and temperature. J. Dairy Res. 1–8.

Silva, F.V., G.S. Lopes, J.A. Nóbrega, G.B. Souza, and A.R.A. Nogueira. 2001. Study of the protein-bound fraction of calcium, iron, magnesium and zinc in bovine milk. Spectrochim. Acta Part B At. Spectrosc. 56:1909–1916.

Singh, H. 2004. Heat stability of milk. Int. J. Dairy Technol. 57:111–119.

Singh, H., and P.F. Fox. 1987. Heat stability of milk: role of β-lactoglobulin in the pH-dependent dissociation of micellar κ-casein. J. Dairy Res. 54:509–521.

Xu, Y., D. Liu, H. Yang, J. Zhang, X. Liu, J.M. Regenstein, Y. Hemar, and P. Zhou. 2016. Effect of calcium sequestration by ion-exchange treatment on the dissociation of casein micelles in model milk protein concentrates. Food Hydrocoll. 60:59–66.

Chapter 6 - Influence of milk protein concentrates with modified calcium content on the dairy beverage formulation: Storage stability

Abstract

Controlling the calcium-mediated storage defects like age gelation and sedimentation were evaluated in high-protein dairy beverages during storage. To investigate the effects of reduced calcium ingredients on storage stability, 2 batches each of milk protein concentrates (MPC) with 3 levels of calcium content were acquired (control, 20% calcium-reduced (MPC-20), and 30% calcium-reduced (MPC-30)). Control and calcium-reduced MPCs were used to formulate 8% (w/w) protein dairy beverages. The formulation also consisted of other ingredients like gums, maltodextrin, potassium citrate, and sucrose. The pH-adjusted formulation was divided into 2 parts, one with 0.15% sodium hexametaphosphate (SHMP) and the other with no SHMP. The formulations were homogenized, and retort-sterilized at 121°C for 15 min. The retort-sterilized beverages were stored at room temperature (25°C) for up to 90 days and particle size and apparent viscosity were measured on days 0, 7, 30, 60, and 90. Beverages formulated using control MPC with 0 and 0.15% SHMP exhibited sedimentation, causing a decrease in apparent viscosity by approximately 10 cP and clear phase separation by day-90. MPC-20 beverages with 0% SHMP exhibited stable particle size and apparent viscosities during storage. Whereas, in presence of 0.15% SHMP, particle size increased rapidly by 40 nm on day-90, implying the start of progressive gelation. On the other hand, highest apparent viscosities leading to gelation were observed in MPC-30 beverages at both concentrations of SHMP studied. These results suggested that the beverages formulated with 20% calcium-reduced MPC and with no SHMP would improve storage stability by maintaining lower apparent viscosities. Further reduction of calcium to 30% resulted in rapid gelation of beverages during storage.

Introduction

Over a decade, ready-to-drink (**RTD**) beverages have been in high demand because of their convenience and nutritional benefits. Milk protein concentrates (**MPC**) are one of the preferred ingredients to formulate dairy beverages because of its same casein-to-whey protein ratio as in milk. By using MPC, protein content in dairy beverages can be increased. However, mineral-protein and protein-protein interactions during storage results in defects like sedimentation and age gelation (Datta and Deeth, 2001; Gazi and Huppertz, 2015).

Several research studies reported various ways to improve storage stability of dairy beverages either by using additives or by modifying the properties of ingredients used in the formulation. Cano-Ruiz and Richter (1998) delayed age gelation by adding cyclic polyphosphates like sodium hexametaphosphate (**SHMP**) to formulation before retort sterilization to dissociate casein micelles into sub-micelles. This study also reported that age gelation in retort-sterilized dairy beverages was effectively controlled by cyclic polyphosphates than linear polyphosphates. As the dissociated casein micelles increased, sedimentable caseins during storage decreased in dairy beverages (Harwalkar, 1982). Chen and O'Mahony (2016) observed the influence of adding glucose polymers to 8.5% protein beverages formulated using milk protein isolate. Their study concluded that maltodextrin reduced sedimentation of proteins in beverages during accelerated physical stability testing. Petersen and Ward (2014) demonstrated that the sensory properties of beverages can be improved by modifying the MPC production. The authors added transglutaminase to the milk during MPC production to produce MPC concentrate with smaller particle size and lesser apparent viscosity, resulting in the smooth-tasting beverage. It was also reported that increased heat treatment induced more casein micelle

interactions with denatured whey proteins, delaying the dissociation of β-lactoglobulin and κ-casein complexes during storage, thus delaying gelation (McMahon 1996).

Challenges in improving the storage stability of dairy beverages are characterized as sedimentation and age gelation. Sedimentation is a phenomenon that occurs due to aggregation of κ-casein depleted casein micelles to form a protein layer at the bottom of a beverage container (Gaur et al., 2018). However, sedimentation can be reversed upon shaking, but over the longer storage period, proteins settled at the bottom, resulting in a separation of a serum top phase and a protein sediment phase (Anema, 2017). Though the initial sedimentation phase was reversible, it still can affect consumer acceptance. The extent of sedimentation increased as storage temperature and storage period increased (Cano-Ruiz and Richter, 1998; Malmgren et al., 2017).

Age gelation is another major storage defect in high-protein dairy beverages that concerns the dairy industry. Physical changes occurring during age gelation in dairy beverages was explained in 4 stages by Datta and Deeth (2001). A short first stage of product thinning, followed by a longer second stage with a slight change in viscosity. The third stage can be identified by an increase in viscosity because of the gelation and during the fourth stage, the viscosity decreases due to the gel breakdown, resulting in syneresis.

Casein micelle stability during storage was determined by factors like ionic calcium, pH, composition of the beverage, and plasmin activity (Datta and Deeth, 2001; Anema, 2017). Partial demineralization of calcium proved to improve functional properties of MPC (Marella et al., 2015) as well as dissociation of casein micelles in skim milk (Xu et al., 2016). An earlier part of this study about determining the physiochemical properties of calcium-reduced MPCs also proved that 20% reduced calcium improved the heat stability without any chelating agent in 8% protein formulations. The objective of this study was to further investigate the influence of

calcium-reduced MPCs and the presence of a chelating agent on the storage stability of high-protein dairy beverages.

Materials and Methods

Experimental Design

MPC powders with 3 levels of calcium percentage, 0 (control), 20 (**MPC-20**), and 30% (**MPC-30**) were obtained from Idaho Milk Products, Jerome, ID, in 2 batches with the composition given in Table 6.1. MPC-20 is also a commercially available calcium-reduced MPC known as IdaPlus 1085. MPC powders with desired calcium concentrations were produced by injecting carbon dioxide into pasteurized skim milk before and during ultrafiltration process as described by Marella et al. (2015). A split-plot study was designed with MPCs of 3 levels of calcium percentage and 2 replicates as whole plot factors, whereas 2 levels of SHMP (with and without SHMP) as sub plot factors. Storage stability of the retort sterilized dairy beverages was evaluated by measuring particle size and apparent viscosity on 0, 7, 30, 60, and 90 days of the storage period, and the color was only measured on day 0.

Table 6.1. Compositions of the MPC powders used to formulate a high-protein dairy beverage. Total solids, protein, and calcium percentage are given as mean ± standard deviation.

MPC	Total solids (%)	Protein (%)	Calcium (%)	% Reduction
Control	94.73±0.18	80.77±0.02	2.21±0.04	-
20% Ca reduced	95.13±0.89	80.77±0.55	1.73±0.02	21.7
30% Ca reduced	94.70±0.17	80.02±0.14	1.47±0.02	33.5

Preparation of High-Protein Dairy Beverages

Dairy beverages were prepared using a formulation given in Table 6.2. MPCs with varying calcium concentrations were reconstituted to 8% (w/w) dry basis protein solutions using two-thirds of the distilled water given in formulation (Table 6.2). Reconstituted solutions were constantly stirred for 30 min using an overhead stirrer with a 4-blade propeller (Caframo, Georgian Bluffs, Ontario, Canada) at approximately 45°C. The solution was placed in a water-bath maintained at 45°C to ensure complete solubilization of the MPC powder. Other ingredients in the formulation (gums, corn maltodextrin, sugar (sucrose), potassium citrate, and canola oil) were mixed in one-thirds of the remaining water using a magnetic stirrer. The two solutions were mixed, and the formulation was stirred for an additional 10 min. pH was adjusted to 7.0 using 0.5 N NaOH if pH of the formulations was <7.0, and if pH was ≥ 7.0, no changes were made. The pH adjusted formulations were divided into 2 equal parts, to which no SHMP and 0.15% SHMP was added. Subsequently, formulations were homogenized at 5000 rpm for 30 s using a hand-held homogenizer (Polytron PT 2500 E, Luzern, Switzerland) and filled in 20 mL glass vials. Sealed vials were retort sterilized in an autoclave (Steris Amsco 3023, Sanford, FL) at 121°C for 15 min. Retort sterilized vials were cooled down and stored undisturbed at room temperature (25°C). Subsequent vials were opened on days 0, 7, 30, 60, and 90 of storage period for the further analysis.

Particle size

The dynamic Light Scattering technique was used to measure particle size with a Zetasizer Nano ZSP (Malvern Instruments Ltd., Malvern, UK) using a method adapted from Silva et al. (2001). The equipment is facilitated with a helium/neon laser at 633 nm wavelength and at a backscattering angle of 173° at 10mW. Retort sterilized beverage vials were vortexed for

10 s to obtain a homogenous mixture and then diluted 50 times in calcium imidazole buffer and transferred into a disposable cuvette for analysis. Average hydrodynamic diameter (z-average mean) was calculated by an autocorrelation function from the intensity scattering of particles measured at 25°C at 20 s intervals for 2 repeated measurements. Mean particle size of replicates was reported in the results and discussion.

Table 6.2. The composition of formulation used to prepare high-protein dairy beverages.

Ingredients	Percent	Sources
MPC85	9.76	Idaho Milk Products, Jerome, ID
Corn Maltodextrin	2.90	Maltrin M100, GPC, Muscatine, IO
Sugar (sucrose)	1.21	C&H Sugar, Crockett, CA
Canola Oil	0.68	Crisco, Orrville, OH
Potassium citrate	0.12	Sigma Aldrich, St. Louis, MO
Cellulose Gum	0.12	TICACEL-700 MCC, TIC Gums, Inc., White Marsh, MD
Carrageenan	0.02	Ticaloid 100, TIC Gums, Inc., White Marsh, MD
Cellulose Gel	0.02	TICACEL-700 MCC, TIC Gums, Inc., White Marsh, MD
Gellan Gum	0.12	Ticagel Gellan DPB, TIC Gums, Inc., White Marsh, MD
Deionized Water	85.05	
Total	100.00	

Apparent Viscosity

The apparent viscosity of retort sterilized dairy beverages were measured using a controlled stress rheometer (ATS RheoSystems, Bordentown, NJ) in a bob and cup geometry at 20°C. A sample volume of 13 mL was used to measure the apparent viscosity at shear rate of 100

s^{-1} and compared statistically. Mean apparent viscosity of replicates was reported in the results and discussion.

Color

L*, a*, and b* parameters of retort sterilized beverages were measured using a hand-held colorimeter (HunterLab, Miniscan XE, Reston, VA). L* is a measure of whiteness, a* is a measure of green-to-red on a positive to negative scale, respectively, and b* is a measure of blue-to-yellow on a positive to negative scale, respectively (Nasirpour et al., 2006). White and green standards provided were used to standardize the colorimeter as suggested by manufacturer.

Statistical Analysis

The results obtained were statistically analyzed using SAS (version 9.1, SAS Institute Inc., Cary, NC). For the analysis of variables on same day of storage, split-plot analysis was used. MPC types was considered as whole plot factors and concentrations of SHMP were considered as sub-plot factors. PROC GLIMMIX procedure was used for the analysis and Tukey's test was used to determine the significant differences between treatment levels and were declared significant when $P \leq 0.05$. For statistical analysis of variables during storage, repeated measures analysis was used. PROC GLM function was used to identify the significant effects of main effects.

Results and Discussion

When a high-protein milk system at neutral pH is heated above 80°C, whey proteins denature and form aggregates between themselves. However, association of denatured whey proteins with casein micelles is limited by the chaperone like activity of κ-casein (Guyomarc'h et al., 2009). In addition to the denaturation and aggregation of whey proteins during heating, calcium phosphate precipitates, leading to mineral imbalance. Consequently, calcium migrates

from the colloidal phase to the serum phase to reestablish the mineral equilibrium (Dalgleish and Law, 1989). Upon further heating, casein micelle destabilizes, and forms aggregates due to lack of sufficient colloidal calcium phosphate (**CCP**). Pyne (1958) observed that chelating agents are added in lower concentrations to stabilize casein micelle and increase the heat stability. However, addition of chelating agents in higher concentrations chelated calcium beyond critical limit, resulting in casein micelle dissociation into non-micellar caseins (Augustin and Clarke, 1990; Singh, 2004). When a chelating agent such as SHMP is added to the high-protein milk system, it binds to the ionic calcium in the serum phase, resulting in migration of the colloidal calcium to the serum phase to reestablish mineral equilibrium. When a heat treatment is given to a milk system with dissociated casein micelles and whey proteins at neutral pH, reversible aggregates are formed at low heating temperatures and time. On the other hand, increasing the severity of heat treatment causes irreversible aggregates of non-micellar caseins and denatured whey proteins (Singh and Fox, 1987; Panouillé et al., 2004).

Effect of Beverage Formulation on Physico-Chemical Properties

In this section, the effect of reduced calcium MPCs in presence or absence of SHMP on the particle size and the apparent viscosity of retort sterilized beverages was studied. The comparison of these properties was done between beverages immediately after the retort sterilization.

Particle Size. The particle size was significantly influenced by the type of MPC, concentration of the SHMP, and the interaction of MPC × SHMP in the beverages as shown in whole-plot in Table 6.3. In the absence of SHMP, no significant difference was observed between beverages formulated with the control MPC (187 nm) and MPC-20 (202 nm). On the other hand, the particle size significantly increased in beverages formulated with MPC-30 (302

nm) as shown in Figure 6.1. The increase in the particle size in beverages formulated with MPC-30 can be attributed to the reduced calcium association with casein micelles and caused casein micelle dissociation resulting in non-micellar caseins. Consequently, when the formulation was heated, non-micellar caseins and denatured whey proteins reaggregated to form approximately 300 nm-size particles.

In the presence of SHMP in the formulation, casein micelles dissociated to form heat-induced reaggregates of non-micellar caseins and denatured whey proteins, causing an increase in the particle size in beverages (Panouillé et al., 2004). However, a significant increase in the particle size was only observed in beverages formulated with control MPC. The particle size significantly increased from 187 (with no SHMP) to 274 nm (0.15% SHMP), in beverages formulated with control MPC. Whereas, in MPC-20 and MPC-30 beverages, further dissociation of casein micelles had no significant difference on the particle size. Significantly higher particle size was observed in beverages formulated with MPC-30, with 302 nm in the absence of SHMP, and 315 nm when 0.15% SHMP was added. As the calcium percentage reduced, casein micelle dissociation occurred easily even in the absence SHMP, resulting in the formation of larger heat-induced protein reaggregates.

Table 6.3. Mean squares (MS) and probabilities (in parentheses) of measured changes in particle size and apparent viscosity in retort sterilized high-protein dairy beverages during 90-day storage.

	Particle size		Apparent Viscosity	
Factors	df	MS	df	MS
Whole-plot				
MPC	2	54367.74(.0001)	2	50417.84(<.001)
Rep	1	130.74(0.3211)	1	8.06(0.7061)
SHMP	1	2837.72(0.0117)	1	7221.11(.0011)
MPC × SHMP	2	26403.41(.0004)	2	6727.81(.0010)
Error	3	92.98	3	46.81
Sub-plot				
Time	4	1770.31(<.0001)	4	505.78(<.001)
Time × MPC	8	846.59(.0004)	8	1368.50(<.001)
Time × SHMP	4	257.8(0.0739)	4	1021.12(<.001)
Time × MPC × SHMP	8	1264.43(<.0001)	8	1227.27(<.001)
Error(Time)	12	91.70	12	21.19

Sodium hexametaphosphate (SHMP)

Apparent Viscosity. The apparent viscosity was significantly influenced by the type of MPC, presence of SHMP, and the interaction of MPC × SHMP in the beverages as shown in whole-plot in Table 6.3. During the retort processing, heat-induced protein reaggregates continue to grow in size and number until they form a gel, leading to increased apparent viscosity (Panouillé et al., 2004). Beverages formulated with control MPC and MPC-20 had no significant difference in the apparent viscosity. Whereas, beverages formulated with MPC-30 had significantly higher apparent viscosities as shown in Figure 6.2. This significant increase was because of the easier dissociation of casein micelles due to the lower calcium content in MPC-30 that increased heat-induced aggregates in the serum phase. The particle size data (Figure 6.1) obtained from beverages formulated with MPC-30 supported the observation made in the apparent viscosity.

When 0.15% SHMP was added to the formulation, SHMP interacted with the available calcium ions in the serum phase, altering the mineral equilibrium. Consequently, CCP was

migrated into the serum phase, resulting in casein micelle dissociation. The dissociated casein micelle facilitates the heat-induced protein reaggregation. In control, when 0.15% SHMP was added, apparent viscosity significantly increased to 50.69 cP from 14.51 cP without SHMP. On the other hand, beverages formulated with MPC-30 have the higher apparent viscosity than beverages formulated with control MPC and MPC-20 beverages. The apparent viscosity of MPC-30 beverages significantly increased from 137.50 cP (without SHMP) to 171.05 cP when 0.15% SHMP was added. As calcium percentage reduced in MPC, heat-induced reaggregates caused an increase in the apparent viscosity (Figure 6.2) and the particle size (Figure 6.1).

Color. L* (whiteness) has significant influence on the type of MPC but no significant effect by the concentration of SHMP. a* (green to red) has no significant influence by both the main effects (type of MPC and concentration of SHMP). On the other hand, b* (blue to yellow) has significant influence by both the main effects. There was no significant interaction effect of MPC × SHMP ($P>0.05$) in the L*, a*, and b* of the beverages after the retort sterilization. Irrespective of presence or absence of SHMP, there was no significant difference in the L* and a* of beverages formulated with control MPC, MPC-20, and MPC-30 as shown in Table 6.3. Whereas, the b* of beverages formulated with control MPC were significantly different from beverages formulated with MPC-20 and MPC-30 with and without SHMP. On the other hand, the b* of beverages formulated using MPC-20 and MPC-30 were in the range of 14.64- 16.69 with no significant difference between them. The increased b* in beverages formulated with MPC-20 and MPC-30 was assumed to be because of the exposed lysine residues due to the increased casein micelle dissociation promoting the interactions with lactose during the retort processing resulting in browning compounds (Devi et al., 2015).

Table 6.4. L*, a*, and b* values of the dairy beverages measured after retort processing on day 0 given as mean ± standard deviation.

MPC	SHMP (%)	L*	a*	b*
Control	0	63.41±1.06^{NS}	3.58±0.01^{NS}	10.86±0.72^{NS}
	0.15	65.36±0.24^{NS}	3.95±0.68^{NS}	13.44±0.49^{NS}
20% Ca reduced	0	62.40±0.02^{NS}	4.81±0.61^{NS}	15.60±0.66^{NS}
	0.15	62.56±1.67^{NS}	4.87±1.04^{NS}	16.69±0.69^{NS}
30% Ca reduced	0	61.83±0.97^{NS}	4.24±0.00^{NS}	14.64±0.37^{NS}
	0.15	62.61±1.04^{NS}	5.12±0.67^{NS}	16.15±1.03^{NS}

Sodium hexametaphosphate (SHMP)
Values were compared within column and with same superscript are not significantly different (P>0.05)
NS- No significant interaction effect between main effects
L* is the measure of whiteness on scale 0-100
a* is the measure green to red from positive to negative scale
b*is the measure of blue to yellow from positive to negative scale

From the results so far, it can be summarized that the extent of casein micelle dissociation determined the size of heat-induced reaggregates. As more non-micellar caseins are present in the formulation before the retort sterilization, the bigger the heat-induced reaggregates formed. Dissociation of casein micelles either by reduced calcium content or the addition of SHMP also affected the b* of color during the retort sterilization.

Physico-Chemical Changes in High-Protein Beverages During Storage

In this section, changes in the particle size and the apparent viscosity of the retort sterilized beverages during the 90-day storage are discussed.

Particle Size. The particle size of beverages during storage was significantly influenced by the type of MPC, presence of SHMP, Time, interactions of MPC × SHMP, Time × MPC, and Time × MPC × SHMP, whereas there was no significant influence of Time × SHMP as shown in the Table 6.3. In the absence of SHMP, the particle size of beverages formulated with control

MPC had no significant difference during storage, as shown in Figure 6.1. But when 0.15 % SHMP was added to the beverages with control MPC, the particle size significantly increased on day-7 and had no significant difference until day-90. The increased particle size on day-7 during storage was attributed to heat-induced protein reaggregation. Though there was no noticeable change in the particle size in the beverages formulated with control MPC irrespective of SHMP present, there was an evidence of visual sedimentation on day-60 and a clear phase separation on day-90. The × sign in Figure 6.1 identifies the visual observation of sedimentation. However, any absence of noticeable changes in the particle size was contributed by the sampling method. During vortexing the vial for 10 s to obtain a homogenous sample for particle size, the protein network was also disrupted.

In case of beverages formulated with MPC-20 with no SHMP, a significant and progressive increase in the particle size was observed until day-30, and no significant increase was observed thereafter until day-90. The progressive increase in the particle size until day-30 was due to continued reaggregation of proteins formed during the retort sterilization. In case of beverages with MPC-20 and 0.15% SHMP, the particle size stayed stable until an increase of approximately 50 nm was observed on day-90. This significant increase in particle size was because of progressive gelation caused by network formation between heat-induced reaggregates (Panouillé et al., 2004; Tsioulpas et al., 2010).

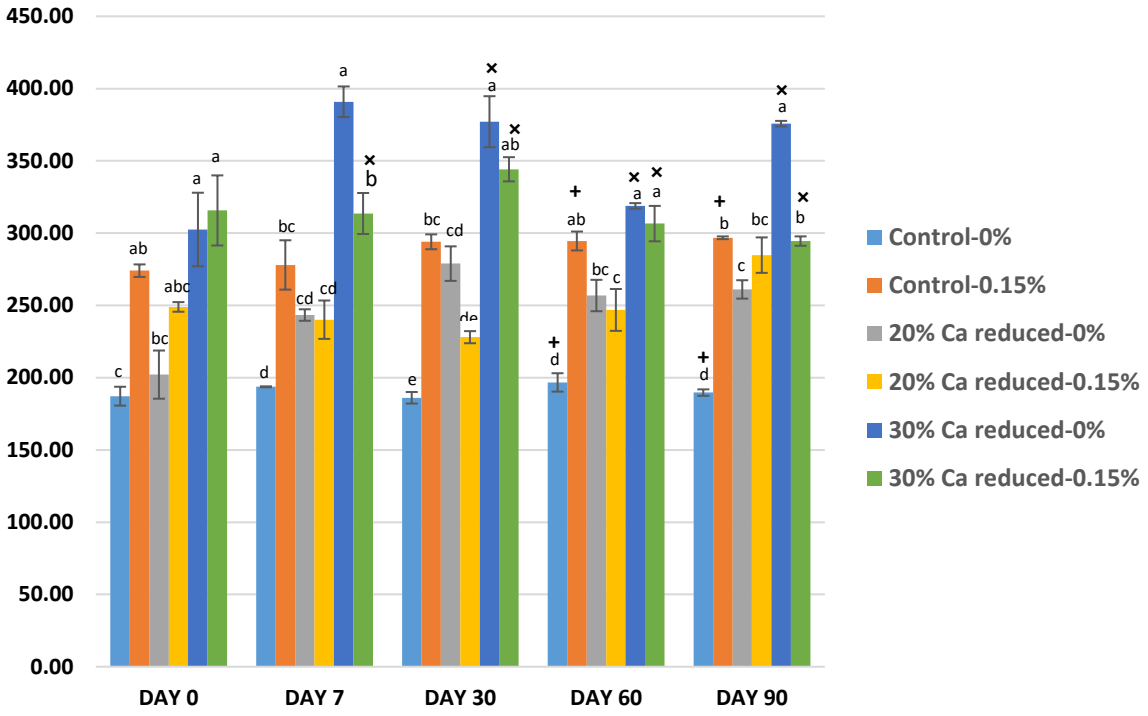

Figure 6.1. Particle size (nm) of retort sterilized dairy beverages during the 90-day storage at room temperature. Formulations were prepared using Control (0% calcium-reduced MPC), MPC-20 (20% calcium-reduced MPC), MPC-30 (30% calcium-reduced MPC) by adding 0 and 0.15% sodium hexametaphosphate (SHMP). (+) indicates the visual observation of sedimentation and (×) indicates visual observation of age gelation during storage of high-protein dairy beverage. Values of six treatment combinations were statistically compared within the same day during storage.

On the other hand, in beverages formulated with MPC-30 with no SHMP, an increase in the particle size by approximately 90 nm was observed on day-7, followed by a steady decrease until day-60. This increase of particle size on day-7 during storage can be attributed to the progressive gel formation because of the network between heat-induced protein reaggregates (Panouillé et al., 2004). Gradual decrease in the particle size followed by age gelation in the MPC-30 beverage was attributed to gel breakage and syneresis. When 0.15% SHMP was added to the formulation, the particle size significantly increased on day-30 followed by a gradual decrease by day-60 with no further change until day-90. From visual observation, it was evident

that gel breakage with syneresis already occurred by day-7 in MPC-30 beverage with 0.15% SHMP.

The results so far imply that reducing the calcium percentage in beverage formulation led to non-micellar caseins which reaggregated with denatured whey proteins and among themselves to increase the particle size during the retort sterilization. But when the particle size continued to increase in number and size during storage, rapid gelation occurred due to the network formed between heat-induced protein reaggregates as evident from MPC-30 beverages (Panouillé et al., 2004). These results also illustrate that the particle size can be a better predictor in determining the gelation than sedimentation.

Apparent Viscosity. The apparent viscosity was significantly influenced by the type of MPC, presence of SHMP, Time, interactions of MPC × SHMP, Time × MPC, Time × SHMP, and Time × MPC × SHMP, as shown in Table 6.3. In case of beverages formulated with control MPC in the absence of SHMP, the apparent viscosity had no significant difference until day-30 followed by a significant decrease by day-60. This significant decrease of approximately 10 cP from day-30 to day-60 can be attributed to the sedimentation. However, a distinct phase separation sediment protein layer at the bottom and top aqueous layer was not observed until day-90. In beverage formulated with control MPC and with no SHMP, a reversible sedimentation was observed by day-7 and showed no significant effect on the apparent viscosity. However, when 0.15% SHMP was added to the control formulations, a significant decrease in the apparent viscosity was observed by day-7 in contrast to beverages with no SHMP. This can be attributed to casein micelle dissociation, resulting in heat-induced protein reaggregates with casein micelles in the presence of SHMP. From Chapter-5, it was evident that casein micelles were not completely dissociated in control as compared to calcium-reduced MPCs when 0.15%

SHMP was added. Hence, it can be assumed that the association of heat-induced reaggregates with casein micelles can occur during the retort sterilization. During storage, these heat-induced reaggregates dissociate from the casein micelles, resulting in prominent reversible sedimentation by day-7 (Datta and Deeth, 2001; Panouillé et al., 2004). During storage, a significant decrease in the apparent viscosity by day-60 and day-90 was also observed in beverages formulated with control MPC with 0.15% SHMP, attributing to the sedimentation and phase separation. However, the particle size (Figure 6.1) in beverages formulated with control MPC with and without SHMP did not exhibit any significant changes during sedimentation or phase separation. Disruption of protein networks occurred during sample preparation for the particle size analysis could be the reason for no change in the particle size.

In case of beverages formulated with MPC-20 and with no SHMP, the apparent viscosity significantly increased by day-7 of storage and decreased by day-30. There was no significant difference in the apparent viscosity until day-90. An increase in the apparent viscosity on day-7 was attributed to the increased size of heat-induced protein reaggregates, facilitated by easier dissociation of casein micelles in MPC-20. These heat-induced reaggregates associate with casein micelles during the retort sterilization and dissociate during storage, leading to reversible sedimentation by day-30 (Datta and Deeth, 2001; Panouillé et al., 2004). The absence of an increase or decrease in the apparent viscosity during storage confirmed that the gelation or the sedimentation had not occurred yet in MPC-20 beverages with no SHMP. On the other hand, when 0.15% SHMP was added, the apparent viscosity in MPC-20 beverages significantly increased by day-7, and thereafter no significant changes were observed. The significant increase of the apparent viscosity by day-7 can be attributed to the increased size of heat-induced protein reaggregates, but the absence of any further decrease in the apparent viscosity suggest that there

was no reversible sedimentation observed. When 0.15% SHMP was added to the beverages formulated with MPC-20, it was hypothesized that the non-micellar caseins formed heat-induced protein reaggregates during the retort sterilization and caused an increase in the particle size and the apparent viscosity by forming a network. On the other hand, when the apparent viscosities of MPC-20 beverages on day-7 at 2 levels of SHMP were compared, the addition of 0.15% SHMP increased the apparent viscosity by approximately 6 times, confirming rapid growth in the network between heat-induced protein reaggregates (Panouillé et al., 2004; Tsioulpas et al., 2010).

In case of beverages formulated with MPC-30 with and without SHMP, significantly higher apparent viscosities were observed throughout the storage. A 30% reduction in calcium in MPC led to increased casein micelle dissociation, consequently forming heat-induced reaggregates between non-micellar caseins and denatured whey proteins. Increased aggregate size and number enabled easier network formation, resulting in rapid gelation (Tsioulpas et al., 2010). Increased apparent viscosity on day-30 of MPC-30 beverages with no SHMP, followed by a decrease with no further changes, was attributed to the age gelation, followed by gel breakage and syneresis. However, in beverages formulated with MPC-30 with 0.15 % SHMP, the apparent viscosity rapidly decreased by approximately 80 cP by day-7. This rapid significant decrease can be attributed to gel breakage and syneresis by day-7, which is evident from the visual observation as well. Because gel matrix was disrupted to obtain a homogenous sample for the particle size analysis, these changes were not exhibited in the particle size data (Figure 6.1). Beverages formulated with MPC-30 and 0.15% SHMP exhibited another significant rapid increase in the apparent viscosity by day-60, which was assumed to be because of stronger gel formation by interlinking with protein reaggregates in the supernatant.

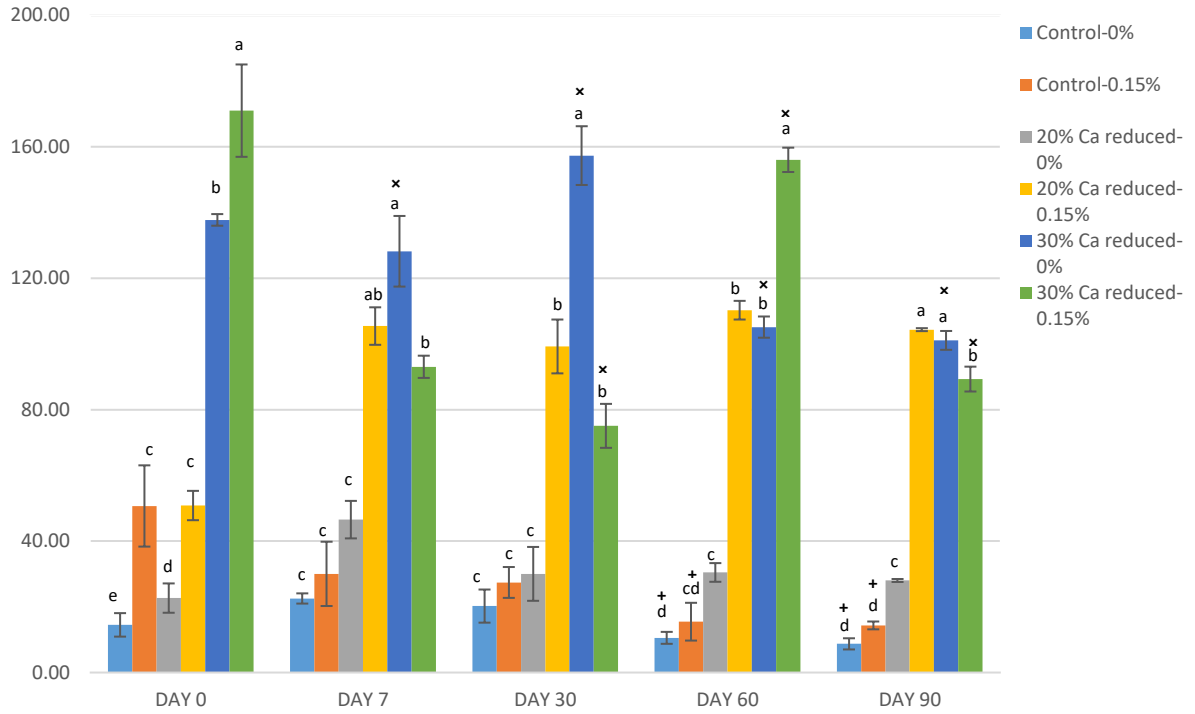

Figure 6.2. Apparent viscosity (cP) at 100s^{-1} shear rate of retort sterilized dairy beverages during the 90-day storage at room temperature. Formulations were prepared using Control (0% calcium-reduced MPC), MPC-20 (20% calcium-reduced MPC), MPC-30 (30% calcium-reduced MPC) by adding 0 and 0.15% sodium hexametaphosphate (SHMP). (+) indicates the visual observation of sedimentation and (×) indicates visual observation of age gelation during storage of high-protein dairy beverage. Values of six treatment combinations were statistically compared within the same day during storage.

It is noteworthy to observe that the apparent viscosities of beverages formulated with MPC-20 and with no SHMP were closer in range of apparent viscosities of control beverages. On the other hand, apparent viscosities of beverages formulated with MPC-20 with 0.15% were higher and closer to apparent viscosities of beverages formulated with MPC-30. Distinct differences in the apparent viscosity of beverages formulated with MPC-20, with and without SHMP, marks the importance of the amount of calcium to be chelated to obtain beverages with the preferred apparent viscosity. Though heat-induced reaggregates were formed in beverages formulated with MPC-20, the amount of calcium reduced was able to keep the reaggregates stable in the beverages. Results from this study also demonstrate that calcium percentage affects

the rate at which gelation occurs. Gelation is distinct and occurred rapidly in beverages formulated with MPC-30 compared to MPC-20 beverages. Tsioulpas et al. (2010) also reported a coagulation in in-can sterilized skim milk when 0.2% SHMP was added. It was explained that coagulation was due to an increase in casein micelle size as the concentration of SHMP increased, supporting the observations made in this study. The particle size and the apparent viscosity results in this study were in agreement with Anema (2017), who also observed an increase in the particle size due to aggregation of casein micelles before the onset of gelation in UHT milk samples.

Summarizing the observation from this and previously published study, it is evident that 20% calcium-reduced MPC application in high-protein dairy beverages improves heat stability and storage stability without the addition of any chelating agent. Because of the different heat treatments employed along with usage of different compositions of dairy beverages in the literature, the apparent viscosities and particle sizes cannot be compared directly to explain the exact phenomenon of sedimentation and age gelation during storage. To develop a high-protein dairy beverage with improved storage stability, further studies to understand the role of non-protein components is necessary.

Conclusions

During a 90-day storage, the retort sterilized beverages formulated using control exhibited no gelation, but the visual sedimentation by end of the 90-day storage was distinct. On the other hand, MPC-20 beverages without SHMP had consistent lower apparent viscosity throughout the storage with no visual sedimentation or gelation but when 0.15% SHMP was added, apparent viscosities significantly increased. Higher particle size and apparent viscosities leading to rapid gelation were found in beverages with MPC-30 with and without SHMP studied.

These results suggest that using 30% calcium-reduced MPC in the beverage formulation could lead to rapid gelation. Whereas, formulating beverages with 20% calcium-reduced MPC improved the storage stability with and without SHMP added. This study presents a way to improve the storage stability of the high-protein dairy beverages by formulating using 20% calcium-reduced MPC with no additives like SHMP.

Acknowledgements

This project is Kansas State Research and Extension contribution number 18-361-J. We would like to acknowledge Idaho Milk Products, Jerome, ID for their generous donation of MPC powders. Kansas State University neither endorses or takes responsibility for any products, goods or services offered by outside vendors. We thank Dr. Chenchaiah Marella and Dr. Lloyd Metzger for their support during this research.

References

Anema, S.G. 2017. Storage stability and age gelation of reconstituted ultra-high temperature skim milk. Int. Dairy J. 75:56–67.

Augustin, M.A., and P.T. Clarke. 1990. Effects of added salts on the heat stability of recombined concentrated milk. J. Dairy Res. 57:213–226.

Cano-Ruiz, M.E., and R.L. Richter. 1998. Changes in Physicochemical Properties of Retort-Sterilized Dairy Beverages During Storage. J. Dairy Sci. 81:2116–2123.

Chen, B., and J.A. O'Mahony. 2016. Impact of glucose polymer chain length on heat and physical stability of milk protein-carbohydrate nutritional beverages. Food Chem. 211:474–482.

Dalgleish, D.G., and A.J.R. Law. 1989. pH-induced dissociation of bovine casein micelles. II. Mineral solubilization and its relation to casein release. J. Dairy Res. 56:727 - 735

Datta, N., and H.C. Deeth. 2001. Age Gelation of UHT Milk—A Review. Food Bioprod. Process. 79:197–210.

Devi, A.F., R. Buckow, T. Singh, Y. Hemar, and S. Kasapis. 2015. Colour change and proteolysis of skim milk during high pressure thermal–processing. J. Food Eng. 147:102–110.

Gaur, V., J. Schalk, and S.G. Anema. 2018. Sedimentation in UHT milk. Int. Dairy J. 78:92–102.

Gazi, I., and T. Huppertz. 2015. Influence of protein content and storage conditions on the solubility of caseins and whey proteins in milk protein concentrates. Int. Dairy J. 46:22–30.

Grygorczyk, A. 2009. Biophysical studies of milk protein interactions in relation to storage defects in high protein beverages. MS Thesis. McGill Univ., MacDonald, Canada.

Guyomarc'h, F., M. Nono, T. Nicolai, and D. Durand. 2009. Heat-induced aggregation of whey proteins in the presence of κ-casein or sodium caseinate. Food Hydrocoll. 23:1103–1110.

Harwalkar, V.R. 1982. Age Gelation of Sterilized Milks. Pages 229-269 in Developments in Dairy Chemistry-1. P. F. Fox, ed. Applied Science Publishers, London, UK.

Malmgren, B., Y. Ardö, M. Langton, A. Altskär, M.G.E.G. Bremer, P. Dejmek, and M. Paulsson. 2017. Changes in proteins, physical stability and structure in directly heated UHT milk during storage at different temperatures. Int. Dairy J. 71:60–75.

Marella, C., P. Salunke, A.C. Biswas, A. Kommineni, and L.E. Metzger. 2015. Manufacture of modified milk protein concentrate utilizing injection of carbon dioxide. J. Dairy Sci. 98:3577–3589.

McMahon, D. 1996. Heat-Induced Changes in Beta-Lactoglobulin and the Stability of UHT Milk. 2nd Biennial Ultra-High Temperature Processing of Milk Symposium, Utah State University, Logan, Utah.

Nasirpour, A., J. Scher, M. Linder, and S. Desobry. 2006. Modeling of lactose crystallization and color changes in model infant foods. J. Dairy Sci. 89:2365–2373.

Panouillé, M., T. Nicolai, and D. Durand. 2004. Heat induced aggregation and gelation of casein submicelles. Int. Dairy J. 14:297–303.

Petersen, B., and L.S. Ward. 2014. Method for Improving Viscosity, Solubility, and Particle Size of Milk Protein Concentrates. U.S. Classification 426/42, assignee. US Pat. No. US20140199436 A1.

Pyne, G.T. 1958. The heat coagulation of milk: II. variations in sensitivity of casein to calcium ions. J. Dairy Res. 25:467–474.

Silva, F.V., G.S. Lopes, J.A. Nóbrega, G.B. Souza, and A.R.A. Nogueira. 2001. Study of the protein-bound fraction of calcium, iron, magnesium and zinc in bovine milk. Spectrochim. Acta Part B At. Spectrosc. 56:1909–1916.

Singh, H., and P.F. Fox. 1987. Heat stability of milk: role of β-lactoglobulin in the pH-dependent dissociation of micellar κ-casein. J. Dairy Res. 54:509–521.

Singh, H. 2004. Heat stability of milk. Int. J. Dairy Technol. 57:111–119.

Tsioulpas, A., A. Koliandris, A.S. Grandison, and M.J. Lewis. 2010. Effects of stabiliser addition and in-container sterilisation on selected properties of milk related to casein micelle stability. Food Chem. 122:1027–1034.

Chapter 7 - Conclusion

Focused beam reflectance measurement (FBRM) as an in-situ tool was used for monitoring isothermal crystallization of lactose at concentrations relevant to industrial application and found that FBRM has potential to monitor the chord length distribution of lactose crystals during crystallization without any need for sample preparation. Isothermal crystallization at 20°C and 50% lactose concentration resulted in the highest mean crystal chord lengths. It was also found that the FBRM-based technique is also a useful tool to detect secondary nucleation during lactose crystallization. In a different study, FBRM and other techniques (HPLC-based, Fourier-transform Infrared Spectroscopy (FTIR), and microscopic analysis) were used to study the effect of different cooling rates on lactose crystallization in deproteinized whey and milk permeates in terms of yield, crystal purity, and mean particle chord length. Reducing the time of crystallization from 17 h to 9 h did not significantly influence the lactose yield and particle chord length distribution at the end of crystallization. The microscopic analysis of lactose crystals suggested that the impurities were embedded at the apex of the crystal. From proximate and mineral analysis of lactose crystals it can be concluded that there were more impurities in crystals obtained milk permeate than deproteinized whey. Overall, this study suggested that the time of crystallization can be reduced by 8 h in production of lactose from concentrated permeates with no significant effect on lactose crystal purity and yield.

In a different study, the use of calcium-reduced MPC in high-protein dairy beverages was evaluated. It was found that 20% calcium-reduced MPC at 8% protein in solution showed highest heat stability when compared with control MPC solutions at the same protein level. Similarly, 20% calcium-reduced MPC in model formulation without any chelating agent exhibited the highest heat stability than control MPC formulation. On the other hand, presence of

chelating agent significantly decreased the heat stability in calcium-reduced MPC formulations. In the next phase of the study model formulations were retort-sterilized and storage stability was evaluated for 90 days. It can be concluded that beverages formulated with control MPC and 20% calcium-reduced MPC without chelating agents exhibited no age gelation during the 90-day storage period. However, beverages formulated with control MPC exhibited sedimentation was observed in control beverages by the end of 90-day storage period whereas, no sedimentation or gelling was observed in beverages with 20% calcium-reduced MPC. These findings show a potential for the use of 20% calcium-reduced MPC without chelating agent in dairy beverage formulations to improve the heat stability and the storage stability.

Appendix A - FBRM Operating Procedure

Step 1. Before FBRM is turned on, make sure desiccant is dry and set the pressure of compressed air at 70 psi.

Step 2. Let the compressed air run for few min before switching the equipment on and connecting the USB to the laptop.

Step 3. On the laptop, access the iC FBRM software to start an experiment as shown in Figure A-1.

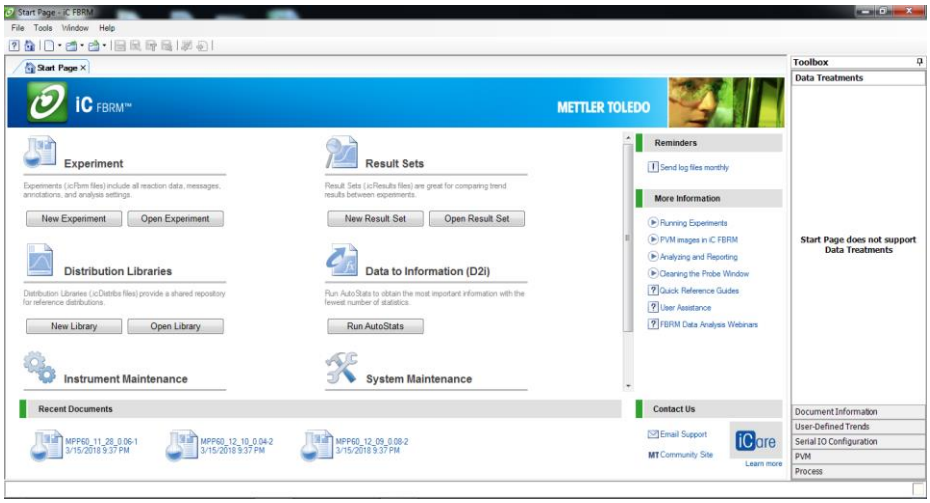

Figure A-1. Accessing iC FBRM program on the laptop.

Step 4. Click on “New Experiment” option in the Experiment section. If an error pops up saying instrument cannot be detected as shown in Figure A-2, please follow instructions on Step 5, if not move to Step 7.

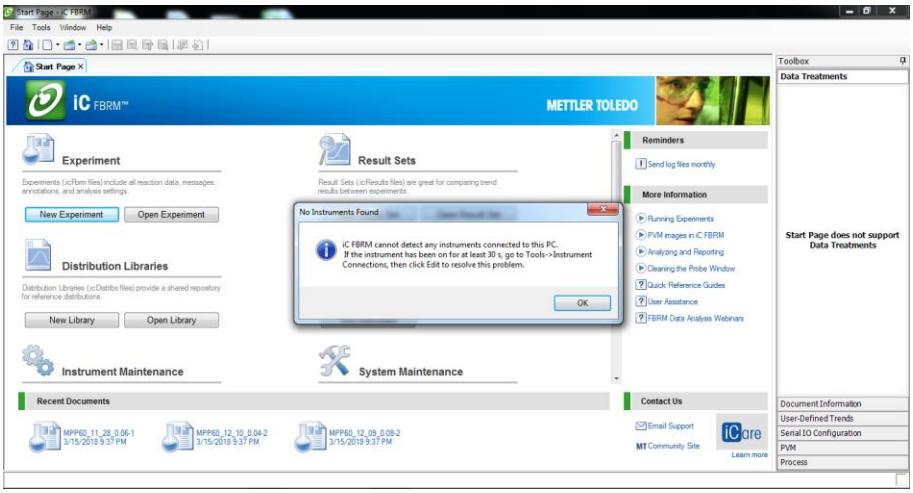

Figure A-2. Error window indicating that the instrument was not detected by the iC FBRM software.

Step 5. In the Tools tab, choose instrument connections and click “Edit” as shown in Figure A-3.

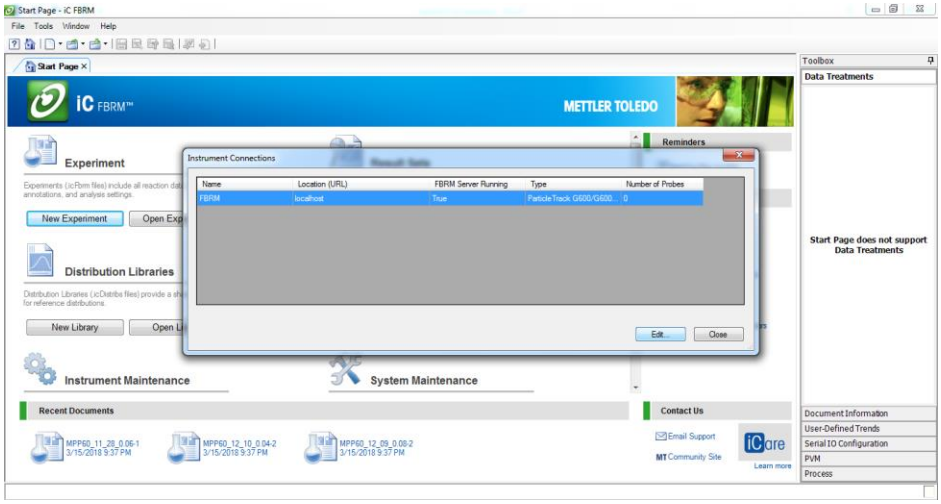

Figure A-3. Troubleshooting the error to start the new experiment.

Step 6. Another pop-up window displays confirming that the Particle Track device is already configured as shown in Figure A-4 and probe was detected changing the “Number of Probes” from 0 to 1 as shown in Figure A-5.

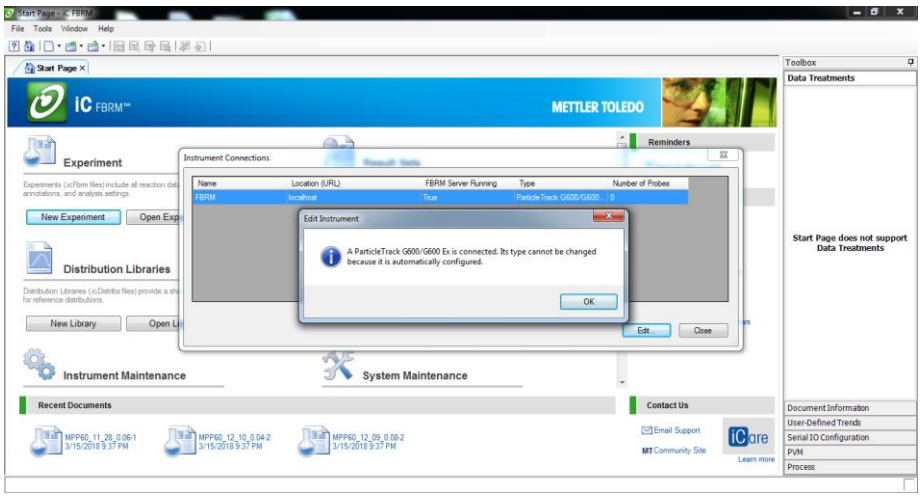

Figure A-4. Particle Track configuration confirmation in the connections.

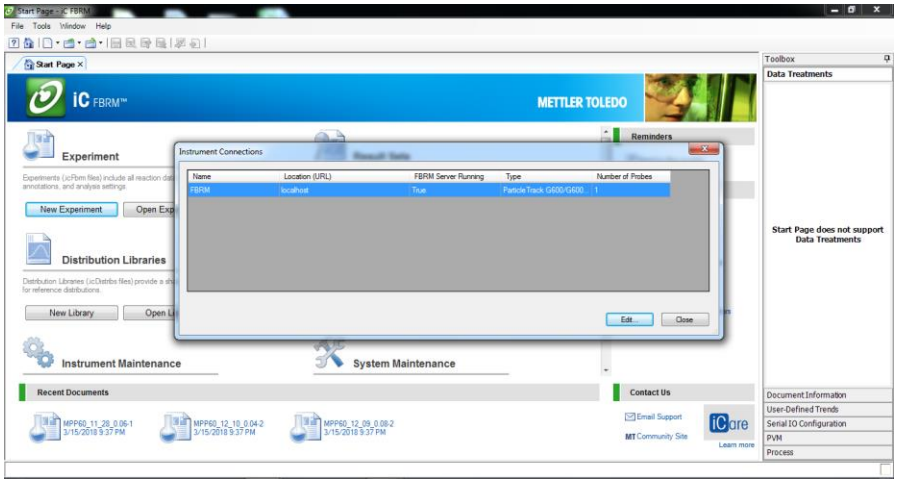

Figure A-5. Probe detected by the iC FBRM software.

Step 7. Now go back to the Start page and start the new experiment to choose file name, folder and template as shown in Figure A-6. In case of calibrating the probe using standard solution, choose “Configure Instrument” and follow the instructions.

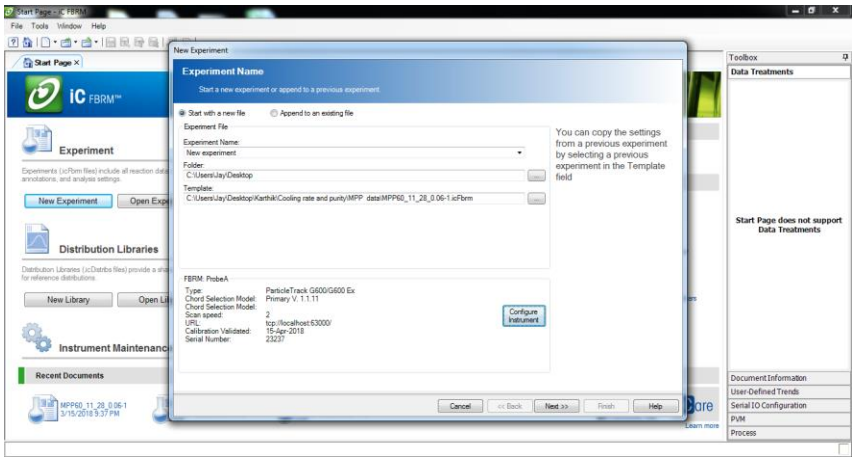

Figure A-6. Experiment information and calibrating the probe using standard solution.

Step 8. Choose the data acquisition settings depending on the experiment planned and go to next step as shown in Figure A-7.

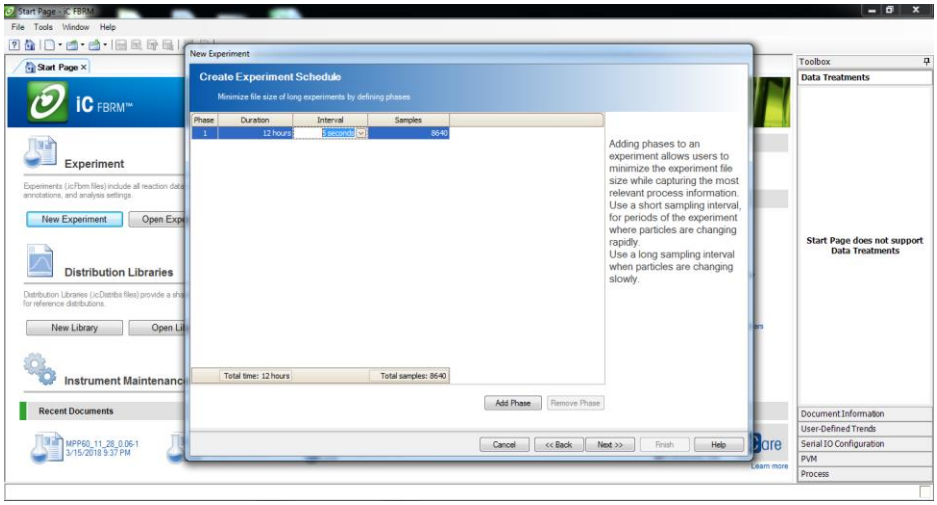

Figure A-7. Data acquisition settings on iC FBRM.

Step 9. Probe must be cleaned following the instructions. Use clean deionized water in a clean glass beaker to clean the probe. If the counts are too high on the probe window, the counts range was shown in red as shown in Figure A-8.

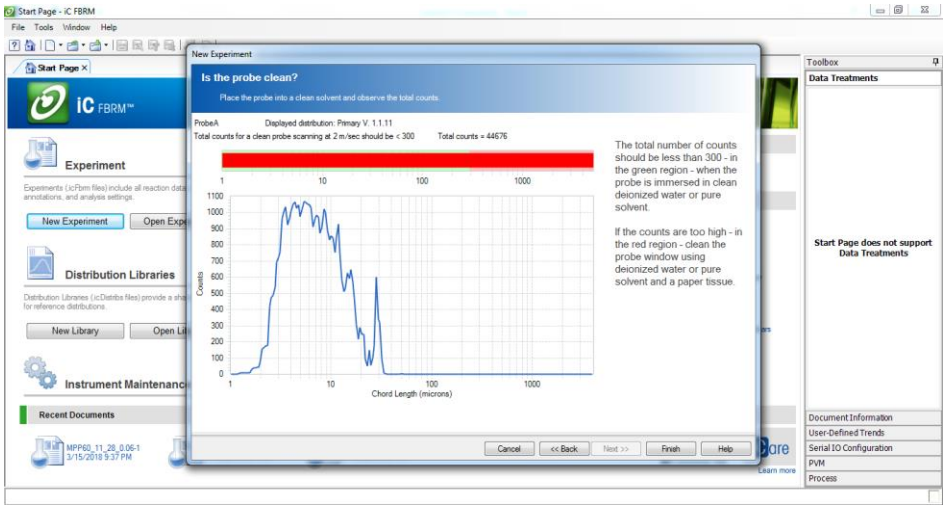

Figure A-8. Instructions to clean a dirty probe window.

Step 10. Once the probe is cleaned following the instructions, the particle counts fall in the green region as shown in Figure A-9.

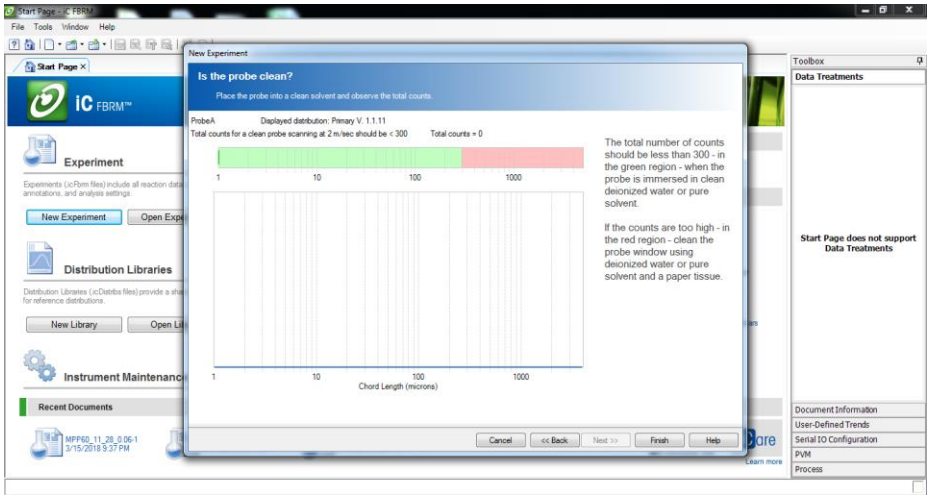

Figure A-9. Clean probe with counts in the green region.

Step 11. After the probe is cleaned, the window with data acquisition is displayed in yellow color as shown in Figure A-10. Cleaned probe can be adjusted into the experimental setup in this step and data acquired during this procedure can be saved or discarded (Figure A-11) depending on the experimental design.

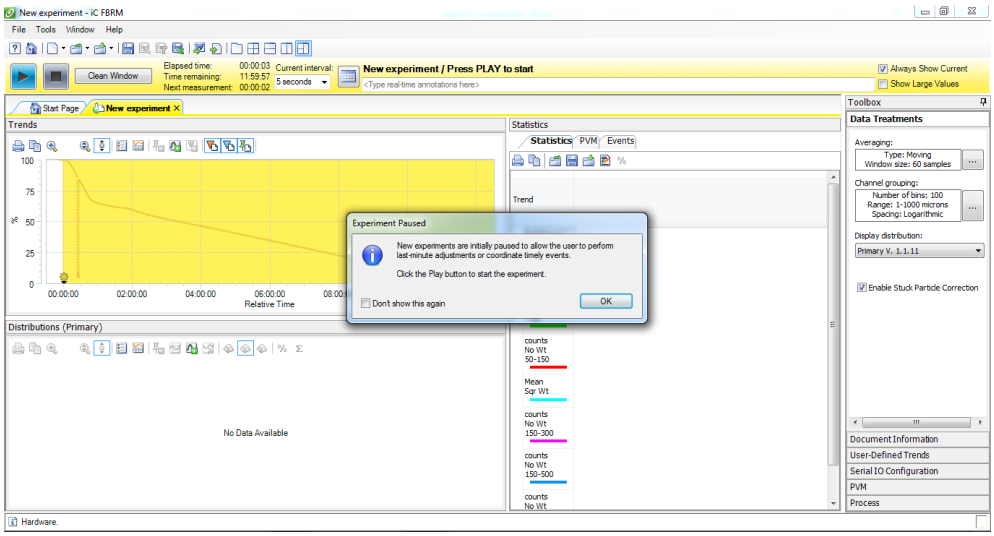

Figure A-10. Starting an experiment

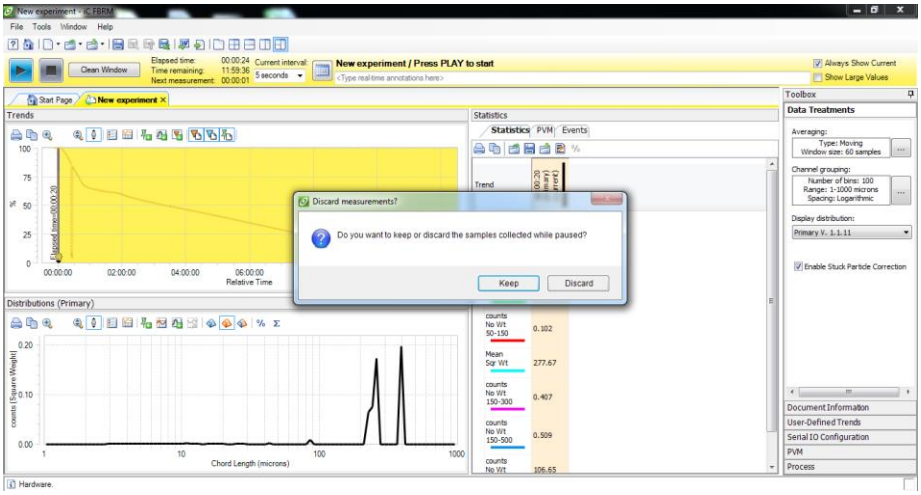

Figure A-11. Data acquired during experimental setup.

Step 12. On choosing to keep or discard the data during experimental setup, the window turns green indicating that data is being acquired based on the settings provided initially as shown in Figure A-12.

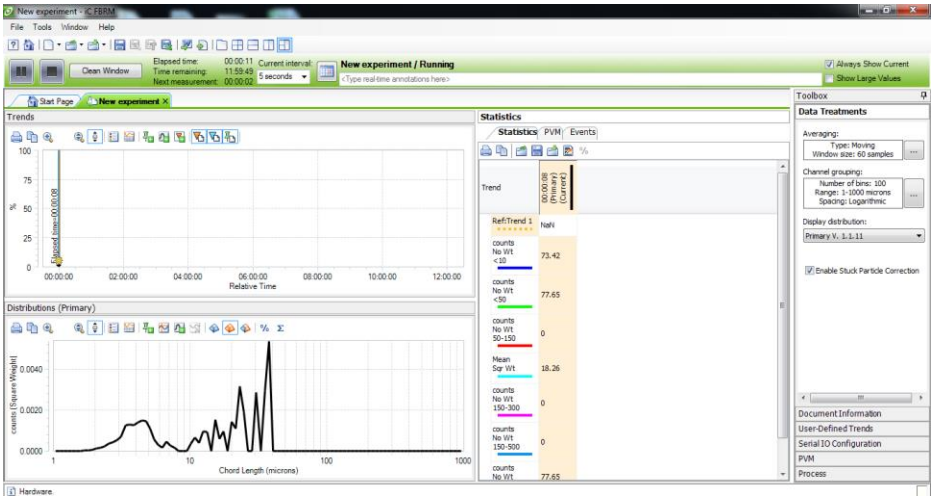

Figure A-12. Data acquisition during the experiment.

Step 13. To end the experiment, click on the stop button the top left corner of the window. A warning window displays to confirming the end process as shown in Figure A-13.

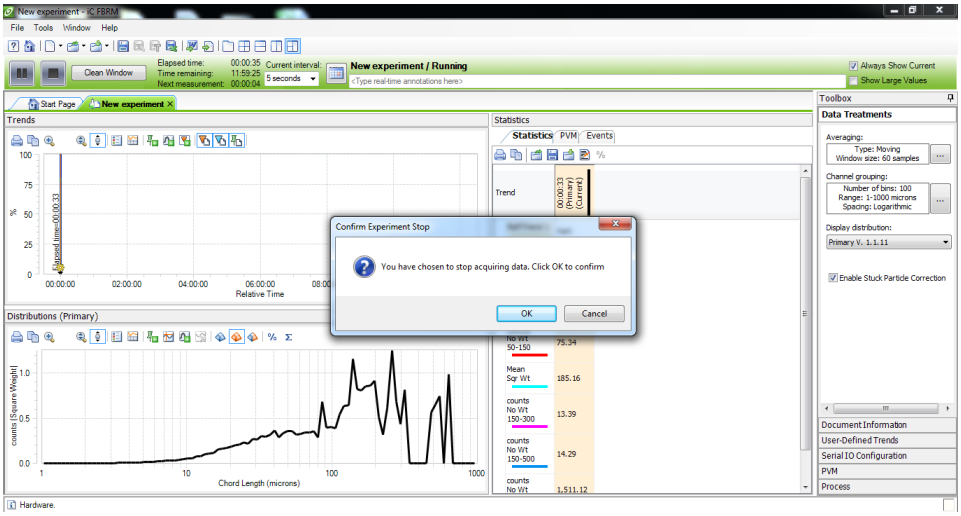

Figure A-13. Procedure to end the experiment.

Appendix B - Calculations to measure the extent of crystallization from lactose concentration in chapter 3: Focused Beam Reflectance Measurement (FBRM) as a Tool for *in situ* monitoring of Lactose Crystallization Process

Extent of crystallization was calculated from the lactose concentration measured using refractometry method. Mass of lactose crystals was calculated using Equation 1.

$$M_{Crystal}(t) = M_{H_2O}(0).\frac{C(0)-C(t)}{95-0.05.C(t)} \qquad \mathbf{1}$$

From the obtained mass of crystals at time *t*, extent of crystallization was calculated by dividing with mass of crystals calculated at the isothermal temperature. The lactose concentration and the extent of crystallization at time t were plotted on y-axis and time was plotted on x-axis as shown in Figure B-1.

1	Run 6: 30 C with 55% concentration, Solubility of Lactose at 30 C is 19.9%						
2	Mass of crystal at solubility point at 30 C =		19.9	84.0114888			
3	Initial Brix at t =0		53.8	54.11431431	2.15917249	0.025700919	37.51431431
4	Time(t)	Temp	Brix	Concentration	Mass of crystals at time t	Extent of crystallization	Concentration difference Δ C
5	0:03:00	29.9	53.7	54.01421421	2.40307161	0.028604083	34.11421421
6	0:06:00	29.9	52.9	53.21341341	4.35331277	0.051818065	33.31341341
7	0:09:00	30.5	49.4	49.70990991	12.8657693	0.153142975	29.80990991
8	0:12:00	30.4	47.4	47.70790791	17.7155723	0.210870829	27.80790791
9	0:15:00	30.2	45.7	46.00620621	21.8296697	0.259841481	26.10620621
10	0:18:00	29.7	45.2	45.50570571	23.0382614	0.27422751	25.60570571
11	0:21:00	29.6	44.6	44.90510511	24.4877107	0.291480499	25.00510511
12	0:24:00	29.5	43.9	44.2044044	26.177549	0.311594871	24.3044044
13	0:27:00	29.5	43.4	43.7039039	27.3837954	0.325952983	23.8039039
14	0:30:00	29.5	43.1	43.4036036	28.107231	0.334564134	23.5036036
15	0:33:00	29.6	42.7	43.0032032	29.0714479	0.346041337	23.1032032
16	0:36:00	29.6	42.1	42.4026026	30.5169938	0.363247864	22.5026026
17	0:39:00	29.6	41.8	42.1023023	31.2394163	0.371846955	22.2023023
18	0:42:00	29.5	41.4	41.7019019	32.2022831	0.383308088	21.8019019
19	0:45:00	29.5	41.3	41.6018018	32.442935	0.386172599	21.7018018
20	0:48:00	29.4	40.9	41.2014014	33.4052833	0.39762756	21.3014014
21	0:51:00	29.4	40.5	40.801001	34.367217	0.409077586	20.901001
22	0:54:00	29.5	40	40.3005005	35.5690518	0.423383186	20.4005005
23	0:57:00	29.5	39.9	40.2004004	35.8093411	0.426243382	20.3004004
24	1:00:00	29.6	39.6	39.9001001	36.5300539	0.434822123	20.0001001
25	1:30:00	30.5	36.4	36.6968969	44.2032023	0.526156636	16.7968969
26	2:00:00	29.8	33.1	33.39359359	52.0885541	0.620017035	13.49359359
27	2:30:00	29.5	30.8	31.09129129	57.5679212	0.685238674	11.19129129
28	3:00:00	29.6	28.8	29.08928929	62.3216263	0.741822663	9.189289289
29	3:30:00	29.5	27.2	27.48768769	66.1172717	0.787002739	7.587687688

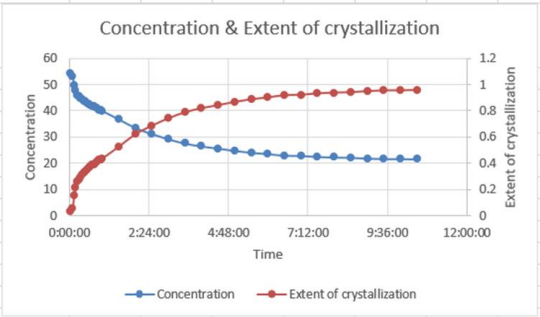

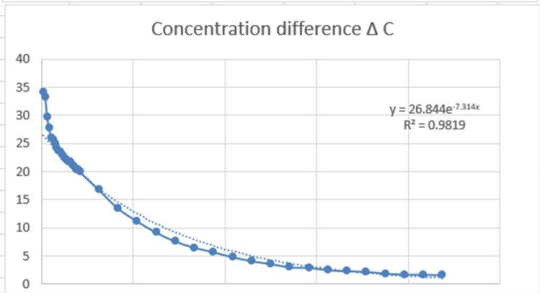

Figure B-1. Calculations to obtain the extent of crystallization during isothermal crystallization of pure lactose in chapter 3.

Appendix C - Data and SAS code for chapter 5: Influence of milk protein concentrates with modified calcium content on the dairy beverage formulation: Physico-chemical properties

Background

The data is organized in 10 columns and variables were arranged in the last 5 columns, Unheated 8% protein solutions prepared from MPC with varying calcium content was given below.

```
data PhaseIUH;
input ID$ Ca$ hexa$ rep$ visc K n L a b particlesize;
datalines;
```

Obs	ID	Ca	hexa	rep	visc	L	a	b	particlesize
1	1	Control	0	1	6.67	74.38	1.19	16.32	192.55
2	2	Control	0	2	6.57	74.38	1.61	14.38	191.72
3	3	Control	0.15	1	16.30	75.35	1.24	15.16	91.25
4	4	Control	0.15	2	15.39	75.34	1.11	13.54	90.16
5	5	Control	0.25	1	50.38	74.06	0.06	9.61	82.87
6	6	Control	0.25	2	62.70	72.23	-1.57	9.40	81.39
7	7	20%reduc	0	1	4.73	78.15	-0.37	10.07	187.37
8	8	20%reduc	0	2	5.34	80.95	-2.53	6.30	185.85
9	9	20%reduc	0.15	1	18.85	79.81	0.10	9.54	87.87
10	10	20%reduc	0.15	2	14.53	76.05	-4.15	4.31	87.17
11	11	20%reduc	0.25	1	29.65	74.22	-3.25	3.98	78.53
12	12	20%reduc	0.25	2	29.75	73.82	-3.04	4.28	74.77
13	13	30%reduc	0	1	8.44	74.41	-1.73	6.09	107.96
14	14	30%reduc	0	2	6.16	74.87	1.29	6.16	109.10
15	15	30%reduc	0.15	1	11.94	76.78	-4.78	-1.62	84.41
16	16	30%reduc	0.15	2	11.47	74.65	1.32	-1.13	82.70
17	17	30%reduc	0.25	1	14.27	57.25	-4.56	-2.37	65.62
18	18	30%reduc	0.25	2	10.78	59.56	1.46	-3.28	65.50

```
;
run;
proc print data=PhaseIUH;
run;
```

```
/*LSMEANS differences for visc*/

ods rtf;
proc glimmix data=PhaseIUH;
class Ca hexa rep;
model visc= Ca|hexa;
random rep rep*Ca rep*hexa(Ca);
lsmeans Ca/ pdiff lines adjust=Tukey;
lsmeans hexa/ pdiff lines adjust=Tukey;
lsmeans hexa*Ca/ pdiff lines adjust=Tukey;
run;

 /*LSMEANS differences for L*/

ods rtf;
proc glimmix data=PhaseIUH;
class Ca hexa rep;
model L = Ca|hexa;
random rep rep*Ca rep*hexa(Ca);
lsmeans Ca/ pdiff lines adjust=Tukey;
lsmeans hexa/ pdiff lines adjust=Tukey;
lsmeans hexa*Ca/ pdiff lines adjust=Tukey;
run;

/*LSMEANS differences for a*/

ods rtf;
proc glimmix data=PhaseIUH;
class Ca hexa rep;
model a = Ca|hexa;
random rep rep*Ca rep*hexa(Ca);
lsmeans Ca/ pdiff lines adjust=Tukey;
lsmeans hexa/ pdiff lines adjust=Tukey;
lsmeans hexa*Ca/ pdiff lines adjust=Tukey;
run;


/*LSMEANS differences for b*/

ods rtf;
proc glimmix data=PhaseIUH;
class Ca hexa rep;
model b = Ca|hexa;
random rep rep*Ca rep*hexa(Ca);
lsmeans Ca/ pdiff lines adjust=Tukey;
lsmeans hexa/ pdiff lines adjust=Tukey;
lsmeans hexa*Ca/ pdiff lines adjust=Tukey;
run;


/*LSMEANS differences for particlesize*/

ods rtf;
proc glimmix data=PhaseIUH;
class Ca hexa rep;
model particlesize = Ca|hexa;
random rep rep*Ca rep*hexa(Ca);
```

```
lsmeans Ca/ pdiff lines adjust=Tukey;
lsmeans hexa/ pdiff lines adjust=Tukey;
lsmeans hexa*Ca/ pdiff lines adjust=Tukey;
run;
```

Heated 8% protein solutions prepared from MPC with varying calcium content was given below.

```
data PhaseIH;
input ID$ Ca$ hexa$ rep$ visc K n L a b particlesize;
datalines;
```

1	Control	0	1	2.81	0.0018	1.1625	75.14	-2.8	6.44	223.2
2	Control	0	2	2.96	0.0026	1.0534	78.4	-3.84	5.12	234.87
3	Control	0.15	1	2.77	0.0044	0.9609	72.15	-3.99	11.38	382.1
4	Control	0.15	2	3.47	0.0031	1.0896	73	0.1	15.48	378.37
5	Control	0.25	1	3.84	0.0041	1.0340	63.47	-4.43	13.16	338.37
6	Control	0.25	2	3.91	0.0038	1.0706	64.96	-1.54	12.77	335.87
7	20%reduced	0	1	3.55	0.0037	1.0497	75.03	-4.33	4.23	232.47
8	20%reduced	0	2	3.93	0.0049	1.0209	72.54	-4.56	2.79	238.47
9	20%reduced	0.15	1	4.90	0.0089	0.8084	54.47	-5.36	-2.09	266.25
10	20%reduced	0.15	2	6.29	0.0087	0.9788	56.2	-5.07	-0.01	274.32
11	20%reduced	0.25	1	5.91	0.0073	1.0473	41.54	-3.58	-4.88	227.17
12	20%reduced	0.25	2	4.77	0.0062	1.0662	42.44	-4.3	-5.26	219.72
13	30%reduced	0	1	4.17	0.0034	1.0639	72.5	-2.7	7.32	234.35
14	30%reduced	0	2	3.13	0.0033	1.0539	69.52	-1.43	8.9	223.97
15	30%reduced	0.15	1	5.55	0.0069	1.0433	59.39	-3.62	1.9	262.15
16	30%reduced	0.15	2	3.75	0.0056	1.0462	57.11	-4.29	1.06	274.65
17	30%reduced	0.25	1	5.33	0.0080	1.0152	46.16	-3.25	2.05	243.6
18	30%reduced	0.25	2	4.38	0.0092	1.0037	44.3	-3.56	4.57	248.89

```
;
run;
proc print data=PhaseIH;
run;

/*LSMEANS differences for visc*/

ods rtf;
proc glimmix data=PhaseIH;
class Ca hexa rep;
model visc = Ca|hexa;
random rep rep*Ca rep*hexa(Ca);
lsmeans Ca/ pdiff lines adjust=Tukey;
lsmeans hexa/ pdiff lines adjust=Tukey;
lsmeans hexa*Ca/ pdiff lines adjust=Tukey;
run;
```

```
/*LSMEANS differences for L*/

ods rtf;
proc glimmix data=PhaseIH;
class Ca hexa rep;
model L = Ca|hexa;
random rep rep*Ca rep*hexa(Ca);
lsmeans Ca/ pdiff lines adjust=Tukey;
lsmeans hexa/ pdiff lines adjust=Tukey;
lsmeans hexa*Ca/ pdiff lines adjust=Tukey;
run;


/*LSMEANS differences for a*/

ods rtf;
proc glimmix data=PhaseIH;
class Ca hexa rep;
model a = Ca|hexa;
random rep rep*Ca rep*hexa(Ca);
lsmeans Ca/ pdiff lines adjust=Tukey;
lsmeans hexa/ pdiff lines adjust=Tukey;
lsmeans hexa*Ca/ pdiff lines adjust=Tukey;
run;

/*LSMEANS differences for b*/

ods rtf;
proc glimmix data=PhaseIH;
class Ca hexa rep;
model b = Ca|hexa;
random rep rep*Ca rep*hexa(Ca);
lsmeans Ca/ pdiff lines adjust=Tukey;
lsmeans hexa/ pdiff lines adjust=Tukey;
lsmeans hexa*Ca/ pdiff lines adjust=Tukey;
run;

/*LSMEANS differences for particlesize*/

ods rtf;
proc glimmix data=PhaseIH;
class Ca hexa rep;
model particlesize = Ca|hexa;
random rep rep*Ca rep*hexa(Ca);
lsmeans Ca/ pdiff lines adjust=Tukey;
lsmeans hexa/ pdiff lines adjust=Tukey;
lsmeans hexa*Ca/ pdiff lines adjust=Tukey;
run;
```

Unheated 8% protein beverage formulations prepared from MPC with varying calcium content was given below.

```
data PhaseIIUH;
input ID$ Ca$ hexa$ rep$ visc K n L a b particlesize;
datalines;
```

Obs	ID	Ca	hexa	rep	visc	L	a	b	particlesize
1	1	Control	0	1	86.61	67.58	-0.95	5.57	234.68
2	2	Control	0	2	84.61	70.45	-1.33	8.16	237.48
3	3	Control	0.15	1	193.54	72.33	-1.62	5.35	179.78
4	4	Control	0.15	2	195.00	77.72	-1.57	9.63	172.93
5	5	Control	0.25	1	445.05	70.97	-1.74	11.97	122.28
6	6	Control	0.25	2	408.00	73.57	-1.42	11.03	123.73
7	7	20%reduc	0	1	33.90	75.18	-2.05	7.34	163.80
8	8	20%reduc	0	2	45.19	77.39	-1.98	12.46	162.38
9	9	20%reduc	0.15	1	97.95	71.07	-2.50	11.08	147.55
10	10	20%reduc	0.15	2	113.10	74.21	-2.27	12.46	149.30
11	11	20%reduc	0.25	1	161.10	60.98	-2.66	5.81	128.95
12	12	20%reduc	0.25	2	168.80	63.88	-2.84	6.01	123.42
13	13	30%reduc	0	1	46.74	69.29	-0.39	10.89	136.70
14	14	30%reduc	0	2	59.73	66.47	0.10	9.97	134.58
15	15	30%reduc	0.15	1	72.60	63.96	-3.15	8.74	113.38
16	16	30%reduc	0.15	2	86.49	64.01	-0.64	10.14	111.19
17	17	30%reduc	0.25	1	66.65	60.59	-1.80	7.40	107.08
18	18	30%reduc	0.25	2	89.54	63.51	-1.46	7.40	103.63

```
;
run;
proc print data=PhaseIIUH;
run;

/*LSMEANS differences for visc*/

ods rtf;
proc glimmix data=PhaseIIUH;
class Ca hexa rep;
model visc= Ca|hexa;
random rep rep*Ca rep*hexa(Ca);
lsmeans Ca/ pdiff lines adjust=Tukey;
lsmeans hexa/ pdiff lines adjust=Tukey;
lsmeans hexa*Ca/ pdiff lines adjust=Tukey;
run;
```

```
/*LSMEANS differences for L*/

ods rtf;
proc glimmix data=PhaseIIUH;
class Ca hexa rep;
model L = Ca|hexa;
random rep rep*Ca rep*hexa(Ca);
lsmeans Ca/ pdiff lines adjust=Tukey;
lsmeans hexa/ pdiff lines adjust=Tukey;
lsmeans hexa*Ca/ pdiff lines adjust=Tukey;
run;

/*LSMEANS differences for a*/

ods rtf;
proc glimmix data=PhaseIIUH;
class Ca hexa rep;
model a = Ca|hexa;
random rep rep*Ca rep*hexa(Ca);
lsmeans Ca/ pdiff lines adjust=Tukey;
lsmeans hexa/ pdiff lines adjust=Tukey;
lsmeans hexa*Ca/ pdiff lines adjust=Tukey;
run;

/*LSMEANS differences for b*/

ods rtf;
proc glimmix data=PhaseIIUH;
class Ca hexa rep;
model b = Ca|hexa;
random rep rep*Ca rep*hexa(Ca);
lsmeans Ca/ pdiff lines adjust=Tukey;
lsmeans hexa/ pdiff lines adjust=Tukey;
lsmeans hexa*Ca/ pdiff lines adjust=Tukey;
run;

/*LSMEANS differences for particlesize*/

ods rtf;
proc glimmix data=PhaseIIUH;
class Ca hexa rep;
model particlesize = Ca|hexa;
random rep rep*Ca rep*hexa(Ca);
lsmeans Ca/ pdiff lines adjust=Tukey;
lsmeans hexa/ pdiff lines adjust=Tukey;
lsmeans hexa*Ca/ pdiff lines adjust=Tukey;
run;
```

Heated 8% protein beverage formulations prepared from MPC with varying calcium content was given below.

```
data PhaseIIH;
input ID$ Ca$ hexa$ rep$ visc K n L a b particlesize;
datalines;
```

Obs	ID	Ca	hexa	rep	visc	L	a	b	particlesize
1	1	Control	0	1	124.32	67.81	-3.22	8.04	264.53
2	2	Control	0	2	125.00	72.52	-3.19	6.88	262.38
3	3	Control	0.15	1	236.22	65.36	-2.45	7.16	255.18
4	4	Control	0.15	2	235.00	65.19	-2.32	10.20	263.38
5	5	Control	0.25	1	225.70	57.72	-0.27	12.37	249.70
6	6	Control	0.25	2	223.00	59.73	-1.74	9.55	243.18
7	7	20%reduc	0	1	102.38	65.23	-2.25	8.32	253.98
8	8	20%reduc	0	2	93.38	63.26	-1.82	10.19	251.75
9	9	20%reduc	0.15	1	117.31	55.47	-2.50	7.11	227.65
10	10	20%reduc	0.15	2	84.25	53.78	-0.52	9.64	222.88
11	11	20%reduc	0.25	1	222.85	51.30	-1.72	5.59	213.48
12	12	20%reduc	0.25	2	252.65	50.22	-2.79	5.54	215.90
13	13	30%reduc	0	1	185.00	61.87	-1.54	10.57	318.98
14	14	30%reduc	0	2	187.75	55.20	-0.16	14.24	311.55
15	15	30%reduc	0.15	1	133.80	53.14	-0.31	12.40	334.53
16	16	30%reduc	0.15	2	203.20	51.88	-1.43	11.23	328.39
17	17	30%reduc	0.25	1	157.87	52.12	-1.69	10.73	305.35
18	18	30%reduc	0.25	2	194.20	51.88	-2.01	8.63	302.28

```
;
run;

proc print data=PhaseIIH;
run;

/*LSMEANS differences for visc*/

ods rtf;
proc glimmix data=PhaseIIH;
class Ca hexa rep;
model visc= Ca|hexa;
random rep rep*Ca rep*hexa(Ca);
lsmeans Ca/ pdiff lines adjust=Tukey;
lsmeans hexa/ pdiff lines adjust=Tukey;
lsmeans hexa*Ca/ pdiff lines adjust=Tukey;
run;
```

```
/*LSMEANS differences for L*/

ods rtf;
proc glimmix data=PhaseIIH;
class Ca hexa rep;
model L = Ca|hexa;
random rep rep*Ca rep*hexa(Ca);
lsmeans Ca/ pdiff lines adjust=Tukey;
lsmeans hexa/ pdiff lines adjust=Tukey;
lsmeans hexa*Ca/ pdiff lines adjust=Tukey;
run;

/*LSMEANS differences for a*/

ods rtf;
proc glimmix data=PhaseIIH;
class Ca hexa rep;
model a = Ca|hexa;
random rep rep*Ca rep*hexa(Ca);
lsmeans Ca/ pdiff lines adjust=Tukey;
lsmeans hexa/ pdiff lines adjust=Tukey;
lsmeans hexa*Ca/ pdiff lines adjust=Tukey;
run;

/*LSMEANS differences for b*/

ods rtf;
proc glimmix data=PhaseIIH;
class Ca hexa rep;
model b = Ca|hexa;
random rep rep*Ca rep*hexa(Ca);
lsmeans Ca/ pdiff lines adjust=Tukey;
lsmeans hexa/ pdiff lines adjust=Tukey;
lsmeans hexa*Ca/ pdiff lines adjust=Tukey;
run;

/*LSMEANS differences for particlesize*/

ods rtf;
proc glimmix data=PhaseIIH;
class Ca hexa rep;
model particlesize = Ca|hexa;
random rep rep*Ca rep*hexa(Ca);
lsmeans Ca/ pdiff lines adjust=Tukey;
lsmeans hexa/ pdiff lines adjust=Tukey;
lsmeans hexa*Ca/ pdiff lines adjust=Tukey;
run;
```

Table C-1. a* of the enteral formulations before and after heating in Phase I and II

		Phase I		Phase II	
MPC	SHMP (%)	Unheated	Heated	Unheated	Heated
Control	0	1.40±0.30	-3.32±0.74	-1.14±0.27	-3.20±0.02
	0.15	1.18±0.09	-1.95±2.89	-1.59±0.04	-2.39±0.09
	0.25	-0.76±1.15	-2.99±2.04	-1.58±0.23	-1.00±1.04
20% Ca reduced	0	-1.45±1.53	-4.45±0.16	-2.01±0.05	-2.03±0.30
	0.15	-2.03±3.01	-5.22±0.21	-2.39±0.16	-1.51±1.40
	0.25	-3.15±0.15	-3.94±0.51	-2.75±0.13	-2.25±0.76
30% Ca reduced	0	-0.22±2.14	-2.07±0.90	-0.14±0.34	-0.85±0.98
	0.15	-1.73±4.31	-3.96±0.47	-1.90±1.77	-0.87±0.79
	0.25	-1.55±4.26	-3.41±0.22	-1.63±0.24	-1.85±0.23

a* was compared within the column irrespective of the phase.
There was no significant interaction effect between main effects

Table C-2. b* of the enteral formulations before and after heating in Phase I and II

		Phase I		Phase II	
MPC	SHMP (%)	Unheated	Heated	Unheated	Heated
Control	0	15.35 ± 1.37^{a}	5.78 ± 0.93^{bc}	6.86 ± 1.83^{a}	7.46 ± 0.82^{NS}
	0.15	14.35 ± 1.15^{ab}	13.43 ± 2.90^{a}	7.49 ± 3.03^{a}	8.68 ± 2.15^{NS}
	0.25	9.51 ± 0.15^{bc}	12.97 ± 0.28^{a}	11.50 ± 0.66^{a}	10.96 ± 2.00^{NS}
20% Ca reduced	0	8.19 ± 2.67^{bc}	3.51 ± 1.02^{bcd}	9.90 ± 3.62^{a}	9.25 ± 1.32^{NS}
	0.15	6.93 ± 3.70^{c}	-1.05 ± 1.47^{de}	11.77 ± 0.97^{a}	8.37 ± 1.79^{NS}
	0.25	4.13 ± 0.21^{cd}	-5.07 ± 0.27^{e}	5.91 ± 0.14^{a}	5.56 ± 0.04^{NS}
30% Ca reduced	0	6.13 ± 0.05^{c}	8.11 ± 1.12^{ab}	10.43 ± 0.65^{a}	12.41 ± 2.60^{NS}
	0.15	-1.38 ± 0.35^{de}	1.48 ± 0.59^{cd}	9.44 ± 0.99^{a}	11.81 ± 0.83^{NS}
	0.25	-2.83 ± 0.64^{e}	3.31 ± 1.78^{bcd}	7.40 ± 0.00^{a}	9.68 ± 1.48^{NS}

Sodium hexametaphosphate (SHMP).
NS- No significant interaction effect between main effects.
Apparent viscosity was compared within the column irrespective of the phase.
Values with the same superscript in the column are not significantly different (P>0.05)

Appendix D - Data and SAS code for chapter 6: Influence of milk protein concentrates with modified calcium content on the dairy beverage formulation: Storage stability

The apparent viscosity of the retort processed beverages were analyzed using repeated measures using SAS code below.

```
data viscositystorage;
input Rep$ MPC$ SHMP$ day0 day7 day30 day60 day90;
datalines;
```

1	Control	0	11.98	23.64	23.79	11.84	7.53
2	Control	0	17.035	21.44	16.66	9.27	9.93
1	Control	0.15	41.95	23.11	24.1	19.54	13.5
2	Control	0.15	59.435	36.95	30.74	11.41	15.18
1	20%reduced	0	19.5	50.57	24.23	28.45	28.33
2	20%reduced	0	25.815	42.5	35.82	32.47	27.7
1	20%reduced	0.15	50.92	109.83	96.84	108.96	102
2	20%reduced	0.15	50.735	101.05	101.635	111.58	106.7
1	30%reduced	0	136.5	135.8	151	102.84	99.045
2	30%reduced	0	138.5	120.6	163.64	107.41	103.11
1	30%reduced	0.15	173.4	95.44	79.8	158.65	91.98
2	30%reduced	0.15	168.7	90.66	70.34	153.41	86.63

```
;
Run;
Proc print; run;
Proc glm data = viscositystorage;
Class Rep MPC SHMP;
Model day0 day7 day30 day60 day90 = MPC Rep MPC*Rep SHMP MPC*SHMP;
Repeated time;
Means MPC Rep MPC*Rep SHMP MPC*SHMP /Tukey;
Run; quit;
```

The particle size of the retort processed beverages were analyzed using repeated measures using SAS code below.

```
data particlesizestorage;
input Rep$ MPC$ SHMP$ day0 day7 day30 day60 day90;
datalines;
1 Control 0 191.8 193.9 188.9 201.2 188.1
2 Control 0 182.57 193.45 183.25 192.2 191.25
1 Control 0.15 270.97 265.9 290.37 289.95 296.1
2 Control 0.15 277.09 290.05 297.65 299.2 297.45
1 20%reduced 0 199.75 240.52 287.35 264.51 256.55
2 20%reduced 0 204.47 246.15 270.45 249.14 265.55
1 20%reduced 0.15 237.15 230.72 230.97 257.1 293.45
2 20%reduced 0.15 260.72 249.5 225.05 236.62 276.1
1 30%reduced 0 320.5 383.42 389.57 320.2 374.4
2 30%reduced 0 284.52 398.4 364.6 317.52 377.1
1 30%reduced 0.15 332.85 323.62 338.27 315.25 292.2
2 30%reduced 0.15 298.55 303.55 350.1 297.92 296.8
;
Run;
Proc print; run;
Proc glm data = particlesizestorage;
Class Rep MPC SHMP;
Model day0 day7 day30 day60 day90 = MPC Rep MPC*Rep SHMP MPC*SHMP;
Repeated time;
Means MPC Rep MPC*Rep SHMP MPC*SHMP /Tukey;
Run; quit;
```

Table D-1. Viscosity (cP) of the enteral formulations at $100s^{-1}$ shear rate measured over storage period

MPC	SHMP(%)	Day 0	Day 7	Day 30	Day 60	Day 90
Control	0	14.51±3.57	22.54±1.56	20.23±5.04	10.56±1.82	8.73±1.70
	0.15	50.69±12.36	30.03±9.79	27.42±4.70	15.48±5.75	14.34±1.19
20% Ca reduced	0	22.66±4.47	46.54±5.71	30.03±8.20	30.46±2.84	28.02±0.45
	0.15	50.83±0.13	105.44±6.21	99.24±3.39	110.27±1.85	104.35±3.32
30% Ca reduced	0	137.50±1.41	128.20±10.75	157.32±8.94	105.13±3.23	101.08±2.87
	0.15	171.05±3.32	93.05±3.38	75.07±6.69	156.03±3.71	89.31±3.78

Table D-2. Particle size (nm) of the enteral formulations at $100s^{-1}$ shear rate measured over storage period in phase III

MPC	SHMP (%)	Day 0	Day 7	Day 30	Day 60	Day 90
Control	0	187.19±6.53	193.68±0.32	186.08±4.00	196.70±6.36	189.68±2.23
	0.15	274.03±4.33	277.98±17.08	294.01±5.15	294.58±6.54	296.78±0.95
20% Ca reduced	0	202.11±3.34	243.34±3.98	278.90±11.95	256.83±10.87	261.05±6.36
	0.15	248.94±16.67	240.11±13.28	228.01±4.19	246.86±14.48	284.78±12.27
30% Ca reduced	0	302.51±25.44	390.91±10.59	377.09±17.66	318.86±1.90	375.75±1.91
	0.15	315.70±24.25	313.59±14.19	344.19±8.37	306.59±12.25	294.50±3.25